“A system for the intracellular generation of triple helix-forming oligonucleotides (TFOs) and the sequence-specific inhibition of human MCP-1 gene expression”

Dissertation

zur Erlangung des Doktorgrades

der Naturwissenschaften

vorgelegt beim Fachbereich

Chemische und Pharmazeutische Wissenschaften

der Johann Wolfgang Goethe-Universität

in Frankfurt am Main

von

Kordula Kautz

aus Oerlinghausen

Frankfurt 2005

(DF1)

Dekan:	Prof. Dr. H. Schwalbe
Gutachter:	Prof. Dr. D. Steinhilber und Prof. Dr. H.H. Radeke

1 Summary

Chemokines play a key role in the cellular infiltration of inflamed tissue. They are released by a wide variety of cell types during the initial phase of host response to injury, allergens, antigens, or invading microorganisms, and selectively attract leukocytes to inflammatory foci, inducing both migration and activation. Monocyte chemoattractant protein-1 (MCP-1), a member of the CC chemokine superfamily, functions in attracting monocytes, T lymphocytes, and basophils to sites of inflammation. MCP-1 is produced by monocytes, fibroblasts, vascular endothelial cells and smooth muscle cells in response to various stimuli such as tumour necrosis factor-α (TNF-α), interferon-γ (IFN-γ), and interleukin-1β (IL-1β). It also plays an important role in the pathogenesis of chronic inflammation, and overexpression of MCP-1 has been implicated in diseases including glomerulonephritis and rheumatoid arthritis.

Oligonucleotide-directed triple helix formation offers a means to target specific sequences in DNA and interfere with gene expression at the transcriptional level. Triple helix-forming oligonucleotides (TFOs) bind to homopurine/homopyrimidine sequences, forming a stable, sequence-specific complex with the duplex DNA. Purine-rich sequences are frequent in gene regulatory regions and TFOs directed to promoter sequences have been shown to prevent binding of transcription factors and inhibit transcription initiation and elongation. Exogenous TFOs that bind homopurine/ homopyrimidine DNA sequences and form triple-helices can be rationally designed, while the intracellular delivery of single-stranded RNA TFOs has not been studied in detail before. In this study, expression vectors were constructed which directed transcription of either a 19 nt triplex-forming pyrimidine CU-TFO sequence targeting the human MCP-1 or two different 19 nt GU- or CA-control sequences, respectively, together with the vector encoded hygromycin resistance mRNA as one fusion transcript. HEK 293 cells were stable transfected with these vectors and several TFO and control cell lines were generated. Functional relevant triplex formation of a TFO with a corresponding 19 bp GC-rich AP-1/SP-1 site of the human MCP-1 promoter was shown. Binding of synthetic 19 nt CU-TFO to the MCP-1 promoter duplex was verified by triplex blotting at pH 6.7. Underlining binding specificity, control sequences, including the GU- and CA-sequence, a TFO containing one single mismatch and a MCP-1 promoter duplex containing two mismatches, did not participate in triplex formation. Establishing a magnetic capture technique with streptavidin microbeads it was verified that at pH 7.0 the 19 nt TFO embedded in a 1.1 kb fusion transcript binds to a plasmid encoded MCP-1 promoter target duplex three times stronger than the controls.

Finally, cell culture experiments revealed 76 ± 10.2% inhibition of MCP-1 protein secretion in TNF-α stimulated CU-TFO harboring cell lines and up to 88% after TNF-α and IFN-γ co-stimulation in comparison to controls. Expression of interleukin-8 (IL-8) as one TNF-α

inducible control gene was not affected by CU-TFO, demonstrating both highly specific and effective chemokine gene repression.

Furthermore, another chemokine target, regulated upon activation normal T cell expressed and secreted (RANTES), which plays an essential role in inflammation by recruiting T lymphocytes, macrophages and eosinophils to inflammatory sites, was analysed using the triplex approach. A 28 nt TFO was designed targeting the murine RANTES gene promoter, and gel mobility shift assays demonstrated that the phosphodiester TFO formed a sequence-specific triplex with the double-stranded target DNA with a K_d of 2.5 x 10^{-7} M. It was analysed whether RANTES expression could be inhibited at the transcriptional level testing the TFO in two different cell lines, T helper-1 lymphocytes and brain microvascular endothelial cells (b-end3 cells). Although there was a sequence-specific binding of the TFO detectable in the gel shift assays, there was no inhibitory effect of the exogenously added and phosphorothioate stabilised TFO on endogenous RANTES gene expression visible.

Additionally, the small interfering RNA (siRNA) approach was tested as another strategy to inhibit expression of the pro-inflammatory chemokines MCP-1 and RANTES. Two different methods were pursuit, describing transient transfection with vector derived and synthetic siRNA. The vector pSUPER containing the siRNA coding sequence was used to suppress endogenous MCP-1 in HEK 293 cells. An empty vector without RNA sequence served as a control. Inhibition due to the siRNA was measured in stimulated and unstimulated cells. In TNF-α stimulated cells MCP-1 protein synthesis was decreased by 35 ± 11% after siRNA transfection. Using a synthetic double-stranded siRNA, the TNF-α induced MCP-1 protein secretion could be successfully inhibited about 62.3 ± 10.3% in HEK 293 cells, indicating that the siRNA is functional in these cells to suppress chemokine expression. The siRNA approach targeting murine RANTES in Th1 cells and b-end3 cells revealed no inhibition of endogenous gene expression.

Gene therapy approaches rely on efficient transfer of genes to the desired target cells. A wide variety of viral and nonviral vectors have been developed and evaluated for their efficiency of transduction, sustained expression of the transgene, and safety. Among them, lentiviruses have been widely used for gene therapy applications. In order to improve the delivery of TFOs or siRNAs into the target cells, cloning of the lentiviral transfer vector SEW, the production of lentiviral particles by transient transfection were performed with the aim to generate lentiviral vector-derived TFOs in further experiments. Here, Th1 cells were transduced with infectious lentiviral particles and transduction efficacy was measured. Transduction efficacy higher than 82% could be achieved using the lentiviral vector SEW, opening optimal possibilities for the TFO or siRNA approach.

2 Introduction

2.1 Chemokines

Chemokines are a family of chemotactic cytokines that were first identified on the basis of their ability to induce the migration of different cell types, particularly those of lymphoid origin. They can be roughly divided into two main categories based on functional expression, the inducible and the constitutive chemokines. Most of them are inducible chemokines and participate primarily in inflammatory responses. The constitutive chemokines are expressed primarily in secondary lymphoid organs and appear to play a major role in lymphocyte homing (Baggiolini and Loetscher 2000; Feng 2000). In the recent years, an expanded role of chemokines has been identified, and they have been shown to activate leukocytes, influence hematopoiesis, and modulate angiogenesis. For example, interferon-inducible protein-10 (IP-10) induces the proliferation of mesangial cells (Romagnani et al. 1999). Interleukin-8 (IL-8) has been shown to stimulate the proliferation of endothelial cells and promote vascularisation (Miller et al. 1998; Simonini et al. 2000). In addition, some chemokines are involved in hematopoiesis (Juarez et al. 2004). Platelet factor 4 (PF4), IP-10, monokine induced by interferon-γ (MIG), and interferon-inducible T cell alpha chemoattractant (I-TAC) can act as angiostatic factors, while the ELR-chemokines IL-8, growth related oncogene-α, -β, -γ (GRO-α, -β, -γ), epithelial neutrophil activating peptide-78 (ENA-78), and stromal cell-derived factor-1 (SDF-1) have been shown to act as angiogenic agents (Belperio et al. 2000; Moore et al. 1998), suggesting that chemokines contribute to tissue remodelling and wound healing (Gillitzer and Goebeler 2001). Tumours transfected with RANTES (regulated upon activation, normal T cell expressed and secreted) and IP-10 have been shown to regress with the subsequent development of tumour immunity (Oppenheim et al. 1997). Chemokines are chemotactic for antigen-presenting dendritic cells and increase their capacity to activate T cells (Cravens and Lipsky 2002; Proietto et al. 2004).

Chemokines play a major role in chemoattraction and activation of blood leukocytes. They are involved in multiple disease processes and are of major importance during acute and chronic inflammation. Chemokines have been associated with a number of inflammatory diseases and conditions, including atherosclerosis, asthma, sepsis, inflammatory bowel disease and respiratory distress syndrome (Conti et al. 1999; Ni et al. 2004; Rose, Jr. et al. 2003). Chemokines are secreted in a stimulus-specific manner from a variety of cell types, including leukocytes, fibroblasts, epithelial cells, mesangial cells, and endothelial cells. (Coletta et al. 2000; Ebnet et al. 1996; Galindo et al. 2001; Murugesan et al. 2003; Schwarz

et al. 1997; Umekawa et al. 2003). The principle steps of inflammatory chemokine action on tethering, rolling, adhesion and transmigration have been described extensively (Johnston and Butcher 2002; Murphy 1994). The attraction of leukocytes out of the circulating blood to the site of injury is initiated by changes in the expression and activity of adhesion molecules on the respective vascular endothelial cells (Johnston and Butcher 2002). These early adhesion events are induced by a number of early response mediators and cytokines, including histamine, tumour necrosis factor-α (TNF-α), and interleukin-1 (IL-1). The early response cytokines and mediators upregulate E- and P-selectin molecules on the endothelial surface and slow the leukocytes from circulatory flow, a phenomenon known as tethering and rolling. Once tethered, the leukocytes roll on the endothelial surface in the direction of the blood flow, but much slower. This process exposes a greater surface of the leukocytes to the endothelial layer, where locally produced inflammatory chemokines are displayed bound to apical glycosaminoglycans of the endothelium. After leukocytes have been sequestered to the inflamed vascular wall, the cells may firmly adhere to the endothelium. During this interaction of adhesion molecules on leukocytes (e.g. lymphocyte-function-associated antigen 1, LFA-1, and very late antigen 4, VLA-4) with members of the immunoglobulin family of adhesion molecules on the endothelial cells (e.g. intercellular adhesion molecule 1, ICAM-1, and vascular-cell adhesion molecule 1, VCAM-1) chemokines are involved in the activation of these adhesion molecules. Adhesion allows the spreading of leukocytes along the endothelial surface (Imhof and Aurrand-Lions 2004). Once firmly adhered to the vascular endothelium, leukocytes then rapidly (in minutes) transmigrate through the endothelial layer without affecting its integrity. Having reached the subendothelial space, leukocytes follow the path to the injured tissue along one or more chemotactic gradients.

A large number of chemokines (~50) and their receptors (~20) have been identified in humans or mice. In general they represent small (8-14 kDa) heparin-binding proteins that are rich in basic amino acids and contain conserved N-terminal cysteines forming essential disulfide bonds between the first and third and the second and fourth cysteines. Chemokines are single polypeptides of 70-130 amino acids in length, which share 20-96% homology in amino acid sequence among each other. Based on the presence of the cysteine containing signature motif at the N-terminal, chemokines have been classified into four subfamilies (Table 2-1).

Table 2-1. Chemokines and their receptors (Ono et al. 2003)

Systematic name	Human ligand	Chemokine receptor
CXC family		
CXCL1	*Growth related oncogene* **GROα**/ *Melanoma growth stimulatory activity* **MGSAα**	CXCR1, CXCR2, Duffy (no signalling)
CXCL2	**GROβ**/ **MGSAβ**	CXCR2
CXCL3	**GROγ**/ **MGSAγ**	CXCR2
CXCL4	*Platelet factor* **PF4**	Unknown
CXCL5	*Epithelial neutrophil activating* peptide **ENA-78**	CXCR2
CXCL6	*Granulocyte chemotactic protein* **GCP-2**	CXCR1, CXCR2
CXCL7	*Neutrophil activating peptide* **NAP-2**	CXCR2, Duffy (no signalling)
CXCL8	*Interleukin* **IL-8**	CXCR1, CXCR2, Duffy (no signalling)
CXCL9	*Monokine-induced by interferon-γ* **MIG**	CXCR3, CCR3 (antagonist)
CXCL10	*IFN-γ inducible protein* **IP-10**	CXCR3, CCR3 (antagonist)
CXCL11	*IFN-inducible T-cell α chemoattractant* **I-TAC**	CXCR3
CXCL12	*Stromal cell-derived factor* **SDF-1α/β**	CXCR4
CXCL13	*B-cell attracting chemokine* **BCA-1**	CXCR5
CXCL14	*Breast and kidney-expressed chemokine* **BRAK**/ bolekine	Unknown
(CXCL15)	Unknown	Unknown
CXCL16		CXCR6
C family		
XCL1	Lymphotactin/ *single C motif* **SCM-1α**/ *Activation-induced, chemokine-related protein* **ATAC**	XCR1
XCL2	**SCM-1β**	XCR1
CX3C family		
CX3CL1	**Fractalkine**	CXCR1
CC family		
CCL1	I-309	CCR8, Duffy (no signalling
CCL2	*Monocyte chemoattractant protein* **MCP-1**/ *Monocyte chemotactic and activating factor* **MCAF**/ *Tumour-derived chemotactic factor* **TDCF**	CCR2, CCR5, Duffy (no signalling)
CCL3	*Macrophage inflammatory protein* **MIP-1α**/ **LD78α**	CCR1, CCR5
CCL3L1	**LD78β**	CCR1, CCR5
CCL4	**MIP-1β**	CCR5
CCL5	**RANTES**	CCR1, CCR3, CCR5, Duffy (no signalling)
(CCL6)	Unknown	Unknown
CCL7	**MCP-3**	CCR1, CCR2, CCR3
CCL8	**MCP-2**	CCR2, CCR3, CCR5
(CCL9/10)	Unknown	CCR1
CCL11	**Eotaxin**	CCR2 (partial antagonist), CCR3, CCR5, CXCR3 (antagonist)
(CCL12)	Unknown	CCR2
CCL13	**MCP-4**	CCR2, CCR3
CCL14	*Human CC chemokine* **HCC-1**	CCR1, CCR5
CCL15	**HCC-2**/ *leukotactin* **Lkn-1**/ **MIP-1δ**	CCR1, CCR3
CCL16	**HCC-4**/ *liver-expressed chemokine* **LEC**	CCR1, CCR2
CCL17	*Thymus- and activation-regulated chemokine* **TARC**	CCR4, CCR8
CCL18	*Dendritic cell-derived CC chemokine* **DC-CK1**/ *Pulmonary and activation regulated chemokine* **PARC**/ *Alternative macrophage activation associated CC chemokine* **AMAC-1**	Unknown
CCL19	**MIP-3β**/ *Ebl-1-ligand chemokine* **ELC**/ **exodus-3**	CCR7
CCL20	**MIP-3α**/ *liver and activation regulated chemokine* **LARC**/ **exodus-1**	CCR6
CCL21	**6Ckine**/ *secondary lymphoid tissue chemokine* **SLC**/ **exodus-2**	CCR7, CXCR3
CCL22	*Macrophage-derived chemokine* **MDC**/ *Stimulated T-cell chemoattractant protein* **STCP-1**	CCR4
CCL23	*Myeloid progenitor inhibitory factor* **MPIF-1**/ *chemokine* **CKβ8**/ **CKβ8-1**	CCR1
CCL24	**Eotaxin-2**/ **MPIF-2**	CCR3
CCL25	*Thymus-expressed chemokine* **TECK**	CCR9
CCL26	**Eotaxin-3**	CCR2 (antagonist), CCR3, CCR10
CCL27	*Cutaneous T-cell-activating chemokine* **CTACK**/ *IL-11 receptor alpha-locus chemokine* **ILC**	CCR10
CCL28	*Mucosa-associated epithelial chemokine* **MEC**	CCR3, CCR10

Most chemokines have four characteristic cysteines. Lymphotactins-α and β (CL1 and CL2) have only two cysteine residues (Kelner et al. 1994). While the CXC subfamily members have two cysteines at the N-terminus of the protein separated by one amino acid, the CC subfamily has two juxtaposed cysteine residues. Members of the C subfamily have only one cysteine at the amino terminal, and the first two cysteine residues are separated by three amino acids in the CX3C chemokine subfamily. In humans, the genes of the CXC chemokines are clustered on chromosome 4, and those of the CC chemokines on chromosome 17.

Chemokines mediate their effects via chemokine receptors that have been also divided into four subfamilies depending on the ligands they bind. Most receptors bind more than one chemokine ligand, often from different families. On the other hand, one chemokine ligand may bind to several receptors. Chemokine receptors may share 25-80% homology in the amino acid sequence. They are membrane molecules which belong to the superfamily of G-protein coupled receptors (GPCR) with seven transmembrane domains (Lefkowitz 2000; Milligan 2001). Chemokine receptors are approximately 350 amino acids in length and have a short extracellular N-terminus and a short intracellular C-terminus. The cytosolic tails contain conserved serine and threonine residues that become phosphorylated on receptor occupancy. The seven transmembrane domains are α-helical, and three intracellular and three extracellular loops exist between the transmembrane domains.
Engagement of chemokine receptors by their appropriate ligands results in the induction of a variety of functions including cell migration and proliferation. The biochemical events include GPCR-dependent calcium influx as well as changes in the intracellular cAMP levels and phosphoinositol lipid metabolism. Phospholipase C activation is triggered through Gβγ and yields inositol (1, 4, 5) triphosphate and diacylglycerol. Inositol triphosphate in turn mobilises the release of calcium from intracellular stores (Maghazachi 2000). Calcium, together with diacylglycerol, then activates multiple protein kinase C isoforms that drive downstream events throughout the cell. Eventually receptor desensitisation appears to operate through G-coupled kinases that associate with Gβγ (Okkenhaug and Vanhaesebroeck 2003). Phospholipase A2 and D can also be activated on chemokine receptor activation, and arachidonic acid release driven by phospholipase A2 is important for optimal cell movement toward a chemokine gradient.
Activation signals following stimulation by chemokine ligands also involve the initiation of a protein tyrosine kinase (PTK)-dependent pathway including activation of a family of focal adhesion kinase (FAK) proteins, which leads to reorganisation of various cytoskeletal proteins as well as activation of phosphatidylinositol 3-kinase and Janus kinase (JAK)/signal

transducer and activator of transcription (STAT) cascades (Dairaghi et al. 1998; Wong and Fish 1998).

2.1.1 MCP-1

MCP-1, a member of the CC chemokine superfamily, functions in attracting monocytes (Uguccioni et al. 1995), T lymphocytes (Carr et al. 1994; Loetscher et al. 1994; Roth et al. 1995), basophils (Weber et al. 1995), and B cells (Frade et al. 1997) to sites of inflammation. MCP-1 is expressed by different cell types including monocytes, T lymphocytes, endothelial cells, fibroblasts, and in case of injury by a number of organ tissue cells, such as renal mesangial cells (Rollins et al. 1990; Rovin et al. 1992; Schwarz et al. 1997).
Several studies have shown that MCP-1 plays a major role in the initiation and progression of various forms of nephritis (Anders et al. 2001; Brown et al. 1996; Liu et al. 2003; Radeke et al. 2002; Tesch et al. 1999). In addition the expression of MCP-1 is associated with the pathogenesis of many other chronic inflammatory diseases, e.g. atherosclerosis (Charo and Peters 2003; Ni et al. 2004) and multiple sclerosis (Baggiolini and Loetscher 2000).
The expression of MCP-1 is regulated by cytokines including tumour necrosis factor (TNF) (Murao et al. 2000; Ping et al. 1996), platelet-derived growth factor (PDGF) (Bogdanov et al. 1998; Ping et al. 1999a; Sridhar et al. 1999), interferon-γ (IFN-γ) (Zhou et al. 2001), and interleukin-1β (IL-1β) (Harkness et al. 2003; Lucio-Cazana et al. 2001), but also stress factors and viral infections cause MCP-1 expression (Glabinski et al. 1996; Rott et al. 2003).
Several regulatory promoter regions have been identified that are important for MCP-1 expression. Two nuclear factor-κB binding sites located approximately 2.6 kb from the transcription initiation site appeared to be critical elements for MCP-1 induction in response to IL-1β and TNF-α (Ping et al. 1999b; Ueda et al. 1994). Additionally, within a 150-bp segment located 5' to the ATG translation start codon, two consensus elements for the AP-1 *trans*-acting factors have been described in the human MCP-1 promoter. The more proximal of these consensus AP-1 elements overlaps with a consensus site for SP-1 that appears to be important for the basal transcription activity of the gene (Ueda et al. 1994). Mutation of the SP-1 binding site proved to be critical for regulation by both TNF and PDGF (Ping et al. 1999a). Thus, both disease findings and gene regulatory studies at molecular level point to a considerable pro-inflammatory role of MCP-1. Several therapeutic strategies including neutralizing antibodies and protein antagonists have been employed to reduce MCP-1 activity in nephritis and other inflammatory diseases (Wenzel et al. 1997). These anti-protein/ -receptor strategies as well as inflammatory disease models in MCP-1 gene deficient mice yielded variable and mostly limited success, which in part might be due to an incomplete inhibition of MCP-1 activity (Tesch et al. 1999).

2.1.2 RANTES

The chemokine RANTES (regulated upon activation normal T-cell expressed and secreted; CCL5) is a member of the CC-chemokine family and plays an essential role in inflammation by recruiting T cells, macrophages and eosinophils to inflammatory sites. RANTES has been implicated in a number of diseases characterised by inflammation. These include asthma (Powell et al. 1996), transplantation rejection (Pattison et al. 1994), atherosclerosis (Pattison et al. 1996), rheumatoid arthritis (Rathanaswami et al. 1993), delayed-type hypersensitivity (Devergne et al. 1994), endometriosis (Hornung et al. 1997), chronic polypus sinusitis (Maune et al. 1996) and respiratory syncytial virus-related bronchiolitis (Becker et al. 1997; Saito et al. 1997). RANTES expression is induced by a variety of cells (Olszewska-Pazdrak et al. 1998; Radeke et al. 2002; Shukaliak and Dorovini-Zis 2000). Cytokines produced during acute inflammation induce RANTES expression by fibroblasts and endothelial and epithelial cells. For example, TNF-α and IL-1β increase the expression of RANTES mRNA by fibroblasts and endothelial cells. Furthermore, TNF-α and IFN-γ were shown to induce RANTES production synergistically by epithelial and endothelial cells (Marfaing-Koka et al. 1995; Stellato et al. 1995).

At nanomolar concentrations, RANTES binds to and activates GPCRs, namely the chemokine receptors CCR1, CCR3, and CCR5. Ligation of these receptors activates a heterotrimeric Gαi protein-coupled signalling pathway, characterised by a transient calcium influx (Bacon et al. 1995; Ward et al. 1998), and triggers activation of cell polarisation and chemotaxis (del Pozo et al. 1995). In addition, RANTES also induces several effects that are triggered through a GPCR-independent pathway. Induction of this pathway is mediated by protein tyrosine kinases (PTKs), occurs at high micromolar concentrations of the chemokine, and leads to a sustained influx of calcium (Bacon et al. 1995). This pathway requires an interaction of RANTES with cell surface glycosaminoglycans (GAGs) and depends on the ability of the chemokine to form oligomers (Chang et al. 2002; Czaplewski et al. 1999). Stimulation of the GPCR-independent pathway by RANTES induces hyperpolarisation and generalised cell activation (Appay and Rowland-Jones 2001). A variety of effects is then triggered, such as induction of proliferation, apoptosis, and release of proinflammatory cytokines (Appay et al. 2000).

Studies have demonstrated that the CC-chemokines RANTES, MIP-1α, and MIP-1β suppress human immunodeficiency type 1 (HIV-1) replication *in vitro*. Infection with HIV-1 requires expression of CD4 antigen and the chemokine receptor CXCR4 (X4) or CCR5 (R5) on the surface of target cells. The engagement of these receptors with the viral surface proteins is essential for the membrane fusion process. RANTES, like MIP-1α and MIP-1β, can inhibit the entry of HIV-1 strains that use CCR5 as an entry co-receptor with CD4 (Dragic

et al. 1996). The chemokines inhibit entry of these R5 viruses by down-regulating CCR5 and by competing with the virus for binding sites on the same receptor. But, RANTES can also enhance HIV-1 replication in a dose dependent manner. These characteristics are critically dependent on its ability to self-aggregate and bind to glycosaminoglycans (Roscic-Mrkic et al. 2003).

2.2 Different strategies to modulate gene expression

In addition to drug development methods designed to modulate the activity of protein targets, the knowledge of disease gene DNA sequences provides an opportunity for a highly rational design of therapeutic agents that act at the DNA/RNA level through sequence-specific interactions. Specific interference with gene expression has wide ranging applications in experimental biology and is an attractive approach for the development of new therapeutics. Several gene-specific inhibitory strategies have been established *in vitro* and *in vivo*.

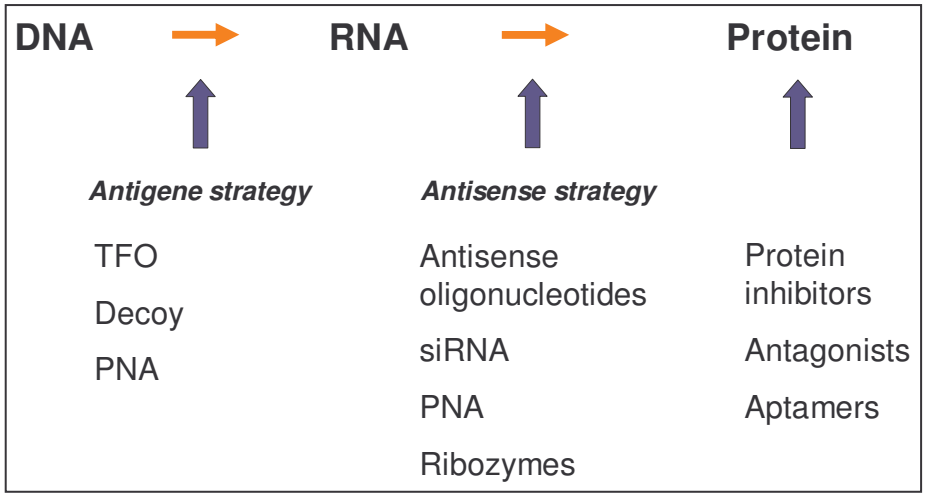

Figure 2-1. Molecular strategies to interfere at the level of gene expression, mRNA or protein activity with a specific factor. Peptide nucleic acid (PNA), triplex helix-forming oligonucleotide (TFO), small interfering RNA (siRNA)

Antisense oligonucleotides

The notion that gene expression could be modified by the use of exogenous nucleic acids derives from studies by Paterson (Paterson et al. 1977), who first used single-stranded DNA to inhibit translation of a complementary mRNA in a cell-free system in 1977. In 1978, Stephenson (Stephenson and Zamecnik 1978) added a synthetic oligonucleotide complementary to the 3' end of the Rous sarcoma virus to the medium of chicken fibroblasts in tissue culture, along with the Rous sarcoma virus itself. The short 13-mer DNA oligonucleotide inhibited the formation of new viruses, and also prevented transformation of chicken fibroblasts into sarcoma cells. In cell-free systems, translation of the viral mRNA was also greatly impaired. The findings showed that antisense oligonucleotides could inhibit mRNA translation in a sequence-specific way.

In the mid 1980s, the existence of naturally occurring RNAs and their role in regulating gene expression was shown (Mizuno et al. 1984; Simons and Kleckner 1983). These observations were important because they stimulated the development of technologies that use nucleic

acids to manipulate gene expression. Since then, various antisense targets, for example in the field of oncology, have been analysed *in vitro* and in animals (Table 2-2).

Table 2-2. Antisense oligonucleotide targets in oncology tested *in vitro* and in animals

Target	Cell type analysed	Biological endpoints	Reference
BCL2	B-cell-lymphoma, melanoma, lung tumour	Apoptosis	(Jansen et al. 1998)
Survivin	Cervical tumour, lung cancer	Apoptosis	(Li et al. 1999; Olie et al. 2000)
MDM2	Multiple tumours	p53 activation	(Wang et al. 1999)
BCLXL	Endothelial cells, lung cancer cells	Apoptosis	(Leech et al. 2000)
RelA	Fibrosarcoma cell line	Cell adhesion, tumourigenicity	(Sharma and Narayanan 1996)
RAS	Endothelial cells, bladder cancer	*CAM* expression, proliferation	(Chen et al. 1996)
RAF	Endothelial cells, smooth muscle cells	*CAM* expression, proliferation	(Cioffi et al. 1997)
BCR-ABL	Primary progenitor bone marrow cells	Adhesion, proliferation	(Mahon et al. 1995)
Jun N-terminal kinase 1 and 2	Renal epithelial cells	Apoptosis	(Cioffi and Monia 2000)
Telomerase	Prostate cell lines	Cell death	(Kondo et al. 2000)
c-MYC	Leukaemia cell lines	Proliferation, apoptosis	(Holt et al. 1988; Wickstrom et al. 1988)
c-MYB	Leukaemia cell lines	Proliferation	(Anfossi et al. 1989)

Adapted from Tamm (Tamm et al. 2001)

Ribozymes and DNAzymes

Another strategy for destabilizing mRNA uses ribozymes or DNAzymes. Ribozymes and DNAzymes are molecules that contain one of a variety of catalytic motifs that cleave the mRNA to which they hybridise and thereby prevent translation. Two ribozymes, the hammerhead ribozyme and the hairpin ribozyme, have been extensively studied owing to their small size and rapid kinetics (Earnshaw and Gait 1997; Shippy et al. 1999). The catalytic motif is surrounded by flanking sequences that are responsible for guiding the ribozyme to its mRNA target and giving stability to the structure. If ribozymes are to work effectively, they not only need to bind to the substrate RNA but also dissociate from the cleavage product to act on further substrates, which might be an important rate limiting step

that controls their usefulness. Ribozymes can be expressed from a vector that offers the advantage of continued intracellular production of these molecules (Irie et al. 1997; Irie et al. 1999).

RNA interference

Double-stranded RNA (dsRNA) can trigger silencing of homologues gene expression by a mechanism termed “RNA interference” (RNAi) (Fire et al. 1998). RNAi is an evolutionary conserved phenomenon and a multistep process that involves the generation of active small interfering RNA (siRNA) *in vivo* through the action of an RNase III endonuclease, “Dicer”. The resulting 21 to 23 nt siRNA mediates degradation of the complementary homologues RNA (Bernstein et al. 2001; Sharp 2001; Zamore 2001). RNAi has been used as a tool to study gene function in multiple model organisms, including plants, *Caenorhabditis elegans*, and *Drosophila*, where dsRNA efficiently induced gene specific silencing (Chuang and Meyerowitz 2000; Misquitta and Paterson 1999; Tuschl et al. 1999). The discovery that synthetic 21nt siRNA triggers gene specific silencing in mammalian cells has further expanded the utility of RNAi into mammalian systems.

Peptide nucleic acid

Peptide nucleic acid (PNA) is a nucleic acid analogue in which the sugar phosphate backbone has been replaced by a synthetic peptide backbone usually formed from N-(2-amino-ethyl)-glycine units, resulting in an achiral and uncharged molecule. It is chemically stable and resistant to hydrolytic cleavage and thus not expected to be degraded inside living cells. PNA is capable of sequence-specific recognition of DNA and RNA obeying the Watson-Crick hydrogen bonding scheme, and the hybrid complexes exhibit extraordinary thermal stability and unique ionic strength effects (Ray and Norden 2000). It may also recognise duplex homopurine sequences of DNA to which it binds by strand invasion, forming a stable PNA-DNA-PNA triplex with a looped-out DNA strand. But, according to the high molecular mass, the delivery of PNA, involving passage through the cell membrane, appears to be critical.

Decoy molecules

Short, double-stranded DNA decoy molecules have also been used to disrupt gene expression at the level of transcription (Kraus et al. 2003; Sharma et al. 1996). These oligonucleotides are designed to compete for transcription factor complexes, with the final aim to distract them from the promoter that they would activate otherwise.

Triple helix-forming oligonucleotides

Normally DNA exists in a duplex form, but under certain circumstances, DNA can acquire triple-helical structures, which are either intra- or intermolecular. Intermolecular triplexes, formed by the addition of a sequence-specific third strand to the duplex DNA, are shown to have an enormous potential as site directed mutagens, repressors of transcription, and inhibitors of replication. These triple helix-forming oligonucleotides (TFOs) bind with high affinity and specificity to homopurine/homopyrimidine sequences in the major groove of the DNA and have proved effective in various gene targeting strategies in living cells and in animals. There are some intrinsic advantages of the antigene over the antisense principle, and interest in oligonucleotides designed to form triple helices with double-stranded DNA is steadily increasing. First, there are only two copies (two alleles) of the targeted gene whereas there may be thousands of copies of a messenger RNA. This should dramatically reduce the amount of oligonucleotide needed for activity. Blocking mRNA translation even by inducing sequence-targeted cleavage of the RNA does not prevent the corresponding gene from being transcribed, thereby repopulating the mRNA pool. Moreover, not only transcriptional activation and deactivation but also gene knockout as well as targeted mutagenesis, targeted recombination and sequence selective manipulation of the genomic DNA can be achieved with the antigene strategy.

2.3 Triple helix formation

2.3.1 Structure and stability of triple helix-forming oligonucleotides

The formation of a triple-helical nucleic acid structure was first observed in 1957 when Felsenfeld et al. demonstrated stable and specific binding of a single-stranded polyuridine oligonucleotide to a polyuridine/polyadenosine duplex. The mechanisms underlying triple helix formation are reasonably well understood (Figure 2-2).

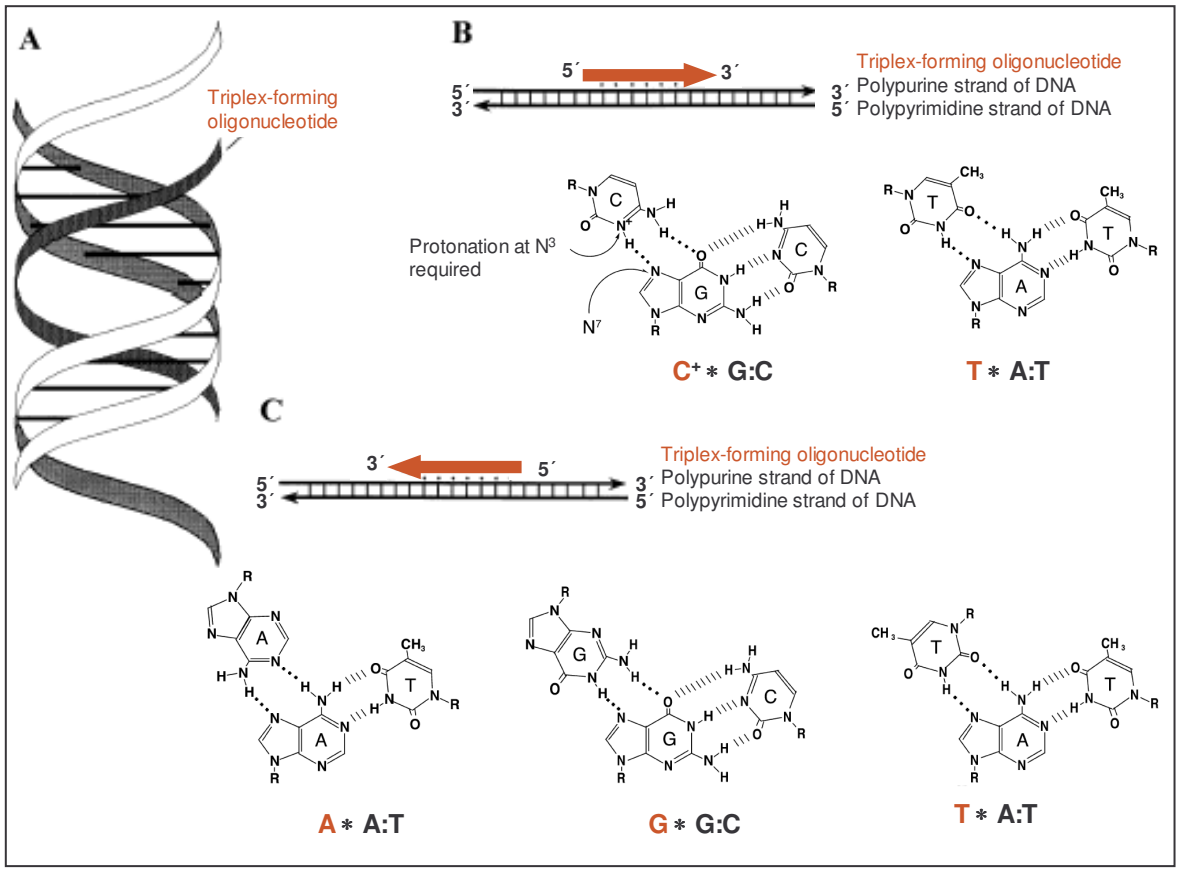

Figure 2-2. Triple-helix formation at the nucleotide level. A: The TFO binds in the major groove of the DNA. **B:** The parallel, pyrimidine binding motif, **C:** The antiparallel, purine binding motif. *Adapted from Chan (Chan and Glazer 1997).*

TFOs specifically bind to the major groove of DNA, forming Hoogsteen or reverse Hoogsteen hydrogen bonds with bases in the purine rich strand of the duplex DNA. Optimal target sequences must harbour 12–14 consecutive purines on one strand (Cheng and Van Dyke 1994) since only purine bases are able to establish two Hoogsteen or reverse Hoogsteen type hydrogen bonds in the major groove of DNA. Two binding motifs have been described: For the pyrimidine motif, a TFO consisting of cytosine (C) and thymine (T) binds with a parallel orientation to the purine strand of DNA via Hoogsteen bonds. Sequence-specificity is mediated by binding of third strand thymines (T) to adenine in A:T base pairs while

protonated cytosines (C^+) bind to guanine in G:C base pairs. Protonation at N^3 of cytosine is required for proper Hoogsteen bonding with N^7 of guanine, therefore mildly acidic conditions are necessary. For the purine binding motif, the TFO binds antiparallel to the purine-rich strand of the DNA via reverse Hoogsteen bonds. In this case triplex formation is mediated by binding of adenine or thymine (A or T) to adenine in A:T base pairs, and guanine (G) to guanine in G:C base pairs. The purine binding motif is largely pH independent.
Both pyrimidine and the purine motifs are stabilised by the presence of divalent cations such as Mg^{2+}, Ca^{2+}, and Zn^{2+} (Felsenfeld et al. 1957) as well as naturally occurring polyamines such as spermine, spermidine, and putrescine (Hampel et al. 1991; Thomas and Thomas 1993). These agents presumably reduce the electrostatic repulsive forces between negatively charged phosphate backbones of the three strands, allowing triplex DNA to form more readily. In general, both polypyrimidine and polypurine TFOs form triplexes efficiently under conditions of high Mg^{2+} ions (10 mM) whereas monovalent cations (Na^+, K^+) at physiological concentrations (140 mM) favour G-quartet formation which competes with triplex formation (Cheng and Van Dyke 1994). Furthermore, formation of both types of triplexes depends on chain length, base composition and temperature (Frank-Kamenetskii and Mirkin 1995).

2.3.2 General modifications which stabilise triplex formation

Various modifications in the sugar-phosphate backbone or the bases, as well as at the 5' and 3' ends of the TFOs, have been introduced to stabilise triplexes and to minimise degradation and increase the half life of these TFOs inside cells and tissues. A generalised approach to improving triplex stability involves coupling non-specific DNA binding agents to TFOs. These agents may improve nuclease resistance and aid in TFO cellular uptake or localisation. Oligonucleotides, when end-conjugated with polyamines such as spermine, also form stable triplexes even in the absence of free polyamines or Mg^{2+} by presumably increasing the effective local polyamine concentration.
Psoralen, a photoreactive intercalating cross-linker, also enhances triplex binding affinity when attached to a TFO. When exposed to long wavelength UV light, psoralen covalently cross-links the triplex strands together, forming mixtures of monoadducts and cross-links (Gunther et al. 1996; Song et al. 2004; Takasugi et al. 1991).
The use of 5-methylcytosine partially alleviates the pH restriction of TFOs in the pyrimidine motif (Lee et al. 1984; Leitner et al. 2000). Cytosine has also been replaced with analogues such as 8-oxoadenine (Jetter and Hobbs 1993; Miller et al. 1996), pseudoisocytidine (Ono et al. 1991), and a 6-keto derivative of 5-methylcytidine (Xiang et al. 1996).

Backbone modifications were performed to optimise triplex stability while keeping sequence-specificity, to minimise self-associations, and furthermore to design oligonucleotides which are resistant towards degradation by cellular nucleases (Figure 2-3).

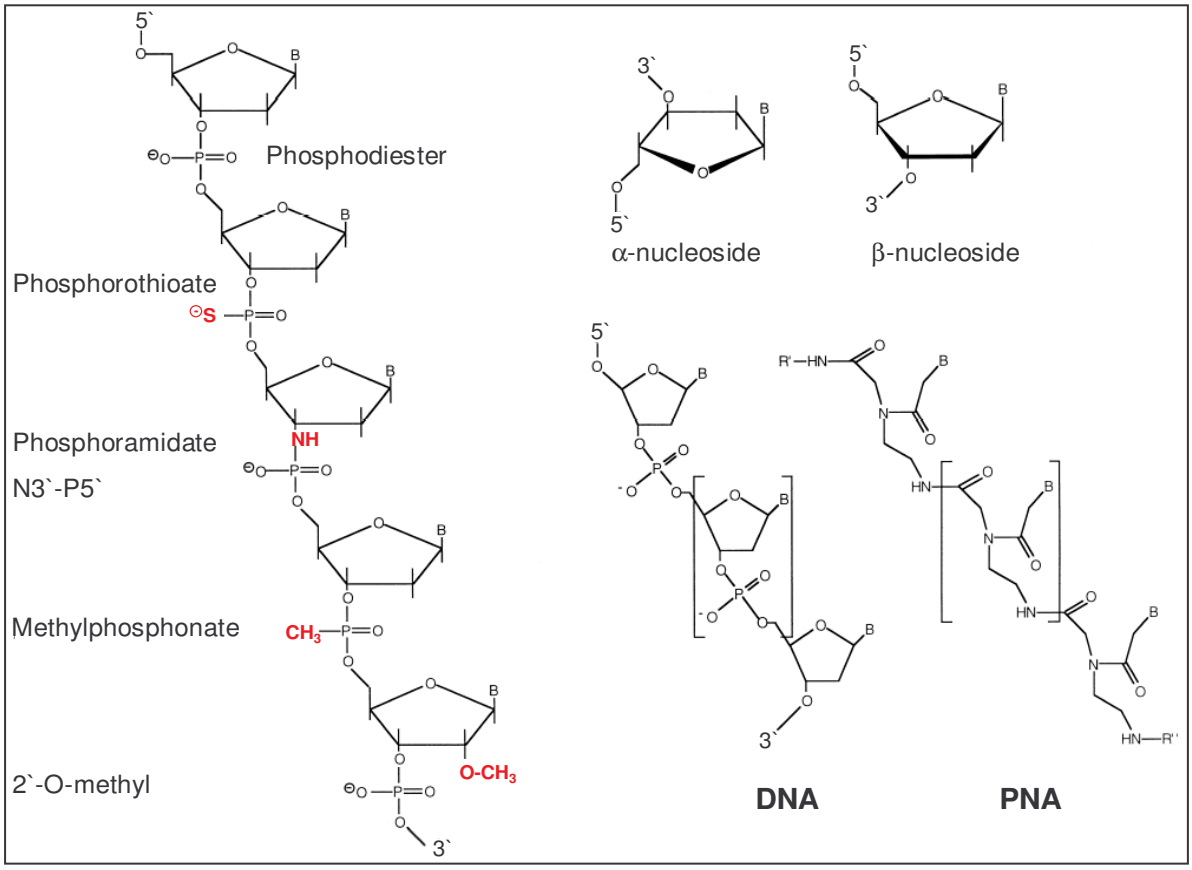

Figure 2-3. Different backbone modifications conferring stability towards intracellular nucleases and used in the antigene strategy. PNA: Peptide nucleic acid. *Adapted from Praseuth (Praseuth et al. 1999).*

Protection of the oligonucleotide against cellular nucleases can be achieved by changing the anomeric configuration of the glycosidic bond from β to α without much incidence on triplex stability (Noonberg et al. 1995b). Another modification was obtained by substitution of deoxyribose for ribose in the third strand of the triplex and this resulted in stabilisation of triple helices for the CU or GU motif with a parallel orientation with respect to the purine target sequence (Escude et al. 1993). The replacement in both purine and pyrimidine TFOs of the phosphate groups with phosphorothioates greatly improves the resistance to nucleases (Cogoi et al. 2001; Joseph et al. 1997). In the pyrimidine motif, the substitution of the phosphodiester linkage with N3'-P5' phosphoramidate linkage in which the 3'-oxygen is substituted with 3'-nitrogen (Escude et al. 1996; Sun et al. 1996; Torigoe 2001) or the substitution of the sugar-phosphate with a morpholino phosphoramidate backbone (Basye et al. 2001) increased significantly the binding to DNA at neutral pH. The substitution of the phosphodiester backbone with methylphosphonate in the pyrimidine motif also increased the half-life and the affinity to the duplex DNA (Cassidy et al. 2000). PNA is a non-ionic nucleic

acid analogue in which the entire sugar-phosphate backbone is replaced by a polyamide backbone to obtain a neutral molecule which minimises unspecific electrostatic interactions with proteins.

2.3.3 Biological activity of TFOs

Accessibility of target sites in the context of chromatin is crucial for the development of the antigene strategy. The first report describing the accessibility of nuclear DNA sequences to an antigene oligonucleotide dealt with a viral HIV-1 sequence in chronically infected cells (Giovannangeli et al. 1997). Triplex formation was detected on one of the two viral polypurine tract sequences present in the integrated HIV-1 proviral genome within cells incubated with a psoralen-modified TFO. Different possibilities of TFOs to interfere with gene expression are shown in Figure 2-4.

Triplex formation induced site-directed mutagenesis and promoted recombination in a site-specific manner (Nagatsugi et al. 2003; Rogers et al. 2002). Triplex-based activity in animals was demonstrated by successfully introducing site-specific genomic modifications in somatic cells of adult mice (Vasquez et al. 2000). Psoralen can form adducts and interstrand crosslinks when it is activated by long wave UV light, and psoralen linked TFOs were used to stimulate homologues recombination in yeast and in mammalian targets and could increase mutation frequencies compared to the control oligonucleotide (Datta et al. 2001; Vasquez et al. 2001b). A psoralen-conjugated TFO designed to bind to a transcription factor in the upstream sequence of the human gamma-globulin gene, mutation frequencies as high as 20% were reported by Xu (Xu et al. 2000).

It has been shown that shorter (10 bp) target sites in a gene can be achieved by using cationic phosphoramidate linkages. *N,N*-diethylethylenediamine and *N,N*-dimethylaminopropylamine phosphodiester TFOs increase the efficiency of targeted mutagenesis by 6-10 fold (Vasquez et al. 2001a). Double strand breaks in the target gene could be induced by TFOs containing radioactive isotopes (Mezhevaya et al. 1999; Panyutin et al. 2001). TFOs containing non-radioactive chemicals have been successfully used to cleave target DNA at specific sites (Arimondo et al. 2001; Nunez et al. 2000). Camptothecin, an antitumour drug, acts by interfering with DNA topoisomerase I. Camptothecin-conjugated TFOs, upon binding to the duplex target DNA, selectively positions the drug at the triplex site where it stimulates topoisomerase I mediated DNA cleavage at this site (Arimondo et al. 2002).

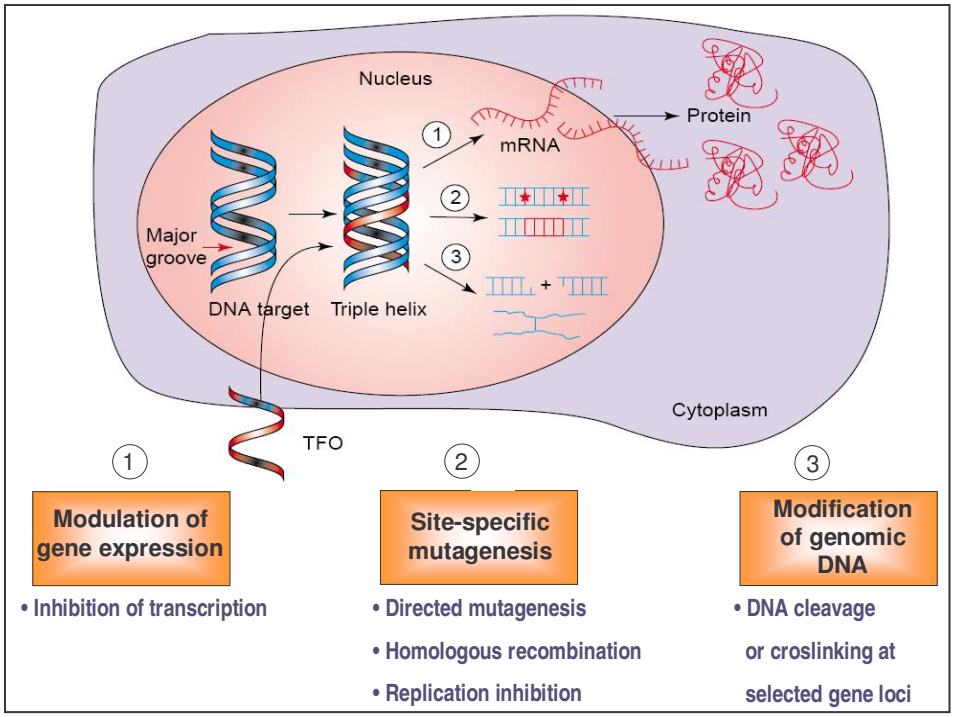

Figure 2-4. Schematic diagram of current oligonucleotide based triplex applications. Triplex DNA can inhibit transcription in two ways. A triplex formed in the regulatory region of a gene can interfere with the formation of the initiation complex, while a triplex formed in the coding region of the target gene can block transcription elongation. Selective modification of the genome includes homologous recombination through triplex delivered donor DNA via DNA repair or site-specific mutagenesis via triplex delivered mutagens like psoralen. Further applications arise from triplex targeted chemical modifications of the gene (e.g. cleavage, site-specific cross-linking or alkylation). *Adapted from Buchini (Buchini and Leumann 2003).*

TFOs can be designed as tools to inhibit gene expression by blocking transcription initiation or elongation. Modulation of transcription by TFOs was described *in vitro* and in cell cultures for several plasmid targets transiently transfected into living cells (Faria et al. 2000; Intody et al. 2000) and for endogenous genes (Carbone et al. 2004). Moreover, it was shown that at a given promoter triplex formation blocked the binding of various transcription factors, including SP-1, thereby inhibiting transcription initiation (Carbone et al. 2003). The triplex mediated antigene approach was used to selectively inhibit a wide array of clinical important genes. Examples include transcriptional inhibition of aldehyde dehydrogenase (Tu et al. 1995), IL-2 receptor (Orson et al. 1991), the human *HER2/neu* gene (Porumb et al. 1996), c-*myc* (Postel et al. 1991; Thomas et al. 1995), and GM-CSF (Kochetkova and Shannon 1996). In Table 2-3, some important examples of TFOs are shown which led to successful inhibition of gene expression inside cells in the range between 40 and 90%. In general, success of transcriptional inhibition might vary depending on the target sequence itself (accessibility, mismatches), TFO delivery, stability of TFO binding, the use of nuclease resistant oligonucleotides, use of stabilizing agents, the binding motif, and other factors.

Table 2-3. Inhibition of transcription in cells using triple helix-forming oligonucleotides

Target	TFO and modification	Control	Biological effect
Human c-myc gene, P2 promoter	Phosphorothioate internucleotide linkages; fluorescein-labelled TFO 23 bp, 1 mismatch	1) scrambled sequence	50 % inhibition of c-myc expression (10 µM TFO) in Northern and Western blots 80 % growth inhibition (10 µM TFO) (McGuffie et al. 2000)
Human c-myc gene	3'-amino-modified phosphodiester TFO -target 1: 27 bp, 3 mismatches -target 2: 23 bp, 1 mismatch -target 3: 25 bp, 3 mismatches -target 4: 21 bp 3 mismatches	2 controls: length and base composition similar to the TFOs but different in nucleotide sequence	Inhibition of c-myc expression and proliferation in CEM cells (sequence and target specific) 50 % reduction of mRNA expression (20 µM TFO), (Catapano et al. 2000)
Human MCP-1 promoter	Phosphorothioate oligonucleotide 19 bp GT, 1 mismatch	Scrambled oligonucleotide	40-45 % inhibition of MCP-1 gene expression (5 µM TFO) (Marchand et al. 2000)
alpha 1(I) procollagen	Phosphodiester and phosphorothioate oligonucleotides Rat C1 region 30 bp Human C1 region 30 bp, 1 mismatch Human C2 region 25 bp, 8 mismatches	Control for human C1 region was a TFO to human C2 region	TFOs specific for human C1 inhibited transcription from human promoter both in vitro in HeLa cell nuclear extracts and in vivo in cultured chicken embryo fibroblasts Triplex formation of human C2 TFO: very inefficiently and at extremely high concentrations (Nakanishi et al. 1998)
Human bcl-2 proto-oncogene	Phosphorothioated at its 5'- and 3'- ends and amino-linked at its 3'- end, 18 bp GT or GA, 1 mismatch	3 different controls 1) inverted 2) scrambled 3) targeted to another sequence (bcl-2 promoter P2)	Downregulation of bcl-2 expression and inhibition of transcription elongation (Shen et al. 2001)
Human rhodopsin	2 psoralen-modified TFOs TFO2: 18 bp GA, 1 mismatch TFO9: 28 bp GA, 2 mismatches	1) Mutated TFO binding site to confirm that the effects of TFOs are mediated through triplex formation 2) Control oligonucleotide which is targeted to another sequence	Each TFO reduced rhodopsin-GFP expression by 70-80 %, treatment with both TFOs reduced expression by 90 % (Intody et al. 2000)

HIV-1 polypurine tract	Oligonucleotide analogues with N3'-P5'np linkages acridine and psoralen-5'modified oligonucleotides 15 bp TCG,	2 control oligonucleotides	Sequence-specific inhibition of transcription elongation in cell cultures 50 % inhibition of luciferase activity (0,5 µM Acr-15 TCG) (Faria et al. 2000)
Insulin-like growth factor type 1 receptor (IGF-IR)	AG-RNA TFO IGF-IR: 24 bp, stable transfection	Control vectors: 1) CT-insert 2) without insert 3) untransfected cells	Suppression of IGF-IR transcription, Inhibition of tumour growth in nude mice (80 %) Downregulation of IGF-I transcription, upregulation of nexin-I mRNA (Rininsland et al. 1997)
GM-CSF	Phosphodiester TFO 15 bp GT, 1 mismatch	15 bp GT, different base composition	Reduction of endogenous GM-CSF level (70 %) 65 % inhibition of the luciferase reporter gene activity (Kochetkova and Shannon 1996)
c-myc P1 promoter	Phosphodiester TFO 27 bp GAT, 3 mismatches	27 bp CTA, scrambled	-The TFO (without chemical modification) can enter the nucleus of HeLa cells and remains intact for 4 h -TFO treatment: 10-fold reduction of P1 c-myc steady state mRNA in Hela cells (Postel et al. 1991)
Rat alpha 1(I) collagen promoter	Phosphodiester and phosphorothioate oligonucleotides, parallel and antiparallel orientation C-1 region: 30 bp GA different 18 bp GA C-2 region: 30 bp GA(CT), 8 mismatches 18 bp GA(T)	18 bp ATGC scrambled	Inhibition of collagen promoter activity in HeLa cells: 18 bp phosphorothioate TFOs resulted in a significant decrease in promoter activity (up to 80 % reduction in CAT activity) (Joseph et al. 1997)
Human bcl-1	Phosphodiester and phosphorothioate oligonucleotides, 18 bp GT, 3 mismatches	1) 18 bp GT in parallel orientation 2) Control plasmid with different promoter target sequence	Luciferase activity: 60 % inhibition (10 µM TFO) (Kim and Miller 1998)
IL-2R alpha	Psoralen conjugated oligonucleotide 15 bp TC	Plasmid with mutated target sequence	70% inhibition of transcription in vitro and in vivo (20 µM TFO) (Grigoriev et al. 1992)

The examples of antigene strategies indicate that TFOs constitute a new class of molecules potentially useful in therapy. However, there are some limitations to oligonucleotide based technology, and in order to use these compounds in clinical applications their delivery to the cells must be improved, as the oligonucleotides have to be delivered to cells in adequate concentrations and they need to be stable in the extracellular and intracellular environments.

Despite any modifications they must be able to bind to their target DNA with high affinity. For some applications high nuclear concentrations must be maintained, and lastly, TFOs must not be immunogenic, even when bound to carrier proteins.

To circumvent the limits on the use of TFOs due to nuclease degradation and delivery to target cells, one possible solution is to generate TFOs endogenously in the target cell by specific recombinant expression vectors. Different strategies have been followed to generate single-stranded DNA (Datta and Glazer 2001) or RNA (Ilves et al. 1996; Noonberg et al. 1994a) inside cells which may bind to the duplex DNA in a triplex mediated way. RNA oligonucleotides can also form triple helices with duplex DNA, and triplexes formed by CU motif TFOs are generally more stable than those formed by their CT motif counterparts (Bates et al. 2002; Han and Dervan 1994; Roberts and Crothers 1992). The data about binding of a purine oligoribonucleotides (GA or GU) to the duplex DNA are controversial. There are studies which exclude the possibility that purine oligoribonucleotides form triplex structures with duplex DNA as determined by electrophoretic mobility shift assays (Semerad and Maher, III 1994). On the other hand, there are positive examples of RNA third stands to form triplexes in the purine binding motif (Cogoi et al. 2000; Ririe and Guntaka 1998), suggesting that the stability of RNA GA and GU motif triplexes are more dependent on the sequence itself.

2.3.4 The intracellular generation of TFOs

Appropriate DNA vectors can be constructed to generate RNA transcripts inside the cell nucleus which allows triplex formation on the targeted DNA sequence. Rininsland (Rininsland et al. 1997) described the specific suppression of the insulin like growth factor type I receptor (IGF-IR) in rat C6 glioblastoma cells and tumour growth in nude mice by using a plasmid-encoded homopurine (AG) RNA effector sequence. Only the RNA containing the homopurine sequence was shown to suppress IGF-IR, whereas a homopyrimidine RNA sequence had no effect.

Noonberg (Noonberg et al. 1994a) constructed a recombinant expression vector containing a promoter, capping, and termination sequences from the human small nuclear U6 gene, surrounding a synthetic sequence incorporating the TFO of interest. *In vivo*, these oligonucleotides were produced constitutively and without cell type specificity at levels up to 5×10^6 copies per cell. The oligonucleotides had an intracellular half life of approximately one hour and were still readily detectable 7 days post-transfection.

Cogoi (Cogoi et al. 2000) demonstrated triplex formation using CU-, GU- as well as GA-oligoribonucleotides targeted against the promoter of the murine c-Ki-*ras* gene. These

oligoribonucleotides led to 38, 40 and 47% inhibition of c-Ki-*ras* promoter activity, respectively, when generated in HEK 293 cells in comparison to a control sequence.
As homopurine RNA may not always form sufficiently stable triplexes with duplex DNA, it has been proposed to use vectors capable to generate single-stranded DNA (Chen et al. 2000). They designed a vector set that directed the *in vivo* production of single-stranded DNA of a desired target sequence. One plasmid was designed to express the Moloney murine leukemia virus (MoMuLV) reverse transcriptase. Another expression plasmid contained the MoMuLV primer binding site at the 3'-end of its RNA transcript so that a single-stranded DNA would be synthesised by the reverse transcriptase when both plasmids were co-transfected into cells. In principle, this single-stranded DNA expression system can generate any sequence of interest *in vivo* for antisense, RNA-cleavage, DNA enzyme, or triplex-forming strategies and represents a promising alternative to extracellular added oligonucleotides.
The synthesis of TFOs *in vivo* circumvents the problem of delivery and could become a powerful tool for triplex applications, but for its successful employment in therapy vectors still need to be optimised.

2.3.5 A TFO targeting the human MCP-1 promoter

A computer search was conducted to identify potential triple helix-forming target sites within the promoter of the human MCP-1- gene. Sequences were scanned for motifs consisting of a continuous stretch of at last 15 purine bases in one strand, with no more than one mismatch. One possible 19 bp TFO target site was identified in the promoter region at bp -66 to -48. The target site in the promoter includes the binding site for SP-1 and partially overlaps a putative AP-1 binding site (Figure 2-5).

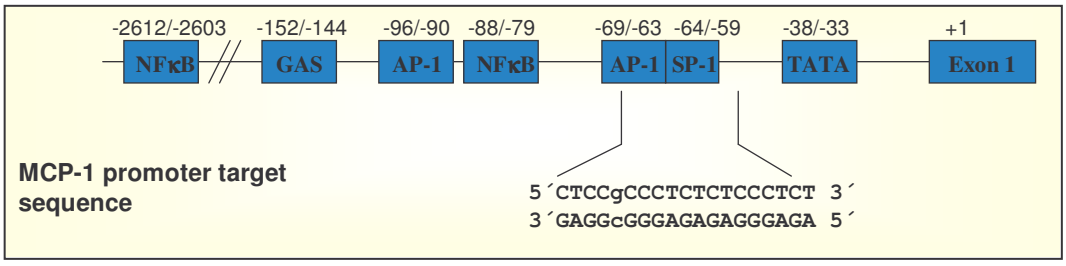

Figure 2-5. Structure of the human MCP-1 promoter and TFO target sequence. The proximal promoter region of the human MCP-1 gene contains putative binding sites for the transcription factors NF-κB, AP-1, GAS, and SP-1 as well as a TATA box. Position +1 corresponds to the major transcriptional start site, as described by Ueda (Ueda et al. 1994). The 19 bp target sequence for the TFO is indicated, a point of mismatch is shown by small capital letters.

Previously it was demonstrated in Prof. Radeke's lab (Medical School Hannover) that a 19 nt purine TFO binding in an antiparallel orientation to the human MCP-1 promoter formed a sequence-specific triplex with the target DNA *in vitro* and blocked *in vitro* binding of nuclear extract proteins and recombinant SP-1 to the promoter DNA. When HEK 293 cells were treated with the TFO, MCP-1 expression gene expression was inhibited by 40-45% in comparison to a control oligonucleotide, as analysed by Northern blots and ELISA (Marchand et al. 2000).

2.3.6 A TFO targeting the murine RANTES

It has been demonstrated that the RANTES promoter contains a large number of potential consensus elements for transcription factors. The murine RANTES promoter contains a single interferon regulatory factor (IRF) and three putative NF-κB binding sites, each of which is well conserved in the human RANTES promoter. Interactions between NF-κB and IRF are crucial for the induction of RANTES promoter activity (Lee et al. 2000). Both NF-κB and IRF transcription factors participate in the induction of the RANTES promoter in response to TNF-α and IFN-γ.

In the RANTES promoter a possible 28 bp TFO target site is located from -265 to -238 relative to the transcriptional start site and about 78 bp downstream to a putative NF-κB1 binding site. This homopurine/homopyrimidine target sequence of 28 bp in length was chosen as a proinflammatory chemokine of interest out of a high number of possible TFO targets in the mammalian genome, which have been found with a proprietary gene bank search algorithm (Radeke HH & Bruno B, unpublished data). The sequence contains no mismatch and a G-content of 78%. In the following study a TFO was designed targeting the RANTES promoter sequence, and it was analysed whether RANTES gene expression could be inhibited using this TFO.

2.4 Design of lentiviral vectors

Lentiviral vectors derived from human immunodeficiency virus (HIV) are highly efficient vehicles for *in vivo* gene delivery, and they have been strongly developed in design, in biosafety and in their ability of transgene expression inside target cells.

Lentiviruses are a family of complex retroviruses inducing chronic and progressive disease typically associated with infection of macrophages. Gene transfer vectors were derived from lentiviruses to complement the successful features of previously developed retroviral vectors - efficient integration in the chromatin, absence of viral genes from the genetic information transferred to the recipient - with the ability to infect non-dividing cells.

The design of viral vectors is based on the separation of cis-acting sequences required for the transfer of the viral genome to the target cell from trans-acting sequences encoding the viral proteins (Mann et al. 1983; Miller et al. 1993). In addition to the structural genes (gag, pol, and env) common to all retroviruses, lentiviruses also contain two essential regulatory (tat and rev) and several accessory genes involved in the modulation of viral gene expression, assembly of viral particles, and structural and functional alterations in the infected cells. The lentivirus replication is partially mediated by cis-acting viral sequences, which do not encode proteins. The trans-acting sequences encode structural, regulatory, and accessory proteins and are included in the packaging construct. Most cis-acting sequences are essential for lentivirus functioning and are usually included in the transfer construct, which is the part of the lentivirus which integrates in the host cell genome and encodes the gene of interest. Both types of constructs are introduced in the same cell to produce vector particles. As the particles can only encapsidate and transfer the vector construct, the infection process is limited to a single round, the transduction. Since the early steps do not depend on viral protein synthesis, all trans-acting genes can be excluded from the transfer construct that encodes only the gene of interest. The required trans-acting sequences are provided by the packaging construct. The efficiency and biosafety of a vector depends on the extent to which segregation of cis- and trans-acting functions of the viral genome is achieved.

Lentiviral vectors were originally designed as replication-defective, hybrid viral particles made from the core proteins and enzymes of HIV-1, and the envelope of a different virus, most often the vesicular stomatitis virus (VSV) (Akkina et al. 1996; Naldini et al. 1996; Reiser et al. 1996). The packaging functions are provided by at least two separate expression plasmids that use transcriptional signals unrelated to those of the virus. One or more core packaging constructs, derived from the lentiviral genome, express the viral proteins but not the env gene that has been deleted. A separate construct expresses a heterologous envelope that is incorporated into the vector particles (pseudotyping) and allows entry into a wide spectrum of target cells (Naldini 1998).

In order to be considered for clinical applications, lentiviral vectors must comply with the strictest safety standards. It is theoretically possible that multiple recombination events join the viral cis-acting sequences in the transfer vector to trans-acting viral genes in packaging constructs to generate replication competent recombinants (RCR). While the use of a heterologous envelope makes the generation of a wild-type lentivirus impossible, contamination of a vector batch by such an RCR may represent a hazard to the recipient. A strategy to improve vector biosafety is to eliminate all the viral genes that are not essential for gene transfer from the packaging constructs. In the first generation packaging construct, all the genes encoding structural and accessory proteins of HIV-1 except for the envelope are maintained. In the second generation packaging construct, all the accessory genes have been deleted. In the third generation packaging construct, the sequences encoding the tat and rev protein have also been eliminated. Tat acts as a transcriptional activator, and it plays an important role in the exceedingly high replication rates that characterise HIV-induced disease. Rev inhibits formation of early regulatory mRNAs and, conversely, promotes the cytoplasmatic export of late viral transcripts expressing the viral structural proteins (gag, pol, and env). As rev is required for expression of the gag and pol genes, recombinants between the packaging and transfer vectors would be non-functional outside vector producer cells (Follenzi and Naldini 2002).

The biosafety of lentiviral vectors is also improved by generating self-inactivating transfer (SIN) vectors (Bukovsky et al. 1999; Iwakuma et al. 1999; Miyoshi et al. 1998; Zufferey et al. 1998). The SIN transfer vector carries a large deletion in the U3 region of the 3' long terminal repeat (LTR) completely inactivating its promoter and enhancer activity. This deletion is duplicated upstream of the vector upon transduction into target cells, thus inactivating both LTRs. The 5' LTR was also modified by substituting the U3 region with a strong constitutive promoter derived from the rous sarcoma virus (RSV) to abolish tat dependence of transcription in vector-producer cells. An improved SIN vector contains the central polypurine tract (cPPT) sequence from the HIV-1 pol gene inserted in front of the internal promoter to improve gene transfer performance (Follenzi et al. 2000; Zennou et al. 2000), and the post-transcriptional regulatory element of the woodchuck hepatitis virus (WPRE) positioned after the transgene to enhance its expression (Deglon et al. 2000; Farson et al. 2001; Zufferey et al. 1999).

Combining a self-inactivating transfer vector with a packaging system of the third generation, it is now possible to achieve a high level of predicted biosafety, theoretically superior to that of retroviral vectors currently in clinical use, and possible acceptable for clinical experimentation.

In the following work the transfer vector pHR'SIN-cPPT-SEW ("SEW") is used which was kindly provided by Dr. M. Grez, Georg-Speyer-Haus, Frankfurt, and is described in detail by

Demaison (Demaison et al. 2002). Here, the internal CMW promoter was replaced by the U3 part of the spleen focus forming virus (SFFV) strain P long terminal repeat sequence (3'LTR SFFV). The incorporation of the HIV cPPT and termination sequence in the lentiviral vector facilitates reverse transcription, nuclear entry, and transduction. It had also been suggested that the cPPT element could enhance gene expression (Figure 2-6).

Figure 2-6. Schematic representation of the lentiviral transfer vector pHR'SIN-cPPT-SEW. Abbreviations: Long terminal repeats (LTR), central polypurine tract (cPPT), spleen focus forming virus (SFFV), enhanced green fluorescent protein (eGFP), post-transcriptional regulatory element of the woodchuck hepatitis virus (WPRE).

2.5 Tasks

The chemokine system has emerged as a central player in human health and disease. Whereas normal chemokine expression is necessary for host defence, inappropriate or exaggerated activation of these genes are a threat to health. One of the major chemokines produced during glomerulonephritis and several other inflammatory diseases is MCP-1, and the modulation of MCP-1 activity and/or expression may be a promising therapeutic strategy for nephritis and possible other inflammatory diseases.

The potential of triple helix-forming oligonucleotides (TFOs) to selectively inhibit expression of target genes is of great interest for gene therapeutic strategies. RNA oligonucleotides that bind homopurine/homopyrimidine DNA sequences by forming triple-helices can be rationally designed, but intracellular delivery of TFOs needs improvement.

The central goal of this study was the establishment of on optimised method for TFO delivery, using expression vectors which generate RNA transcripts that are capable of triplex formation.

The study is divided into four parts:

1. Validation of triplex formation *in vitro*

Two TFO target sequences were found in the human MCP-1 promoter and the mouse RANTES promoter. Triplex formation should be examined *in vitro* via gel mobility shift assays and following, the capacity of extracellular added TFOs to inhibit gene expression was analysed in different cell systems.

2. *In vivo* synthesis of TFOs

To improve TFO delivery and to make the TFO application a powerful gene-therapeutic tool, a system for the *in vivo* synthesis of TFOs should be established. First, specific binding of the RNA CU-TFO to the MCP-1 promoter fragment had to be verified *in vitro* in comparison to unrelated control oligoribonucleotides. To generate RNA-TFOs targeting the human MCP-1 *in vivo*, an expression vector was cloned which directed transcription of either a 19 nt triplex-forming CU-TFO sequence or two different 19 nt GU- or CA-control sequences. These sequences were transcribed together with the RNA of a hygromycin resistance gene as one fusion transcript. The inhibitory effects of the vector-derived CU-TFO on endogenous MCP-1 gene expression should be analysed in stable transfected HEK 293 cells. A set of control experiments had to be established to rule out unspecific binding of the TFO to the target sequence, including control and target sequences with single mismatches, RT-PCR using nuclear and total RNA containing the cytosolic fraction, and a novel magnetic capture technique to show binding of the fusion transcript to its MCP-1 target sequence.

3. siRNA technique

In addition to the TFOs the siRNA technique was tested to inhibit the expression of proinflammatory chemokines MCP-1 and RANTES, as there is no siRNA sequence described in the literature for these two chemokines till now. Here, different strategies were followed. Experiments were performed using vector-derived siRNAs; therefore several expression vectors (pSUPER) had to be cloned. On the other hand, transient transfections were performed using synthetic siRNAs to suppress translation of the gene of interest.

4. Production of lentiviral vectors

Gene therapy approaches rely on efficient transfer of genes to the desired target cells. A wide variety of viral and nonviral vectors have been developed and evaluated for their efficiency of transduction, sustained expression of the transgene, and safety. Among them, lentiviruses have been widely used for gene therapy applications.

Here, the cloning of the lentiviral transfer vector SEW, the production of lentiviral particles by transient transfection, determination of the viral titre, and the transduction of T helper 1 cells were performed.

In the future it should be possible to generate lentiviral vector-derived TFOs, which then could be easily tested in variety of cell lines or animal models.

3 Materials and Methods

3.1 Molecular biological methods

3.1.1 Isolation of nucleic acids

Table 3-1. Materials nucleic acids

Gibco RBL, Life Technologies, Eggenstein	Phosphate buffered saline (PBS)
Invitrogen GmbH, Karlsruhe	Trizol reagent
Qiagen GmbH, Hilden	Qiafilter Maxiprep Kit Qiafilter Maxiprep Kit, endotoxin-free Qiaprep spin Miniprep Kit
Sigma-Aldrich Chemie GmbH, Deisenhofen	DEPC, 0.1% (v/v) DEPC in Millipore H_2O, autoclaved Nonidet P-40

3.1.1.1 RNA isolation of eukaryotic cells

Isolation of total RNA was performed using Trizol reagent according to the supplier's protocol. Cells grown in a monolayer were washed twice with PBS and lysed directly in the culture dish with 1ml Trizol reagent per 10 cm^2. Cells grown in suspension were pelleted by centrifugation, washed once with PBS and lysed in 1 ml Trizol reagent per 10 x 10^6 cells. RNA was redissolved in RNase free water and stored at -20°C or -80°C. RNA quality was checked on a denaturing agarose gel, showing two predominant ribosomal RNA bands at ~5 kb (28S) and at ~2 kb (18S), and low molecular weight RNA between 0.1 and 0.3 kb (tRNA, 5S).

3.1.1.2 Ethanol precipitation of nucleic acids

TE buffer: 10 mM Tris/HCl, pH 8.0
1 mM Na_2EDTA

DNA or RNA from dilute, aqueous solutions can be precipitated by the addition of monovalent cations and ethanol. 2.5 volumes of ice-cold 95% ethanol and 0.1 volume of 3 M sodium acetate (pH 5.2) were added to the nucleic acid solution, mixed, and incubated at -20°C at least for 1 h. Following centrifugation for 30 min at 12,000 x *g*, 4°C, the supernatant was carefully discarded. The pellet was washed once with 70% ethanol to remove remaining salt and centrifuged for additional 10 min at 12,000 x *g*, 4°C (Sigma 3K30 Laboratory Centrihuges). The DNA or RNA precipitate was briefly air dried and dissolved in sterile H_2O (RNase-free) or TE buffer.

3.1.1.3 Quantification of nucleic acids

Determination of DNA or RNA concentration was done by spectrophotometry at 260 nm (GeneQuant *Pro* RNA/DNA calculator, Amersham Pharmacia Biotech, Freiburg). Nucleic acids absorb UV light of 250 to 270 nm wavelength, with a maximum at 260 nm. The reading at 260 nm allows calculation of the concentration of nucleic acid in the sample. The absorbance of 1 unit at 260 nm (A_{260}) corresponds to approximately 50 µg/ml for double-stranded DNA and 40 µg/ml for single-stranded DNA and RNA. The ratio between the readings at 260 nm and 280 nm provides an estimate for the purity of the nucleic acid. Pure preparations of DNA and RNA have ratios of 1.8 and 1.95, respectively.

3.1.1.4 Isolation of nuclei and extraction of RNA

NP-40 lysis buffer:	10 mM Tris/HCl, pH 7.4
	10 mM NaCl
	3 mM $MgCl_2$
	0.5% (v/v) Nonidet P-40
Glycerol storage buffer:	50 mM Tris/HCl, pH 8.3
	40% (v/v) glycerol
	5 mM $MgCl_2$
	0.1 mM EDTA

For cultures of adherent cells (~5 x 10^7 cells): The medium was removed from monolayer cultures and the cells were placed on ice. Cells were washed twice and scraped into ice-cold PBS and pelleted by centrifugation at 500 x *g* for 5 min, 4° C (Hermle Labortechnik GmbH, Wehingen). The cell pellet was loosened by gently vortexing 5 sec, and 4 ml NP-40 lysis buffer were added, continuing to vortex as buffer was added, followed by incubation for 5 min on ice. After complete lysis, nuclei were pelleted by centrifugation at 500 x *g* for 5 min, 4° C. The nuclear pellet was resuspended in 4 ml NP-40 lysis buffer as described, the nuclei were pelleted by centrifugation again and the supernatant was discarded. Nuclei were resuspended in 100 to 200 µl glycerol storage buffer and frozen and stored in liquid nitrogen up to one year. RNA was isolated using Trizol reagent according to the manufacturer's instructions.

3.1.1.5 Isolation of plasmid DNA

The alkaline/SDS lysis describes the lysis of bacterial cells by a NaOH/SDS solution. Chromosomal and plasmid DNA are denatured under these alkaline conditions. Addition of potassium acetate results in a precipitate containing chromosomal DNA and other cellular compounds, while plasmid DNA stays in solution and reanneals to its supercoiled structure.

Purification of plasmids from E.coli overnight cultures containing the appropriate antibiotics were routinely performed using the QIAprep spin Miniprep or Maxiprep according to the manufacturer's protocol. Plasmids for transfection of eukaryotic cells were purified under endotoxin free conditions. Plasmid DNA was eluted in H_2O or TE buffer and stored at -20°C.

3.1.2 Gel electrophoresis

Table 3-2. Materials electrophoresis

AppliChem GmbH, Darmstadt	Acrylamide 30%
Carl Roth GmbH, Karlsruhe	Agarose APS Ethidium bromide MOPS TEMED
Invitrogen GmbH, Karlsruhe	50 bp DNA marker
MBI Fermentas, St. Leon-Roth	6 x DNA loading buffer 2 x RNA loading buffer
New England BioLabs, Beverly MA	X174 DNA *Hae*III Digest
Promega GmbH, Mannheim	RNA marker

Gel electrophoresis allows separation and identification of nucleic acids based on charge migration. Migration of nucleic acid molecules in an electric field is determined by size and conformation, allowing nucleic fragments of different sizes to be separated. Agarose gel analysis is the most commonly used method for analyzing DNA fragments between 0.1 and 25 kb. The concentration of agarose (usually 0.7-1.5%) used for the gel depends primarily on the size of the DNA fragments to be analyzed.

Ethidium bromide was included in the gel matrix to enable fluorescent visualisation of the DNA fragments under UV light. Agarose gels were submerged in electrophoresis buffer in a horizontal electrophoresis apparatus (Sub Cell Gel Electrophoresis Systems, BioRad).

3.1.2.1 Analytical DNA gels

50 x TAE buffer	2 M Tris·acetate 50 mM EDTA, pH 8.0

The amount of agarose depending on the concentration required was added to the appropriate volume of 1 x TAE buffer in a bottle and heated in a microwave until the agarose dissolved. Reduced volume of liquid was made up to the original volume with distilled water to ensure correct agarose and buffer concentrations. The cooled agarose (55-60°C) was mixed with 1 µl of ethidium bromide (1 µl per 30 ml agarose) and poured onto the gel tray (BioRad) to a thickness of 3-5 mm. A comb was inserted into the gel immediately after

pouring the gel, and the gel was left to set for 20 min. Following, the comb was removed and the tank containing the gel was filled with 1 x TAE buffer. For DNA sample preparation, 1 volume of 6 x DNA loading buffer was mixed with 5 volumes of DNA solution, the samples were applied to the wells of the gel and a molecular-weight marker was included to enable analysis of DNA fragment sizes in the samples. Electrodes were connected so that the DNA would migrate towards the anode. The gel was run at 1-10 V/cm until the dyes have migrated an appropriate distance.
Ethidium bromide–DNA complexes display increased fluorescence compared to the dye in solution. Illumination of a stained gel under UV light (254–366 nm) allows bands of DNA to be visualised against a background of unbound dye.

3.1.2.2 Polyacrylamide gels

Polyacrylamide gel (12.5%)	5.8 ml H_2O
	4 ml acrylamide (30%)
	0.2 ml 50 x TAE
	4 µl TEMED
	100 µl 10% APS

Polyacrylamide gels were chosen for small DNA fragments or electrophoretic mobility gel shift assays (EMSA). Electrophoresis was performed in a mini vertical electrophoresis system (BioRad).

3.1.2.3 Denaturing RNA gels

10 x MOPS buffer	200 mM MOPS
	50 mM sodium acetate
	10 mM EDTA, pH 7.0
1 x FA gel buffer (1 l)	100 ml 10 x MOPS buffer
	20 ml 37% formaldehyde
	880 ml RNase-free water

The integrity and size distribution of total RNA can be checked by denaturing agarose gel electrophoresis and ethidium bromide staining. The respective ribosomal bands should appear as sharp bands on the stained gel. Unlike DNA, RNA has a high degree of secondary structure, making it necessary to use a denaturing gel. Formaldehyde in the gel disrupts secondary RNA structure so that RNA molecules can be separated by their charge migration. To prepare a gel of 15 x 15 cm, 1.5 g of agarose was mixed with 15 ml of 10 x MOPS buffer and 132.3 ml RNase-free water. The agarose was dissolved by heating in a microwave and

cooled to 65-70°C in a water bath. After cooling, 2.7 ml of 37% formaldehyde and 1.5 µl of ethidium bromide were added. The agarose was poured onto the gel tray and the comb was inserted. Prior to running, the gel was equilibrated in 1 x FA gel buffer for at least 30 min. For RNA sample preparation, 1 volume of RNA was mixed with 1 volume of 2 x RNA loading buffer, denatured for 10 min at 65°C, and chilled on ice. For each run an appropriate RNA weight marker was included. The gel was run at 5 V/cm until the bromophenol blue dye has migrated approximately 2/3 through the gel. For longer runs overnight, electrophoresis was performed at 4°C at 0.75 V/cm, optimal with re-circulating the electrophoresis buffer.

3.1.3 PCR

Table 3-3. Materials PCR and RT-PCR

Invitrogen GmbH, Karlsruhe	0.1 M DTT 10 mM dNTP-Mix 50 mM $MgCl_2$ Oligo $(dT)_n$ *Pfx* polymerase (2.5 U/µl) + buffer Random Hexamers RNase Out (40 U/µl) *Taq* polymerase (5 U/µl) + buffer ThermoScript RT-PCR System

Table 3-4. Primers (Qiagen, Hilden)

Primer	**SEQUENCES 5'- 3'**
T3rev	5'GCTACGTAATTAACCCTCACTAAAG
T7for	5'GCTACGTAAATACGACTCACTATAG
RANTES35for	5'GTACCA TGAAGATCTCTGC
RANTES465rev-r	5'AGAGCCGGTCGGAGCGGAT
MCP-1 104for	5'GCTCATAGCAGCCACCTTC
MCP-1 608rev-r	5'GGTAGAACTGTGGTTCAAG
fw_TVHygro	5'AGCAGAGCTCTCTGGCTAA
rev_TVHygro	5'TCGGCGAGTACTTCTACAC
pcDNA31/Hygro1_fw	5'TCTCCCTCTCTCCCACCTC
pcDNA31/Hygro2_fw	5'GAGGTGGGAGAGAGGGAGA
pcDNA31/Hygro3_fw	5'CTCTCTCCCTTCCTCTCCC
pcDNA31/Hygro4_rev	5'TCACGCCATGTAGTGTAT
pcDNA31/Hygro5_fw	5'GTGGTGGGTGTGTGGGTGT
pcDNA31/Hygro6_fw	5'CACACACCCAACCACACCC
pGL3_for	5'AGAGATACGCCCTGGTTCCT
pGL3_rev	5'AGACCAGTAGATCCAGAGGA
pGL3_for II	5'AAGCTTTCCTGCTTGACTCC

Polymerase chain reaction (PCR) is an *in vitro* method for enzymatically synthesizing defined sequences of DNA. The reaction uses two oligonucleotide primers that hybridise to opposite strands and flank the target DNA sequence that is to be amplified. The elongation of the primers is catalyzed by a heat-stable DNA polymerase (such as *Taq* DNA polymerase). A repetitive series of cycles involving template denaturation, primer annealing, and extension of the annealed primers by the polymerase results in exponential accumulation of a specific DNA fragment. The ends of the fragment are defined by the 5' ends of the primers. Prerequisites for successful PCR include the design of optimal primer pairs, the use of appropriate primer concentrations, and optimisation of the PCR conditions.
Routinely, the PCR was performed in a total volume of 50 µl in a DNA thermal cycler (Biometra, Göttingen), using Platinum *Taq* polymerase.

3.1.3.1 Standard PCR

Following conditions were chosen:

Components	Volume	Final concentration
10 x PCR buffer	5 µl	
50 mM $MgCl_2$	1.5 µl	1.5 mM
10 mM dNTP-Mix	1 µl	200 µM
H_2O	38 µl	
10 µM primer forward	1 µl	200 nM
10 µM primer reverse	1 µl	200 nM
Taq polymerase (5 U/µl)	0.5 µl	2.5 U
DNA	2 µl	~50-100 ng
	∑ 50 µl	

The program for standard PCR contained the following steps: 94°C for 2 min followed by 35 cycles of 94°C for 30 sec, 55°C for 30 sec and 72°C for 1 min, and a final step of 72°C for 10 min. The reaction was maintained at 4°C and stored at -20°C until analysis on a gel.

Platinum *Pfx* DNA polymerase amplifies genomic templates up to 12 kb and plasmid templates up to 20 kb and can be used for demanding PCR applications such as site-directed mutagenesis and expression cloning. Besides providing high specificity, the *Pfx* polymerase offers the benefit of proofreading activity. Its 3', 5' exonuclease activity eradicates mismatched base pairings, resulting in fewer errors in the PCR product.
The program for *Pfx* PCR contained the following steps: 94°C for 2 min followed by 25-30 cycles of 94°C for 15 sec, 55°C for 30 sec and 72°C for 1 min, and a final step of 72°C for 10 min. The reaction was maintained at 4°C and stored at -20°C until analysis on a gel.

Components	Volume	Final concentration
10 x *Pfx* buffer	5 µl	
50 mM $MgCl_2$	1 µl	1 mM
10 mM dNTP-Mix	1.5 µl	300 µM
H_2O	38 µl	
10 µM primer forward	1 µl	300 nM
10 µM primer reverse	1 µl	300 nM
Pfx polymerase (2.5 U/µl)	0.5 µl	1.25 U
DNA	2 µl	~50-100 ng
	∑ 50 µl	

3.1.4 RT-PCR

RNA Primer Mix	1-2 µg RNA
	1 µl Oligo $(dT)_n$
	1 µl Random Hexamers
	ad 10 µl H_2O
RT-Master Mix:	4 µl 5 x cDNA synthesis buffer
	1 µl 0.1 M DTT
	1 µl H_2O
	2 µl 10 mM dNTP mix
	1 µl RNase Out (40U/µl)
	1 µl ThermoScript RT (15 U/µl)

Sensitive methods for the detection and analysis of rare mRNA transcripts or other RNAs present in low abundance are an important aspect of most cell/ molecular biology studies. RNA cannot serve as a template for PCR, so it must first be reverse transcribed into cDNA (e.g. with reverse transcriptase from Moloney murine leukemia virus (MoMuLV) or avian myeloblastosis virus). RT-PCR is a combined technique in which reverse transcription (RT) is coupled with PCR amplification of the resulting cDNA.

First strand synthesis was done with ThermoScript RT-PCR System using 1-2 µg RNA. The RNA-primer mix was denatured by heating for 5 minutes at 65°C and chilled on ice. Following RNA denaturation, 10 µl of the RT-Master Mix was applied to the RNA-primer mix and incubated for the following cycles: 25°C 10 min, 50°C 45 min, 85°C 5 min. Optional, 1 µl RNaseH was added at 37°C for 20 minutes.
PCR was performed using Platinum *Taq* DNA polymerase. Cycler conditions: 94°C for 2 min followed by 30 cycles of 94°C for 30 sec, 55°C for 30 sec and 72°C for 1 min. Oligonucleotide primers were used at a 200 nM final concentration.

3.1.5 Cloning

Table 3-5. Materials cloning

	Vectors pSUPER and pHR'SIN-cPPT-SEW were provided by Dr. M. Grez, Georg-Speyer-Haus Haus, Frankfurt a. M.
Invitrogen GmbH, Karlsruhe	Vector pcDNA3.1/Hygro
MBI Fermentas, St. Leon-Roth	10 x buffer 0^+ 10 x buffer R^+ ATP Calf intestine phosphatase (CIP) + buffer Restriction enzymes: *Apa*I, *Sma*I, *Bam*HI, *Xho*I, *Bgl*II, *Hind*III, *Eco*RI *Sna*BI + 10 x buffer T4 DNA ligase + buffer T4 poly-nucleotide kinase (PNK) + buffer
New England BioLabs, Beverly, MA	*Nco*I
Promega GmbH, Mannheim	pGL3 control vector
Qiagen GmbH, Hilden	Qiaquick gel extraction kit Qiaquick nucleotide removal kit

3.1.5.1 Vector system for short interfering RNA

Annealing buffer	100 mM potassium acetate 30 mM HEPES 2 mM Mg-acetate pH 7.4

The vector pSUPER is designed for the expression of double-stranded short interfering RNAs (siRNA). Therefore, a pair of 64 nt oligonucleotides containing the siRNA coding sequences targeting MCP-1 and RANTES were annealed and ligated into the vector between *Bgl*II and *Hind*III sites of the vector.

Using the same method, oligonucleotides containing the coding sequences for single-stranded RNA TFOs (without stem loop) targeting MCP-1 and RANTES were cloned.

Table 3-6. Oligonucleotides (siRNA and TFO) for cloning pSUPER (Qiagen, Hilden)

RANTESf_si1	5′GATCCCCGTGCTCCAATCTTGCAGTCTTCAAGAGAGACTGCAAGATTGGAGCACTTTTTGGAAA
RANTESr_si1	5′AGCTTTTCCAAAAAGTGCTCCAATCTTGCAGTCTCTCTTGAAGACTGCAAGATTGGAGCACGGG
MCP-1f_si1	5′GATCCCCCTTCACCAATAGGAAGATCTTCAAGAGAGATCTTCCTATTGGTGAAGTTTTTGGAAA
MCP-1r_si1	5′AGCTTTTCCAAAAACTTCACCAATAGGAAGATCTCTCTTGAAGATCTTCCTATTGGTGAAGGGG
MCP-1 19cufor	5′GATCCCCTCTCCCTCTCTCCCACCTCTTTTTGGAAA
MCP-1 19curev	5′AGCTTTTCCAAAAAGAGGTGGGAGAGAGGGAGAGGG
RANTES25Cufor	5′GATCCCCCTCCCCCTCCCCCTCCCCCTCCTTCTTTTTGGAAA
RANTES25Curev	5′AGCTTTTCCAAAAAGAAGGAGGGGGAGGGGGAGGGGGAGGGG

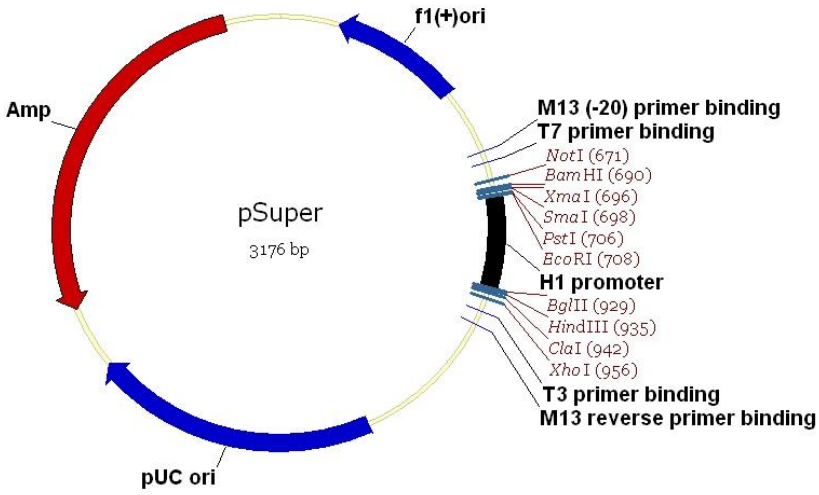

Figure 3-1. Vector pSUPER

The oligonucleotides were dissolved in sterile H_2O to a concentration of 1 mM. The annealing reaction was assembled by mixing 1 µl of each oligonucleotide (forward and reverse) in 48 µl annealing buffer. The mixture was incubated for 4 min at 95°C in a cycler (Biometra, Göttingen), followed by a slow cool-down to room temperature at a rate of 1°C/min. Samples were cooled further to 4°C and for longer storage kept at -20°C until needed.

To prevent vector reclosures during the ligation step, the linearised vector was CIP-treated (CIP=calf intestine alkaline phosphatase) and the annealed oligonucleotides were phosphorylated.

Phosphorylation of oligo	2 µl of annealed oligonucleotides
	1 µl T4 poly-nucleotide kinase (PNK) buffer
	1 µl 10 mM ATP (final concentration 1 mM)
	5 µl H_2O
	1 µl T4 PNK

The reaction was incubated for 30 min at 37°C, heat inactivated at 70°C for 10 min and chilled on ice. Prior to ligation, the reaction was purified using the Qiaquick nucleotide removal kit and eluted in 30 µl H_2O.

Linearisation of pSUPER	Plasmid DNA 20 µg x µl
	H_2O y µl, x + y = 123 µl
	*Hind*III 2 µl (100 U)
	*Bgl*II 10 µl (100 U)
	10 buffer R^+ 15 µl

The reaction was incubated for 3 h at 37°C, heat inactivated at 70°C for 10 min and chilled on ice. Following digestion, the linearised vector was gel purified on a 1% agarose gel (Qiaquick gel extraction kit) to remove the insert sequence and separate the preparation from any undigested circular plasmid to decrease the background in ligation and transformation.

CIP-treatment of linearised plasmid	7.25 µl H_2O
	1 µl 10 x CIP buffer
	0.75 µl linearised plasmid (~0.5 µg)
	1 µl CIP

The reaction was incubated for 1 h at 37°C, heat inactivated at 70°C for 10 min in the presence of 5 mM EDTA and chilled on ice. Prior to ligation, the reaction was purified using the Qiaquick nucleotide removal kit and eluted in 30 µl H_2O.

Ligation	2 µl of the annealed and phosphorylated oligos
	5 µl H_2O
	1 µl 10 x T4 DNA ligase buffer
	1 µl plasmid linearised and CIPed
	1 µl T4 DNA ligase

The reaction was incubated over night at 20°C and was ready for transformation. After transformation and plasmid preparations correct inserts were confirmed by restriction analysis with *Bgl*II or *Hind*III/*Eco*RI for 1-2 h at 37°C:

*Hind*III/*Eco*RI restriction	15.8 µl H_2O
	1 µl plasmid DNA (~1µg/µl)
	2 µl 10 x buffer R^+
	1 µl *Eco*RI (10 U)
	0.2 µl *Hind*III (10 U)

*Bgl*II restriction	16 µl H_2O
	1 µl plasmid DNA (~1µg/µl)
	2 µl 10 x buffer 0^+
	1 µl *Bgl*II (10 U)

Insert sizes were analysed on a 1% agarose gel. Additionally, the presence of the correct insert was confirmed by sequencing (MWG, Ebersberg).

3.1.5.2 Cloning of a lentiviral transfer vector

For SEW vector construction, confirmed inserts in the vector pSUPER were amplified by PCR using the primers T7for and T3rev (Table 3-4) which both contained a 5' *Sna*BI restriction site. Resulting expression cassettes were subcloned into the *Sna*BI linearised SEW.

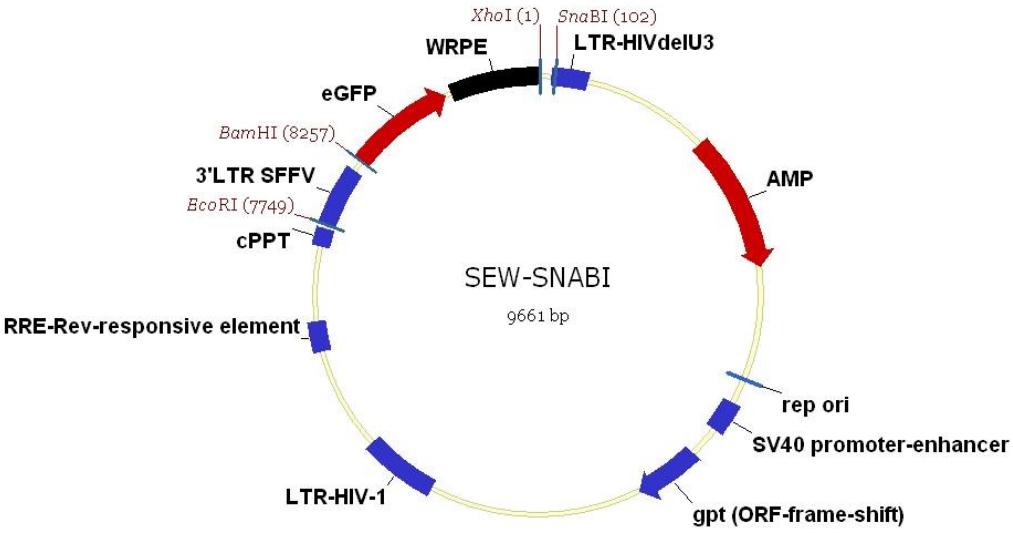

Figure 3-2. Lentiviral transfer vector pHR'SIN-cPPT-SEW (SEW)

Blunt end ligation	2 µl PCR product, *Sna*BI digested
	4 µl H_2O
	1 µl 10 x T4 DNA ligase buffer
	1 µl plasmid *Sna*BI linearised (~50-400 ng)
	2 µl T4 DNA ligase

PCR products (~378 bp ± different inserts), containing the *Sna*BI restriction sites were purified using the Qiaquick nucleotide removal kit and eluted in 30 µl H_2O. The whole reaction was *Sna*BI (10 U/µl) digested and additionally purified.

Insert sizes were analysed on a 1% agarose gel. Additionally, the presence of the correct insert was confirmed by sequencing (MWG, Ebersberg).

3.1.5.3 Construction of vectors TVHygro-CU, TVHygro-GU and TVHygro-CA

Table 3-7. Oligonucleotides (MWG, Ebersberg) for TVHygro

TVHygro-CU_for	5′ GTCGACAAGCTTCTCGAGTCTCCCTCTCTCCCACCTCGGATCCCGCGAT 3′
TVHygro-CU_rev	3′ CAGCTGTTCGAAGAGCTCAGAGGGAGAGAGGGTGGAGCCTAGGGCGCTA 5′
TVHygro-CA_for	5′ AAGCTTCTCGAGCACACACCCAACCACACCCGGATCC 3′
TVHygro-CA_rev	3′ TTCGAAGAGCTCGTGTGTGGGTTGGTGTGGGCCTAGG 5′
TVHygro-GU_for	5′ AAGCTTCTCGAGACACCCACACACCCACCACGGATCC 3′
TVHygro-GU_rev	3′ TTCGAAGAGCTCTGTGGGTGTGTGGGTGGTGCCTAGG 5′

Transfection vectors were constructed to drive transcription of either RNA containing the 19 nt pyrimidine triplex forming sequence targeting the MCP-1 promoter (CU-TFO) or RNA containing two different 19 nt control sequences (GU-control or CA-control). The vector TVHygro was derived from the eukaryotic expression vector pcDNA3.1/Hygro with the sequences spanning the region 1002-2079 deleted by restriction with the enzymes *Apa*I and *Sma*I. The resulting *Apa*I overhang was end-filled and the vector re-ligated. Three different DNA sequences have been cloned into the 5' untranslated region of the hygromycin resistance gene, resulting in the vectors TVHygro-CU, TVHygro-CA and TVHygro-GU. The constructs leading to TVHygro-CU and TVHygro-CA were digested with the enzymes *Hind*III and *Bam*HI, and cloned into TVHygro in *Hind*III/*Bam*HI orientation. The construct leading to vector TVHygro-GU was *Bam*HI and *Xho*I digested and cloned into TVHygro in *Bam*HI/*Xho*I orientation. Each of the cloned sequences is transcribed in line with the hygromycin resistance mRNA under the control of the constitutive cytomegalovirus (CMV) promoter, resulting in one fusion transcript. TVHygro served as an additional control vector without insert.

Cloning of vector TVHygro was carried out by Dr. Mario Schwarz and correct inserts were confirmed by sequencing (MWG, Ebersberg).

Table 3-8. Summary vector constructs

Construct	Vector	Modification	Cloning
TVHygro	pcDNA3.1/Hgro	Deletion *Apa*I/*Sma*I	No insert
TVHygro-CU	pcDNA3.1/Hgro	Deletion *Apa*I/*Sma*I	Insert between *Hind*III/*Bam*HI, ***CU-TFO***
TVHygro-CA	pcDNA3.1/Hgro	Deletion *Apa*I/*Sma*I	Insert between *Hind*III/*Bam*HI, ***CA-control***
TVHygro-GU	pcDNA3.1/Hgro	Deletion *Apa*I/*Sma*I	Insert between *Bam*HI/*Xho*I, ***GU-control***
pS-MCP-1_si	pSUPER		Insert between *Hind*III/*Bgl*II, ***MCP-1 siRNA***
pS-RANTES-si	pSUPER		Insert between *Hind*III/*Bgl*II, ***RANTES siRNA***
pS-MCP-1_TFO	pSUPER		Insert between *Hind*III/*Bgl*II ***MCP-1 TFO***
SEW(-)	pHR'SIN-cPPT-SEW		T7/T3 amplification of vector pSUPER, insert in *Sna*BI
SEW-RANTES-si	pHR'SIN-cPPT-SEW		T7/T3 amplification of vector pS-RANTES-1_si, insert in *Sna*BI, ***RANTES siRNA***
SEW-MCP-1_si	pHR'SIN-cPPT-SEW		T7/T3 amplification of vector pS-MCP-1_si, insert in *Sna*BI, ***MCP-1 siRNA***
SEW-MCP-1_TFO	pHR'SIN-cPPT-SEW		T7/T3 amplification of vector pS-MCP-1_TFO, insert in *Sna*BI, ***MCP-1 TFO***
pGL3-MCP-1	pGL3-control vector		Insert between *Hind*III/*Nco*I, ***39 bp MCP-1 target sequence***
pGL3-MCP-1_a	pGL3-control vector		Insert between *Hind*III/*Nco*I, ***39 bp MCP-1 target sequence, antisense orientation***

3.1.6 Northern blots

Table 3-9. Materials Northern Blot

Amersham Pharmacia Biotech, Freiburg	[α-^{32}P]-dCTP Hybond^{TM}-N nylon membrane
Invitrogen GmbH, Karlsruhe	Denhardt's reagent Salmon sperm DNA
MBI Fermentas, St. Leon-Rot	HexaLabel^{TM} DNA Labelling
Merck, Darmstadt	SDS
Qiagen GmbH, Hilden	Qiaquick nucleotide removal kit
Riedel-de Haën, Seelze	Formaldehyde

20 x SSC	3 M NaCl 0.3 M sodium citrate pH 7.0
20 x SSPE	3 M NaCl 200 mM NaH_2PO_4 x H_2O 20 mm EDTA

After separating RNA molecules based on charge migration in a denaturing gel (standard formaldehyde agarose gel, prepared and run as described), RNA molecules in the gel were transferred to a nylon membrane by capillary transfer. The RNA of interest can then be identified by hybridisation to radioactive probes and visualised by autoradiography.

A buffer tray was filled with 1 l 20 x SSC and a glass plate was placed across the tray. Whatman 3MM filter paper (pre-soaked in 20 x SSC) was placed over the glass plate so that the ends contacted the bottom of the tray. Immediately after gel electrophoresis, the gel was soaked for 10 min in RNase-free water with gentle shaking, then for 15 min in 0.05 NaOH, and finally for 10 min in 10 x SSC to neutralise the NaOH. Following, the gel was positioned upside-down on the filter paper covering the plate. The pre-soaked nylon membrane was placed on top of the gel so that it covered the entire surface, followed by 3 sheets of Whatman filter paper and a 10-15 cm stack of dry paper towels. A second glass plate was placed on top of the paper towels and fixed with a weight of about 500 g. The transfer was carried out for 16-18 h. After the transfer was complete, filters and paper towels were removed, the positions of the gel lanes on the nylon membrane were marked, and the membrane was washed for 1 min in 10 x SSC. The RNA was fixed by UV cross-linking (150 mJ/cm^2). The blot could be stored at 4 °C wrapped in plastic wrap.

3.1.6.1 Preparation of the radioactive probe

For detection of the TFO/hygromycin mRNA in the stable transfected cell lines, a part of the hygromycin resistance gene included in the vector pCDNA3.1/Hygro was amplified by PCR, resulting in a product of 522 bp. The DNA was [α-^{32}P]-dCTP labelled using Klenow fragment according to the supplier's protocol and unbound nucleotides were removed using the Qiaquick nucleotide removal kit. Before hybridisation, the radioactive probe was denatured for 10 min at 70°C.

3.1.6.2 Prehybridisation and hybridisation

Hybridisation buffer	50% deionised formamide
	5 x Denhardt's reagent
	5 x SSPE
	1% SDS
	150 µg/ml salmon sperm DNA

The nylon membrane was washed once in 5 x SSPE, placed into the hybridisation tube using tweezers, and prehybridysed at 42°C for 2 h in hybridisation buffer (~10 ml) with gentle rotation in a hybridisation oven (Kendro Laboratory Products GmbH). After prehybridisation, the buffer was removed and replaced with fresh hybridisation buffer containing the denatured radio-labelled probe. Hybridisation was performed for 22 h at 42°C. For stringency washes, membranes were washed sequentially, starting with 15 min in 1 x SSC/ 0.1% SDS at room temperature, then 15 min in 0.2 x SSC/ 0.1% SDS at 62°C. Washed membranes were left damp, wrapped in plastic wrap and exposed to Phospho-Imager screens (Fuji, Kanagawa,

Japan), visualised using a Fuji BAS-MS Phospho-Imager (Fuji Imaging, Tokio, Japan) and analyzed by Phospho-Imager software (TINA, Raytest Company, Straubenhardt)

3.1.7 TFO targets

Table 3-10. TFO targets

Target	Acc.-nr.	Description
Mouse RANTES	MMU02298	28 bp TFO target site from -265 to -238. +1 corresponds to the transcriptional start site described by Danoff (Danoff et al. 1994)
Human MCP-1	D26087	19 bp TFO target site from -66 to -48. +1 corresponds to the major transcriptional start site described by Ueda (Ueda et al. 1994)

3.1.7.1 Preparation of synthetic double-stranded RANTES promoter fragment

annealing buffer	10 mM Tris/HCl, pH 8.0
	1 mM EDTA
	0.1 M NaCl

The oligonucleotides for the 48 bp double-stranded promoter fragment corresponded to the region between -275 to -228 of the mouse RANTES promoter. For radioactive labelling, *Hind*III and *Nco*I restriction site were added to the 3' and 5' ends of the sequences, leading to a 5' overhang after annealing (Table 3-11). Annealing of the oligonucleotides was achieved by mixing them in equimolar amounts in annealing buffer, incubation at 95°C for 10 min, followed by a slow cool-down to room temperature at a rate of 1°C/min. Quantitative annealing of the single-stranded oligonucleotides to duplex DNA was confirmed by native polyacrylamide gel electrophoresis through 12.5% gels, followed by ethidium bromide staining. The resulting 5' overhang of the duplex DNA was end-filled and [α-^{32}P]-dCTP radio-labelled using Klenow fragment exo$^-$ (Fermentas) in the presence of 0.02 mM of each dGTP, dATP and dTTP and 1.85 MBq [α-^{32}P]-dCTP (Amersham Pharmacia Biotech). Unincorporated nucleotides were removed by using the Qiaquick nucleotide removal kit.

Table 3-11. Oligonucleotides (Qiagen, Hilden) for RANTES promoter fragment

RANTES_for	5'AGCTTCGGCAGATCT**GAGGGGGAGGGGGAGGGGGAGGAAGAAA**TTTTCCCCTAC 3'
RANTES_rev	5'CATGGTAGGGGAAAA**TTTCTTCCTCCCCCTCCCCCTCCCCCTC**AGATCTGCCGA 3'

*The 28 bp RANTES TFO target site is shown in bold letters. Hind*III *restriction site is shown in blue, and Nco*I *restriction site in red.*

3.1.7.2 Preparation of radio-labelled double-stranded MCP-1 promoter fragment

The 39 bp double-stranded promoter fragment corresponded to the region between bp –76 and bp –38 of the human MCP-1 promoter. A modified luciferase pGL3-control vector (Promega) containing the 39 bp target sequence between *Hind*III and *Nco*I restriction sites (pGL3-MCP-1, see Table 3-8) was digested with the respective restriction enzymes *Hind*III (Fermentas) and *Nco*I (New England BioLabs). The resulting fragment contained the 39 bp MCP-1 promoter duplex plus 5' overhang on each side due to the restriction sites. The fragment was electrophoretically fractionated with a 1% agarose gel, excised by a scalpel and DNA extracted using the Qiaquick gel extraction kit. The resulting 5' overhang of the duplex DNA was end-filled and [α-^{32}P]-dCTP radio-labelled as described above. Alternatively, synthetic oligonucleotides containing the same 39 bp MCP-1 promoter sequence or oligonucleotides containing two mismatches in the triplex binding site were annealed and radio-labelled as described above.

Table 3-12. Oligonucleotides (Qiagen, Hilden) for MCP-1 promoter fragment

MCP-1_for	5'AGCTTTCCTGCTTGA**CTCCGCCCTCTCTCCCTCT**GCCCGCTTTCC 3'
MCP-1_rev	5'CATGGGAAAGCGGGC**AGAGGGAGAGAGGGCGGAG**TCAAGCAGGAA 3'
MCP-1_2Mfor	5'AGCTTTCCTGCTTGA**CTCCGCCCTCTATCCCTCG**GCCCGCTTTCC 3'
MCP-1_2Mrev	5'CATGGGAAAGCGGGC**CGAGGGATAGAGGGCGGAG**TCAAGCAGGAA 3'

The 19 bp MCP-1 TFO target site is shown in bold letters. HindIII restriction site is shown in blue, and NcoI restriction site in red, respectively. Positions of mismatches are underlined.

3.1.7.3 Labelling of the plasmid pGL3 control containing a MCP-1 promoter fragment

For labelling of the plasmid pGL3 control containing the 39 bp MCP-1 promoter duplex the vector was linearised by *Bgl*II restriction digestion. About 100 ng were [α-^{32}P]-dCTP labelled using Klenow fragment (Fermentas) according to the supplier's protocol.

3.1.7.4 TFOs

19 nt MCP-1 TFO and 28 nt RANTES TFO were designed according to the sequences described in Table 3-10. Oligonucleotides were HPLC purified and desalted. Oligonucleotides used in cell culture experiments were phosphorothioated.

Table 3-13. TFOs with desoxyribonucleotide backbone targeting RANTES

RANTES GT-TFO	5'TTTGTTGGTGGGGGTGGGGGTGGGGGTG 3'	Qiagen, Hilden
RANTES GT-control	5'TGGTGGGTGGGTGTGTGGGTGGGTGGGT 3'	Qiagen, Hilden
RANTES GT-pTFO	5'T*TTGTTGGTGGGGGTGGGGGTGGGGGT*G 3'	Qiagen, Hilden
RANTES GT-pcontrol	5'T*GGTGGGTGGGTGTGTGGGTGGGTGGG*T 3'	Qiagen, Hilden

** Phosphorothioate modification*

Table 3-14. TFOs with desoxyribonucleotide backbone targeting MCP-1

TFO MS1	5′G*TGGTGGGTGTGTGGGTGT* 3′	Thermo Hybaid, Ulm
control MS2	5′G*GGTGTGGTTGGGTGTGTG* 3′	Thermo Hybaid, Ulm
TFO MS3	5′G*TGGTGGGTGTGTGGGTGT* 3′	GeneScan, Freiburg
control MS34	5′G*GGTGTGGTTGGGTGTGTG* 3′	GeneScan, Freiburg
TFO MS5	5′G*TGGTGGGTGTGTGGGTGT* 3′	metabion, Martinsried
control MS6	5′G*GGTGTGGTTGGGTGTGTG* 3′	

** Phosphorothioate modification*

Table 3-15. TFOs with ribonucleotide backbone targeting MCP-1

rCU-TFO	5′UCUCCCUCUCUCCCACCUC 3′	MWG, Ebersberg
rGA-control	5′GAGGUGGGAGAGAGGGAGA 3′	MWG, Ebersberg
rGU-control	5′GUGGUGGGUGUGUGGGUGU 3′	MWG, Ebersberg
rCA-control	5′CACACACCCAACCACACCC 3′	MWG, Ebersberg
19CU_M	5′UCACCCUCUCUCCCACCUC 3′	MWG, Ebersberg

3.1.8 Electrophoretic mobility gel shift assay (EMSA)

Triplex buffer	10 mM Tris/HCl, pH 7.4 10 mM $MgCl_2$ 5% sucrose
10 x TB buffer + $MgCl_2$	890 mM Tris 890 mM boric acid 100 mM $MgCl_2$
Polyacrylamide gel	4.9 ml H_2O 4 ml acrylamide (30%) 1 ml 10 x TB buffer+ $MgCl_2$ 4 µl TEMED 100 µl 10% APS

The double-stranded target DNA was end-labelled as described previously. About 10 nM of the labelled duplex DNA (~10 fmol/µl in a 25 µl reaction) was incubated for 1 h at room temperature with the indicated concentrations of triple helix-forming or control oligonucleotides in triplex buffer. Immediately following incubation, the samples were electrophoresed through 12.5% native polyacrylamide gels buffered with 1 x TB containing 10 mM $MgCl_2$. Electrophoresis was performed at 8 V/cm for 3 h at 4°C. Gels were dried on a gel dryer (Scie-Plas gel dryer, model GD5040, Southam, UK) for 2 h at 80°C and exposed to Phospho-Imager screens (Fuji), visualised using a Fuji BAS-MS Phospho-Imager and analysed by Phospho-Imager software (TINA, Raytest Company).

3.1.9 Triplex blotting

Blotting buffer:	17 mM NaH_2PO_4 8 mM Na_2HPO_4
Wash buffer:	200 mM sodium acetate 2 mM EDTA adjusted to pH 5.5 or 6.7 0.1% SDS
5xNAE:	500 mM sodium acetate 5 mM EDTA adjusted to pH 5.5 or 6.7
Hybridisation buffer:	5xNAE, pH 5.5 or 6.7 5x Denhardt's solution 1% SDS 20 µg/ml of salmon sperm DNA

Triplex blots were started by electrophoretic separation of the 19 nt oligoribonucleotides by 7 M urea (Roth), 6% polyacrylamide gels. Nucleic acids were transferred to nylon filters (Hybond^{TM}-N, Amersham Pharmacia Biotech) in blotting buffer, followed by UV cross-linking (150 mJ/cm^2). Then, filters were pre-hybridised for 1 h at 30° or 37°C in hybridisation buffer at pH 5.5 or 6.7. Following pre-hybridisation blots were hybridised overnight with the radio-labelled duplex DNA containing the target sequence in the same solution at 30° or 37°C with gentle shaking. Subsequently, filters were washed twice by shaking in wash buffer for 20 min at 30° or 37°C. Filters were exposed to Phospho-Imager screens (Fuji), visualised using a Fuji BAS-MS Phospho-Imager and analyzed by Phospho-Imager software (TINA, Raytest Company).

3.1.10 *In vitro* transcription

The vector encoded TFO or control sequences and in addition part of the hygromycin resistance gene were amplified by PCR using the upstream primer fw_TVHygro 5' AGC AGA GCT CTC TGG CTA A 3' and downstream primer rev_TVHygro 5' TCG GCG AGT ACT TCT ACA C 3' (Table 3-4) at a 200 nm final concentration and Platinum *Taq* DNA polymerase (Invitrogen GmbH, Karlsruhe). Cycler conditions: 94°C for 2 min followed by 35 cycles of 94°C for 30 sec, 55°C for 30 sec and 72°C for 1 min. Products were purified using the Qiaquick PCR Purification kit. The PCR product was used as template for *in vitro* transcription. Product amplification included the T7 promoter sequence of the vector. *In vitro* transcription was performed with the T7 Ribomax^{TM} Express Large Scale RNA Production

System (Promega) according to the supplier's protocol. Correct sizes (1.1 kb) of the transcribed RNA were proven by electrophoresis with 1% agarose gels.

3.1.11 Magnetic capture of triplex complexes

Table 3-16. Materials magnetic capture assay

Miltenyi Biotec, Bergisch Gladbach	µMACS MicroBeads conjugated to streptavidin MACS separation columns, M columns VarioMACS
Triplex buffer	20 mM Tris/HCl, pH 7.0 1.5 mM $MgCl_2$ 140 mM KCl 3% glycerol

Annealing of the biotinylated oligonucleotide 5' biotin - GCG CTT CTG CGG GCG ATT TGT GTA CGC CCG 3', HPCL purified (MWG, Ebersberg) to *in vitro* transcribed RNA (denatured 90°C for 5 min) was achieved by mixing 400 pmol RNA with 400 pmol biotinylated oligonucleotide in annealing buffer (100 mM potassium acetate, 30 mM HEPES, 2 mM magnesium acetate, pH 7.4). The reaction was incubated for 1 h at room temperature. Quantitative annealing of the oligonucleotide to the single-stranded RNA was confirmed by gel electrophoresis through a 1% agarose gel. The annealing reaction was incubated with 2 µg of the vector pGL3-MCP-1 (Promega) containing a 39 bp MCP-1 promoter target sequence. Incubation was performed in triplex buffer for 1 to 24 h to allow proper triplex formation (pH usually 7.0) in the presence of RNase inhibitor (100 U, Invitrogen). A small aliquot of each reaction was saved for PCR analysis to confirm that equal amounts of plasmid were used. The reaction was incubated with 100 µl of the streptavidin micro beads for 5 min at room temperature. Dilution of the beads in the binding reaction was between 1:2 and 1:10. For magnetic separation the column was placed in the magnetic field of the VarioMACS separator and rinsed once with 250 µl of the equilibration buffer provided by the manufacturer and 3 times with 250 µl of triplex buffer. After that the binding reaction was applied onto the top of the column matrix. The solution passed through the column by gravity and the magnetically labelled complexes were retained in the column. The column was rinsed 4 times with 250 µl of triplex buffer to remove non-specifically interacting plasmid. For elution the column was removed out of the magnetic field and 250 µl of triplex buffer or H_2O were applied directly onto the top of the column. Elution and washing fractions were saved for RNA and PCR analysis. To evaluate the quantity of RNA which was bound to the micro beads, 40 µl of each fraction were subjected to electrophoresis through a 1% agarose gel and the relative amount of RNA in the elution fraction was quantified densitometrically (TINA).

3.2 Microbiological methods

Table 3-17. Materials E.coli

BD Biosciences Clontech, Heidelberg	S.O.C. medium
Carl Roth GmbH, Karlsruhe	Tryptone Yeast extract
Gibco RBL, Life Technologies, Eggenstein	E.coli strain: MAX Efficiency DH5α competent cells Genotype: F^-Φ80d*lac*ZΔM15 Δ(*lac*ZYA-*arg*F)U169 *deo*R *rec*A1 *end*A1 *hsd*R17(r_K^-, m_K^+) *pho*A *sup*E44 λ^- *thi*-1 *gyr*A96 *rel*A1
Sigma-Aldrich Chemie GmbH, Deisenhofen	Agar

3.2.1 Cultivation of E.coli

LB (Luria Bertani) medium	1% (w/v) NaCl 1% (w/v) tryptone 0.5% (w/v) yeast extract pH 7.5, autoclave
LB agar	LB medium 1.5% (w/v) agar, autoclave
S.O.C. medium	2% (w/v) tryptone 0.5 % (w/v) yeast extract 10 mM NaCl 10 mM KCl, autoclave and cool to 55°C 20 mM Mg^{2+} (10 mM $MgCl_2$, 10 mM $MgSO_4$ 20 mM glucose -Filter complete medium through a 0.22 µM filter unit

Bacterial strains carrying plasmids or genes with antibiotic selection marker were cultured in liquid or on solid medium containing the selective agent. Stock solutions of antibiotics were sterilised by filtration and aliquots stored at -20°C. Antibiotics were added to freshly autoclaved medium (cooled to below 50°C), and stock and working concentrations for the antibiotics are shown in Table 3-18.

Table 3-18. Concentrations of antibiotics

Antibiotic	**Stock solutions**		**Working concentrations**	
	Concentration	Storage		Dilution
Ampicillin	50 mg/ml in water	-20°C	100 µg/ml	1/500
Tetracycline	5 mg/ml in ethanol	-20°C	50 µg/ml	1/100
Streptomycin	10 mg/ml in water	-20°C	50 µg/ml	1/200
Chloramphenicol	34 mg/ml in ethanol	-20°C	170 µg/ml	1/200

3.2.1.1 Agar plates

E.coli strains can be streaked and stored on LB plates containing 1.5% agar and the appropriate antibiotic. With a flamed and cooled wire loop an inoculum of bacteria from a glycerol stock was streaked on top of a fresh agar plate, and incubated upside down at 37°C for 12-14 h until colonies developed.

3.2.1.2 Liquid cultures

Bacterial liquid cultures were grown for plasmid preparations. A starter culture was prepared by inoculating a single colony from a freshly streaked selective plate into 2-5 ml LB medium containing the appropriate antibiotic. The culture was grown for ~8 h at 37°C with vigorous shaking (~250 rpm). The starter culture was diluted 1/500 to 1/1000 into a larger volume of selective LB medium and grown overnight (12-16 h) at 37°C with shaking (~250 rpm). Cells were harvested by centrifugation at 6000 x g for 15 min, and following the cell pellet was treated as indicated in the appropriate plasmid purification protocols.

3.2.1.3 Glycerol stocks

E.coli strains can be stored for many years at -80°C in 15% glycerol. 0.15 ml glycerol were placed into a 2 ml screw-cap vial and sterilised by autoclaving. 0.85 ml of the E.coli culture were added and vortexed to ensure even mixing of the bacterial culture and the glycerol. Samples were frozen in liquid nitrogen and stored at -80°C.

3.2.2 Transformation of E.coli

Competent cells were removed from the -80°C freezer and thawn on wet ice and aliquots of 100 µl of cells were placed into chilled polypropylene tubes. Following, 1 µl from the ligation reaction (1-10 ng DNA) was added to the cells, moving the pipette through the cells while dispensing. Cells were incubated for 30 min on ice and heat-shocked for 45 sec in a 42°C water bath afterwards. Then, cells were placed on ice for 2 min, and 0.9 ml of room temperature S.O.C medium was added. The culture was incubated for 1 h at 37°C with shaking (225 rpm). Following, cells were centrifuged at 10000 rpm for 2 min and resuspended the in 100 µl S.O.C. 90 and 10 µl of this suspension were plated on LB plates containing the antibiotic and incubated overnight upside-down at 37°C.

3.3 Immunological methods

3.3.1 Enzyme-linked immunosorbent assay (ELISA)

Wash buffer	0.05% Tween 20 in PBS, pH 7.4
Block buffer	1% BSA 5% Sucrose 0.05% NaN_3 In PBS
Reagent diluent	1% BSA in PBS pH, 7.3 0.22 µm filtered
Stop solution	2 N H_2SO_4

Concentrations of secreted chemokines were measured by ELISA. ELISA is a method that is used for the quantitative assay of proteins in solution. In an ELISA, first antibody (capture antibody) is immobilised on a solid support (wells of a 96-well plate) and used as capture molecule to bind the protein that is being assayed. After a wash step to remove non-specifically bound material, a secondary antibody (detection antibody) is added. This secondary antibody is usually conjugated to an enzyme that allows its detection by chromogenic or chemiluminescent methods.

The human MCP-1 ELISA and murine RANTES ELISA were performed with reagents from R&D Systems (Wiesbaden); IL-8 was determined with the OptEIA™ human IL-8 Set from BD Bioscience Pharmingen (Heidelberg) according to the supplier's protocol.

In general, 100 µl of diluted capture antibody were added to each well and incubated overnight. After three aspiration/wash steps the plate was blocked for 1 h using 300 µl block buffer. Following three aspiration/wash steps 100 µl of standard or sample were added to each well for 2 h at room temperature. After washing, 100 µl of diluted detection antibody was added for 2 h. The wash steps were repeated and 100 µl of Streptavidin conjugated to horseradish peroxidase were incubated for 20 min. After three aspiration/wash steps 100 µl of substrate solution was added to each well for 20 min in the dark. 50 µl of stop solution were added, and absorbance was read at 450 nm (Tecan SpectraFluorPlus reader including XFluor-software version V3.21). Readings at 540 nm were subtracted from readings at 450nm for correction.

3.4 Methods of cell biology

3.4.1 Cultivation of mammalian cells

Table 3-19. Materials cell culture

BioWhittaker, Verviers	Fetal calf serum (FCS)
Bissendorf Peptides, Hannover	TNF-α
Cell Concepts GmbH, Umkirch	IFN-γ
Gibco RBL, Life Technologies, Eggenstein	Dulbecco's modified eagle medium (DMEM) PBS RPMI 1640
Invitrogen GmbH, Karlsruhe	Penicillin/Streptomycin Trypsin NEA
Pharmacia Diagnostics GmbH	Concanavalin A (ConA)
Roche, Penzberg	Interleukin-2 (IL-2)
Sigma-Aldrich Chemie GmbH, Deisenhofen	DMSO

Table 3-20. Cells

T helper-1 lymphocytes (Th1 IF12)
brain microvascular endothelial cells (b-end3)
Human embryonic kidney (HEK) 293 (CRL 1573, American Type Culture Collection)
293T cells

Th1 medium	500 ml RPMI 5 ml L-Glutamine 5 ml Penicillin/Streptomycin 5 ml NEA 50 ml 10% FCS 5 µg/ml IL-2
Medium for b-end3 cells, HEK 293 cells, 293T cells	500 ml DMEM 50 ml 10% FCS 5 ml Penicillin/Streptomycin

Cells were incubated in an incubator (Kendro Laboratory Products GmbH) and grown at 37°C and 5% CO_2 with saturating humidity (95%), except brain microvascular endothelial cells were grown in 10% CO_2.

3.4.1.1 Passaging cells

Cells were splitted routinely twice a weak. Cells were harvested either by trypsinisation (adherent cell cultures) or by centrifugation at 1000 rpm for 5 min (suspension cell cultures).

For trypsinisation, the medium was removed from the flask and cells were washed carefully with PBS to remove residual medium. 1-2ml of prewarmed Trypsin solution was added to the flask (175 cm^2) and incubated at 37°C until cells have detached (1-2 minutes). Trypsinisation was blocked by adding a few ml of medium. Following, cells were resuspended in an appropriate volume of prewarmed growth medium containing serum.
Appropriate dilutions of Th1 cells were transferred in 10 ml medium containing 5 µg/ml IL-2 to a fresh cell culture flask (175 cm^2).
Typically, when splitting confluent HEK 293 cells in a 1:10 ratio, confluency was reached again after 3-4 days.

3.4.1.2 Cell freezing and thawing

The cells were trypsinised first if necessary, resuspended in medium containing serum, centrifuged at 1000 rpm for 5 min, and then resuspended in freezing medium. 1 ml of the cell suspension (approximately 3-5 x 10^6 adherent cells or 5-10 x 10^6 suspension cells) was transferred into each freezing vial. Freezing vials were placed into a Cryo freezing container (Nalgene) and stored in a -80°C freezer overnight. This allowed freezing of the cells at a rate of 1°C/min. The following day vials were transferred to a liquid nitrogen chamber.
For cell thawing, a vial of frozen cells was removed from liquid nitrogen and placed in a 37°C water bath until thawed. To remove DMSO from the freezing medium, the cell suspension was pipetted into a centrifuge tube containing prewarmed medium, and centrifuged at 1000 rpm for 5 min. The supernatant was discarded, cells were resuspended in fresh growth medium and transferred to the cell culture flask. Cells were incubated overnight under their usual growth conditions, and the medium was replaced the next day.

3.4.1.3 Cytokine treatment and mitogen activation

For analysis of cytokine induced stimulation of chemokine production, HEK 293 and b-end3 cells were plated in 6-well or 24-well plates in medium as described above (between 1.5 x 10^5 and 6 x 10^5 cells/well) and grown overnight. After 18 h culture media were replaced with fresh medium, and cells were treated with different concentrations of the cytokines (500 U/ml TNF-α and/or 200-1000 U/ml IFN-γ) for 24 h. Then, culture media were harvested, centrifuged for 5 min at 12,000 x g to remove cell debris and stored at –20°C until further analysis of secreted proteins by ELISA.

Th1 cells plated in 6-well plates at a density of 1 x 10^6 cells/well were activated using 5 µg/ml ConA for 24 h. Following the incubation time, the culture media were harvested and the concentration of secreted RANTES was determined by ELISA.

3.4.2 Transfection of mammalian cells

Table 3-21. Materials transfection

Gibco RBL Life Technologies, Eggenstein	Lipofectamine
PAA Laboratories GmbH, Cölbe	Hygromycin
Qiagen GmbH, Hilden	Effectene reagent Enhancer Polyfect transfection reagent

3.4.2.1 Transient transfection of plasmid DNA

HEK 293 or b-end3 cells were seeded in appropriate dishes overnight until 40-80% confluent. Transfection was performed using Polyfect transfection reagent or Lipofectamine according to the supplier's protocol. Suspension cells (Th1) were transfected using Effectene reagent and the enhancer.

After transfection, cells were incubated for 18-48 h, followed by cytokine treatment as indicated.

3.4.2.2 Transient transfection of double-stranded siRNA or TFOs

Phosphorothioated TFOs (Table 3-13 and 3-14) or synthetic siRNA were usually transfected using Lipofectamine. After transfection, cells were incubated for 18-24 h, followed by cytokine treatment as indicated.

Table 3-22. Synthetic siRNA

rRANTES si1	Accession-number NM_013653	5′ GUGCUCCAAUCUUGCAGUCUU UUCACGAGGUUAGAACGUCAG	MWG, Ebersberg
rMCP-1 si1	Accession-number NM_002982	5′ CUUCACCAAUAGGAAGAUCUU UUGAAGUGGUUAUCCUUCUAG	MWG, Ebersberg
control		5′ CUUCACCAAUAGAGAGAUCUU UUGAAGUGGUUAUCUCUCUAG	MWG, Ebersberg
CCL2-361	Accession-number NM_002982	5′ GGAUUCCAUGGACCACCUGtt gtCCUAAGGUACCUGGUGGAC	Ambion, Huntingdon, UK

siRNA sequences were screened using the Ambion siRNA target finder. Single strands ordered from MWG were mixed in equimolar amounts in annealing buffer composed of 100 mM potassium acetate, 30 mM HEPES, and 2 mM magnesium acetate, pH 7.4 and incubated at 95°C for 5 min, followed by a slow cool-down to room temperature at a rate of 1°C/min. The sequence CCL2-361 (double-stranded) was ordered as a validated siRNA sequence (Ambion). Usually, cells were transfected with 100-150 nM siRNA.

3.4.2.3 Transfection of HEK 293 cells with TFOs without transfection reagent

HEK 293 cells plated in 24-well or 96-well plates at different densities (5 x 10^4 to 1.5 x 10^5 cells/well) were pre-treated with 0.5, 2.0 or 5.0 µM phosphorothioated TFO or control oligonucleotides for 24 h. Thereafter, the medium (200 µl/well) was replaced with medium containing the same concentration of oligonucleotides as before, and the cells were cultured for additional 24 h in the absence or presence of 500 U/ml TNF-α. At the end of incubation time, the culture supernatants were harvested and the concentrations of MCP-1 were determined by ELISA.

3.4.2.4 Stable transfection of HEK 293 cells

HEK 293 cells were transfected with the constructed vectors TVHygro-CU, TVHygro-GU, TVHygro-CA or TVHygro (no insert) using Polyfect transfection reagent according to the manufacturer's instructions. Selection of TVHygro-CU, TVHygro-GU, TVHygro-CA and TVHygro transfectants was carried out in the presence of 250 µg/ml hygromycin. Single transfectants were isolated and single cell clones of each of the transfectants were expanded under continuing selection pressure.

3.4.3 Production of lentiviral vectors by transient transfection

Table 3-23. Materials lentiviral vectors

Sigma-Aldrich Chemie GmbH, Deisenhofen	0.1 x TE buffer, filtered 0.22 µm 100 µM chloroquine stock solution, dissolved in PBS, filtered 0.22 µm 2.5 M $CaCl_2$ tissue culture grade, filtered 0.22 µm Double processed tissue culture water dH2O, endotoxin-free HEPES Na_2HPO_4 Polybrene

2 X HBS	281 mM NaCl 100 mM HEPES 1.5 mM Na_2HPO_4 0.22 µm filtered
Fixing solution	1% formaldehyde in PBS
FACS buffer	1% FCS in PBS 0.1% sodium azide

3.4.3.1 Production of lentiviral VSV-G pseudotyped vectors

One day before transfection 5 x 10^6 293T cells were plated in a 10 cm tissue culture dish in 10 ml DMEM and incubated overnight. At the time of transfection cells should be around 80% confluent. 2 h before transfection, the medium was replaced with 10 ml fresh DMEM. Cells were co-transfected with 10 µg pHR'SIN-cPPT-SEW, 6.5 µg packaging plasmid pCMV Δ8.91, and 3.5 µg envelope plasmid pMD2.VSV.G using the calcium phosphate DNA precipitation method. The components were placed in 12 ml snap cap tube (Greiner, Kremsmünster) in the following order:

H_2O: 0.1 x TE (1:3)	ad 450 µl
pHR'SIN-cPPT-SEW	10 µg
pCMV Δ8.91	6.5 µg
pMD2.VSV.G	3.5 µg
2.5 M $CaCl_2$	50 µl
	∑ 500 µl

500 µl 2 x HBS were added dropwise to this mixture under vigorous vortexing, and the solution was incubated at room temperature for no longer than 5-10 min. During that time 1 µl chloroquine (100 mM) was added to the cells to a final concentration of ~10 µM, and the DNA precipitation mix was added to the cells, followed by an incubation overnight (14-16 h) under normal cell culture conditions. Next morning the medium was exchanged for 5 ml fresh medium. Supernatants containing the virus were collected after 24 and 48h and cleared through a 0.45 µm filter (prewashed with 1 ml PBS) and stored in aliquots at -80°C.

3.4.3.2 Titration of lentiviral vectors

One day before transfection, 1 x 10^5 cells were plated in 0.5 ml DMEM per well in a 24-well plate. The following day medium was replaced with 0.5 ml of fresh DMEM containing 4 µg/ml polybrene per well. Serial ten-fold dilutions of the viral stocks were prepared and added to the cells resulting in final dilutions from 10^{-2} to 10^{-4}. Plates were centrifuged for 90 min at 1250 x *g*, 32°C, followed by incubation for 2.5 h and a medium exchange (0.5 ml DMEM per well). Cells were incubated under normal cell culture conditions for 2-3 days.

For FACS analysis, cells were harvested, washed twice in PBS containing 1% FCS and 0.1% sodium azide and fixed in PBS containing 1% formaldehyde. FACS analyses for eGFP expression and titre calculation were performed using a FACScan flow cytometer (BD Biosciences) and Cell Quest software (BD Biosciences).

3.4.3.3 Transduction of target cells

Th1 cells (1 x 10^5 cells/400 µl in a 24-well plate) were transduced with different dilutions of the viral supernatant in the presence of 4 µg/ml protamine sulfate. After spinoculation (1250 x *g*, 90 minutes, 32°C), the cells were incubated for 16 hours at 37°C with the virus. The following day, 200 µl per well were removed, and an additional transduction of the virus (200 µl + 400 µl = 600 µl) was performed as described (1250 x *g*, 90 minutes, 32°C). After 6 h incubation, 1 ml of fresh medium was added, followed by a medium exchange the next day. EGFP expression was analyzed by FACS analysis and fluorescence microscopy (Nikon Eclipse TE300) at various time points.

4 Results

4.1 Binding of synthetic TFOs to double-helical DNA *in vitro* and in cells

Triplex formation was examined with two different chemokine targets, RANTES and MCP-1. The ability of synthetic TFOs to bind to the duplex DNA was investigated by gel shift analysis. Furthermore it was tested whether the 28 nt and 19 nt TFOs, respectively, were able to specifically inhibit gene transcription of their target genes in different cell lines. A triplex formed in gene regulatory regions can interfere with the initiation complex, while a triplex formed in the coding region of the target gene may block transcription elongation. Different backbone modifications of oligonucleotides exist that have been proposed to increase the half-life of TFOs and the stability of the triple-helical complexes. With regard to those findings phosphorothioated TFOs were used in cell culture experiments.

4.1.1 Binding of a 28 nt TFO to the murine RANTES promoter

The murine RANTES promoter was tested as a new target for triplex formation. This homopurine/homopyrimidine target sequence of 28 bp in length was chosen as a proinflammatory chemokine of interest out of a high number of possible TFO targets in the mammalian genome, which have been found with a proprietary gene bank search algorithm (Radeke HH & Bruno B, unpublished data). Here specifically, the purine binding motif (GT) was selected, leading to an antiparallel binding of the TFO to its target. Within the RANTES promoter the TFO target site is located at nucleotide position -265 to -238 relative to the transcriptional start site and about 78 bp downstream of a putative NF-κB1 binding site. Interactions between NF-κB and an interferon regulatory factor (IRF) are crucial for the induction of RANTES promoter activity. The capacity of the TFO to interfere with RANTES gene transcription was evaluated in T helper-1 lymphocytes and brain microvascular endothelial cells.

4.1.1.1 In vitro binding of the TFO to the RANTES promoter

To assess the ability of the TFO to form triple helices with the target site in the RANTES promoter, gel mobility shift assays were performed. In gel mobility shift assays, triplex DNA migrates more slowly than duplex DNA because of its decreased charge density. A 48 bp promoter fragment spanning the TFO target sequence and flanking regions was [α-^{32}P]-dCTP end-labelled to allow detection. The promoter fragment was incubated with

different concentrations of the unmodified TFO based on the antiparallel (GT) purine binding motif (for details of the sequences see “Materials and Methods”, Table 3-13) or control oligonucleotide which was a scrambled oligonucleotide of the same base composition. (Figure 4-1). The RANTES TFO binds in a sequence-specific manner to the duplex DNA (10 nm), and a shift from duplex to triplex formation is visible at a TFO concentration of 4.0 x 10^{-7} M. No shift occurs using the scrambled control oligonucleotide, even at the highest concentration (1.6 x 10^{-5} M), demonstrating sequence-specific binding of the TFO.

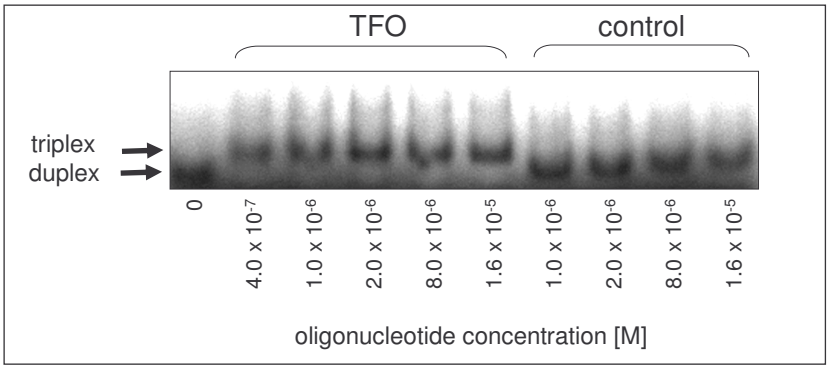

Figure 4-1. *In vitro* determination of triple helix formation by gel mobility shift analysis. Binding of the TFO to duplex DNA was assayed by native gel electrophoresis through 12.5% polyacrylamide gels. The target duplex was the [α-^{32}P]-dCTP end-labelled 48 bp fragment spanning bp -275 to -228 of the murine RANTES promoter. The duplex DNA was incubated for 1 h at room temperature with different concentrations of the TFO, as indicated, in a buffer consisting of 10 mM Tris/HCl (pH 7.4), 5% sucrose, and 10 mM $MgCl_2$. Electrophoresis was performed at 4°C with 80 V. After electrophoresis the gels were dried and exposed to Phospho-Imager screens.

In the experiment shown in Figure 4-2 A, TFO was added at increasing concentrations to samples containing 10 nM of the corresponding radio-labelled RANTES duplex DNA.

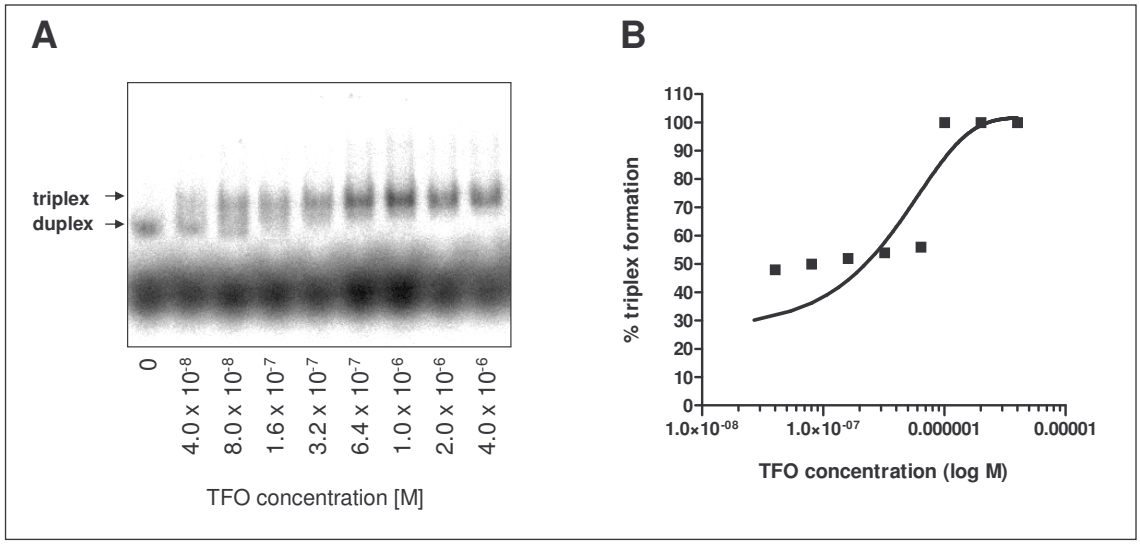

Figure 4-2. Electrophoretic mobility shift assay of triplex formation by RANTES targeting TFO. (**A**): RANTES duplex DNA (10 nM) was incubated with increasing concentrations of TFO. (**B**): Graphic representation of the titration curve.

Binding of the TFO to the target sequence resulted in a shift from duplex to triplex DNA. The 28 nt RANTES TFO formed a triplex DNA even at low concentrations. A distinct band migrating more slowly than duplex DNA was already detected at TFO concentrations of 4.0 x 10^{-8} M, which is a 4-fold molar excess relative to the target DNA. The equilibrium dissociation constant (K_d) for third strand binding was evaluated as the concentration of TFO at which apparent binding was half maximal (Durland et al. 1991). Figure 4-2 B represents the titration curve, and a K_d of 2.5 x 10^{-7} M was determined.

4.1.1.2 Biological effects of the TFO on endogenous RANTES gene expression

Inflammatory cytokines such as TNF-α and INF-γ synergistically activate expression of RANTES. The murine RANTES promoter contains one putative interferon regulatory factor, IRF, and three putative NF-κB binding sites. Both NF-κB and IRF-1 transcription factors mediate the induction of RANTES expression when cells are stimulated by TNF-α and IFN-γ. Here, brain microvascular endothelial cells (b-end3 cells) were incubated for 24 h with TNF-α and IFN-γ (Figure 4-3).

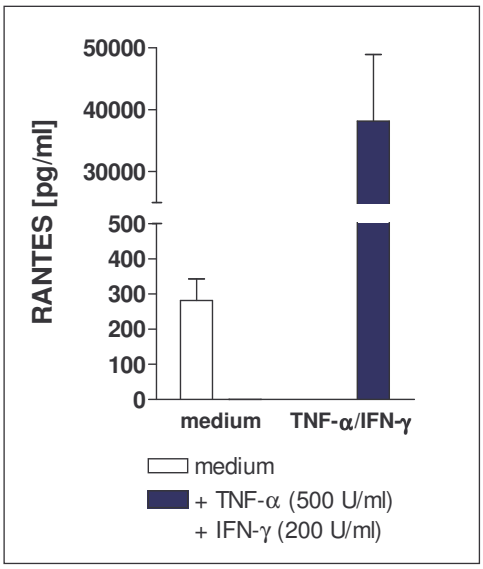

Figure 4-3. Cytokine-induced secretion of the chemokine RANTES by murine brain microvascular endothelial cells. B-end3 cells plated in 6-well plates at a density of 600,000 cells/well were left unstimulated or treated with the indicated cytokines for 24 h. Following cytokine treatment, the culture media were harvested and the concentrations of secreted RANTES were determined by ELISA; error bars indicate the SEM.

In this experimental setup cytokine treatment resulted in a 135-fold upregulation of RANTES protein secretion as measured by ELISA. As a next step the ability of the 28 nt RANTES TFO to bind to the RANTES promoter target sequence and inhibit endogenous RANTES gene expression was analysed. B-end3 cells were transfected with 4.5 µM phosphorothioated TFO (5', 3' end-modified) or scrambled control oligonucleotide (Figure 4-4).

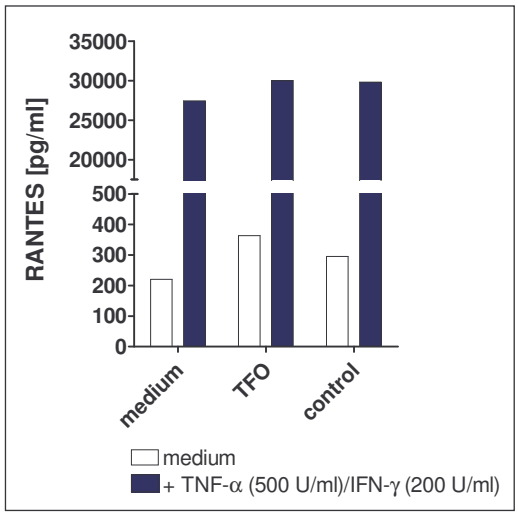

Figure 4-4. Transfection of b-end3 cells with TFOs. B-end3 cells plated in 6-well plates at a density of 600,000 cells/well were transfected with 4.5 µM phosphorothioated 28 nt TFO or control oligonucleotide targeting murine RANTES. After 18 h the cells were left unstimulated or treated with 500 U/ml TNF-α and 200 U/ml IFN-γ for additional 24 h. Following the incubation time, the culture media were harvested and the concentration of secreted RANTES was determined by ELISA. One experiment of three with similar results is shown.

Although there was a sequence-specific binding of the TFO detectable in the gel shift assays, there was no inhibitory effect of the exogenously added and phosphorothioate stabilised TFO on endogenous RANTES gene expression visible, neither in the unstimulated nor in the cytokine treated cells. Furthermore, potential inhibitory effects of the TFO were examined in another cell line.

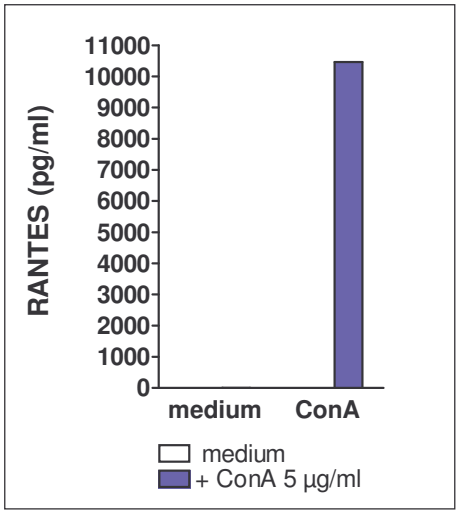

Figure 4-5. Secretion of RANTES by Th1 cells. Th1 cells plated in 6-well plates at a density of 1 x 10^6 cells/well were left unstimulated or treated with 5 µg /ml ConA for 24 h. Following the incubation time, the culture media were harvested and the concentration of secreted RANTES was determined by ELISA.

Murine Th1 cells exhibited an inducible RANTES protein secretion to up to 10 ng/ml after incubation with 5 µg/ml ConA for 24 h, but there was no basal RANTES secretion measurable in untreated cells (Figure 4-5).

In a subsequent experiment, Th1 cells were transfected with phosphorothioated TFO or scrambled control oligonucleotide at the indicated concentrations (Figure 4-6). Here, TFO treatment did not result in the proposed inhibition of RANTES gene expression, but led to variable and inconsistent effects on RANTES protein secretion. These results might be due to different efficiencies of oligonucleotide transfection.

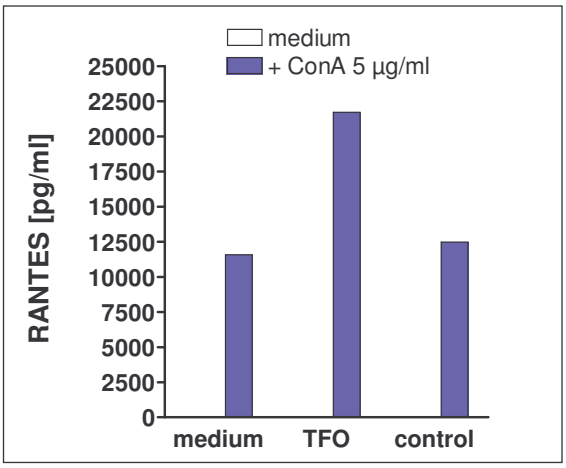

Figure 4-6. Transfection of Th1 cells with TFO. Th1 cells were plated in 6-well plates at a density of 1 x 10^6 cells/well and transfected with 4.7 µM phosphorothioated 28 nt TFO or control oligonucleotide against murine RANTES. After 18 h the cells were left unstimulated or treated with 5 µg/ml ConA for additional 24 h. Following the incubation time, the culture media were harvested and the concentration of secreted RANTES was determined by ELISA.

In summary, with respect to the chemokine RANTES, binding of the 28 nt TFO to the promoter target sequences could be shown in a cell-free system *in vitro*, but the TFO did not functionally inhibit endogenous RANTES gene expression in two different cell systems tested. Even when lower or higher oligonucleotide concentrations were used they had no inhibitory effect (data not shown).

Oligonucleotides must be delivered to the cell nucleus in adequate concentrations and must be stable in extracellular and intracellular environments. The use of synthetic TFOs *in vivo* might be limited by their susceptibility to endogenous nucleases or inefficient cellular uptake. The RANTES TFO is G-rich and contains several Gs in a row (5'TTT GTT GGT GGG GGT GGG GGT GGG GGT G 3'), therefore it might tend to self-association into unfavourable structures in the presence of intracellular concentration of K^+, which then would compete with triplex formation. Thus, to increase the capacity of TFOs as gene modifying agents, it appeared necessary to establish an improved TFO delivery system.

4.1.2 Binding of a 19 nt TFO to the MCP-1 promoter

A possible TFO target site consisting of 19 bp was identified in the promoter region of the human MCP-1 at bp -66 to -48 relative to the transcriptional start site. The TFO target site includes the binding site for the transcription factor SP-1 and a partially overlaps with a putative AP-1 binding site.

4.1.2.1 Triplex formation with the MCP-1 promoter

As described before, triplex formation was demonstrated by gel mobility shift analysis. A 39 bp promoter fragment (10 nM) spanning the TFO target sequence and flanking regions was [α-^{32}P]-dCTP end-labelled to allow detection. The promoter fragment was incubated with 10 µM of the 19 nt TFO based on the antiparallel purine binding motif (GT) or the control oligonucleotide which was a scrambled oligonucleotide of the same base composition (for details of the sequences see “Materials and Methods”, Table 3-14). The aim was to develop a TFO that could be tested in biological systems, therefore oligonucleotides contained a 3’ and 5’ phosphorothioate modification since it confers resistance to nuclease degradation. Under the conditions used, triple helical complexes are stable during the course of the electrophoresis run and migrate significantly slower than the corresponding duplex target (Figure 4-7). The triple helix formation was sequence-specific, because the control oligonucleotide did not bind to the MCP-1 promoter fragment. To further confirm sequence-specificity, the TFO and control were incubated with a RANTES promoter sequences as a control duplex DNA. No binding occurred using this unrelated target sequence.

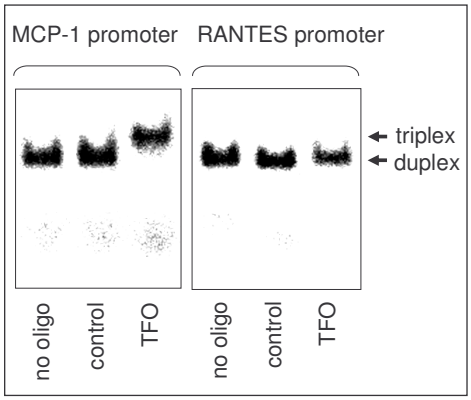

Figure 4-7. *In vitro* determination of triple helix formation by gel mobility shift assay. Binding of the TFO or control oligonucleotide to duplex DNA was assayed by native gel electrophoresis through 12.5% polyacrylamide gels. The target duplex was the [α-^{32}P]-dCTP end-labelled 39 bp fragment spanning bp -76 to -38 of the human MCP-1 promoter. The promoter fragment was incubated with 10 µM TFO or control oligonucleotide. The RANTES promoter served as a control duplex to exclude unspecific binding.

4.1.2.2 Inhibition of the expression of endogenous MCP-1 in cultured cells

A next aim was to test whether the TFO can inhibit expression of MCP-1 in cultured cells. Human MCP-1 is produced in a wide variety of cell types, including monocytes, fibroblasts, vascular endothelial cells, and smooth muscle cells, in response to various stimuli such as LPS, IL-1β, TNF-α, PDGF, IFN-γ and TPA: Here, HEK 293 cells were screened by ELISA for cytokine induced secretion of MCP-1. These cells were found to produce low basal concentrations of MCP-1, and TNF-α and IFN-γ alone or in combination dose dependently induced secretion of higher levels of this chemokine (Figure 4-8).

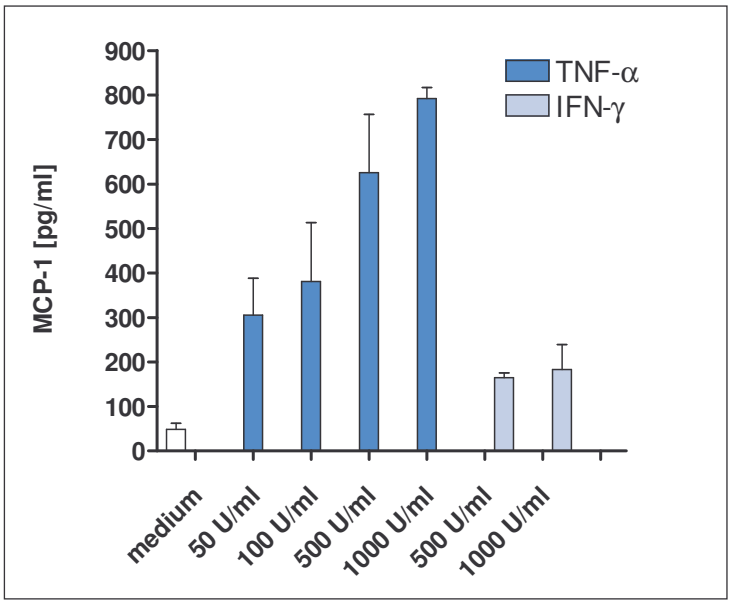

Figure 4-8. Cytokine inducible secretion of the chemokine MCP-1 by HEK 293 cells. HEK 293 cells plated in 24-well plates at a density of 250,000 cells/well were left unstimulated or treated with the indicated cytokines for 24 h. Following cytokine treatment, the culture media were harvested and the concentrations of secreted MCP-1 were determined by ELISA. The cell cultures were performed in duplicates; the error bars indicate the SEM.

After 24 h, TNF-α increased the amount of secreted MCP-1 up to 16-fold and IFN-γ up to 3.8-fold in comparison to unstimulated cells. PDGF (5-25 ng/ml) was used as another stimulus but had no significant inducing effect in these cells (data not shown). HEK 293 cells can therefore serve as a model system to study MCP-1 gene expression, and this cell line was chosen for additional experiments, employing TNF-α as an effective and concentration dependent stimulus. To analyse the effect of the TFO on MCP-1 gene expression, cells were treated with various concentrations of phosphorothioated TFO for 24 h (Figure 4-9). Incubation of the cells with 0.5 µM TFO inhibited TNF-α stimulated MCP-1 protein secretion about 23% in comparison to the scrambled control oligonucleotide, as determined by ELISA. At 2 µM concentration the inhibition was 25% in comparison to the control. But, at this concentration, the control oligonucleotide itself resulted in a slight decrease of MCP-1 protein secretion in comparison to the medium control, suggesting that higher concentrations of

oligonucleotides might not be beneficial in this experimental setup. Higher concentrations of the oligonucleotides resulted in decreased cell viability with decreased secretion of MCP-1 (data not shown). No inhibitory effect of the TFO at different concentrations was observed in unstimulated cells.

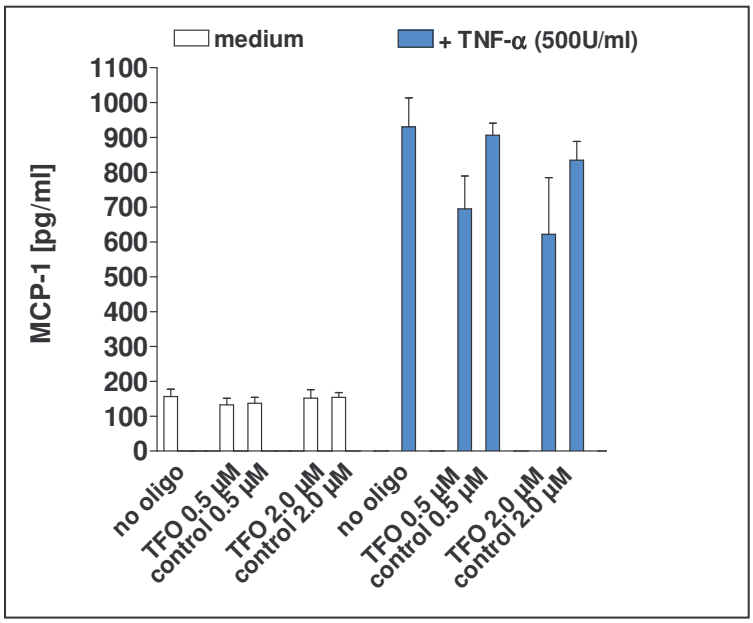

Figure 4-9. Inhibition of MCP-1 secretion by incubation with the TFO. HEK 293 cells plated in 96-well plates at a density of 50,000 cells/well were pre-treated with 0.5 µM or 2 µM phosphorothioated TFO or control oligonucleotides, as indicated, for 24 h. Thereafter, the medium (200 µl/well) was replaced with medium containing the same concentration of oligonucleotides as before, and the cells were cultured for additional 24 h in the absence or presence of 500 U/ml TNF-α. At the end of incubation time, the culture supernatants were harvested and the concentrations of MCP-1 were determined by ELISA. The cell culture was performed in quadruplicates; the error bars indicate the SEM.

As the TFO activity depends on the amount of oligonucleotides reaching the nucleus, the procedure of administration of the oligonucleotides to the cell is an important issue. Oligonucleotides are anionic molecules whose capacity to cross the cell membranes is poor and dependent on the type of cells. Apart from other possible solutions to approach these problems an intracellular, vector-based delivery of TFOs seemed promising. Generating oligonucleotides *in vivo* avoids the problems of e.g. immunogenicity, cellular uptake and dosing. In the following experiments, establishment of the intracellular synthesis of a RNA TFO targeting the human MCP-1 gene will be described.

4.2 Inhibition of MCP-1 gene expression by intracellular generated TFOs

In order to generate TFOs directly inside the cell an expression vector was constructed generating single-strand RNA transcripts, which may act as TFOs and thereby inhibit MCP-1 expression (Figure 4-10 A).

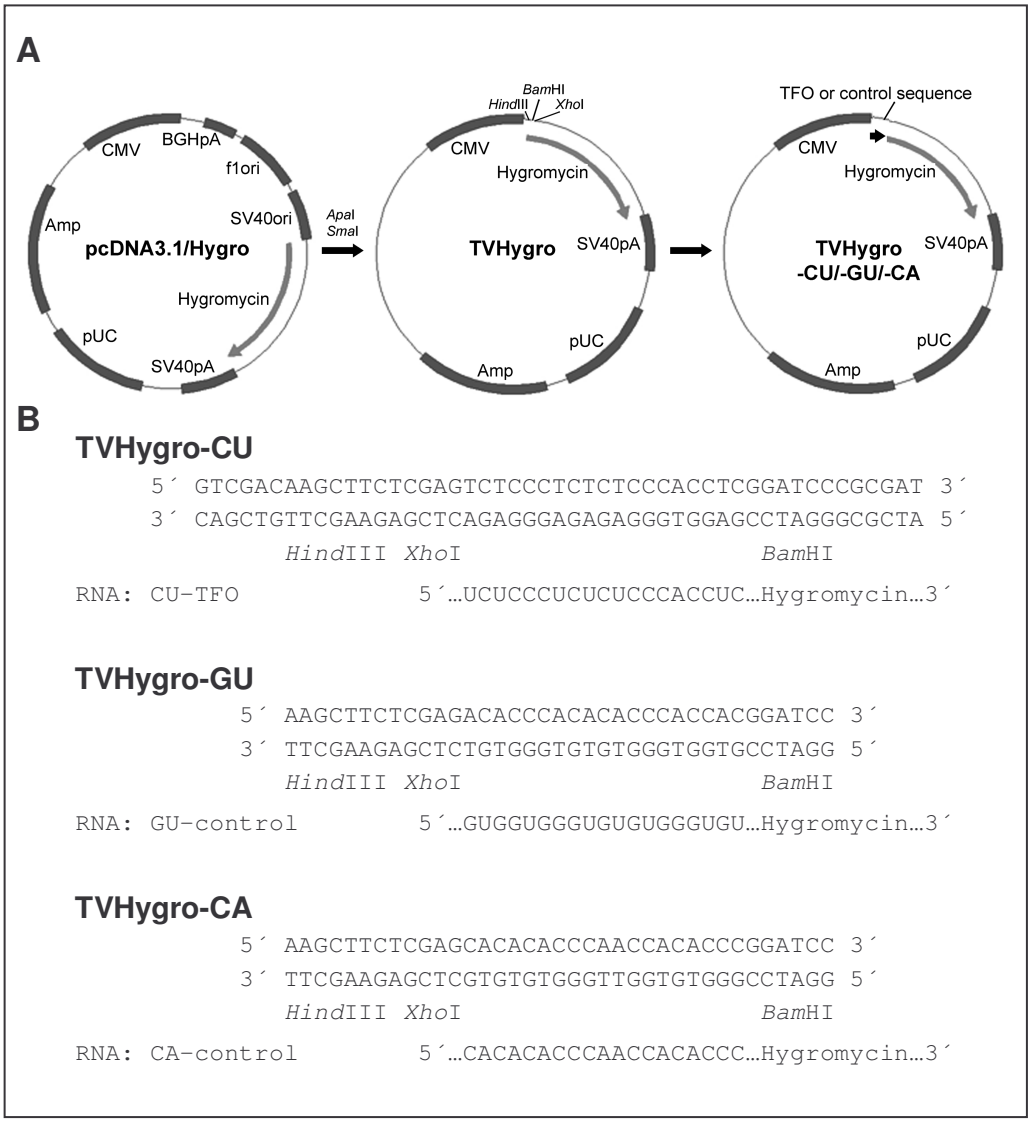

Figure 4-10. Schematic representation of the vector construction. (**A**): The vector TVHygro was derived from the eukaryotic expression vector pcDNA3.1/Hygro with the sequences spanning the region 1002-2079 deleted by restriction digestion with *Apa*I and *Sma*I. The resulting *Apa*I overhang was end-filled and the vector re-ligated. TFO-RNA or control-RNA coding sequences were cloned into the 5' untranslated region of the hygromycin resistance gene. Transcription of this TFO/hygromycin and control/hygromycin fusion transcript, respectively, is driven by the constitutive CMV promoter. Vectors were constructed to drive transcription of either a pyrimidine triplex forming RNA sequence targeting the MCP-1 promoter (CU-TFO) or two different control sequences (CA-control and GU-control). The three different constructs which were cloned into TVHygro are shown in (**B**), leading to the vectors TVHygro-CU, TVHygro-GU and TVHygro-CA, respectively. Vector TVHygro without insert was used as a third control vector.

DNA fragments coding for a 19 nt parallel binding CU-TFO or different control sequences were inserted into the 5' untranslated region of the hygromycin resistance gene of the eukaryotic expression vector TVHygro (Figure 4-10 B). The pyrimidine motif carrying TFO was chosen because triplex formation is unlikely to occur in the purine motif with RNA binding to a DNA duplex (RNA∗DNA:DNA) (Noonberg et al. 1994a; Semerad and Maher, III 1994). Furthermore, the formation of undesired structures which compete for triplex formation is reduced with a pyrimidine oligoribonucleotide (Lacroix et al. 1996). In a first experiment it was analysed whether the 19 nt pyrimidine TFO binds to the MCP-1 promoter sequence.

4.2.1 Triplex formation with RNA-TFOs

The experiments revealed that the synthetic 19 nt TFO (rCU-TFO) effectively and specifically initiated triplex formation with the 39 bp MCP-1 promoter duplex *in vitro*. The capacity of synthetic oligoribonucleotides to bind to the MCP-1 promoter was investigated by a method termed triplex blotting. Triplex blotting is a general technique described for the detection of specific RNA molecules capable of triplex formation (Noonberg et al. 1994b). Here, different concentrations (0.025 – 1.0 nmol) of the oligoribonucleotides were electrophoretically fractionated, transferred to a nylon filter, and hybridised with the radio-labelled 39 bp MCP-1 promoter template.

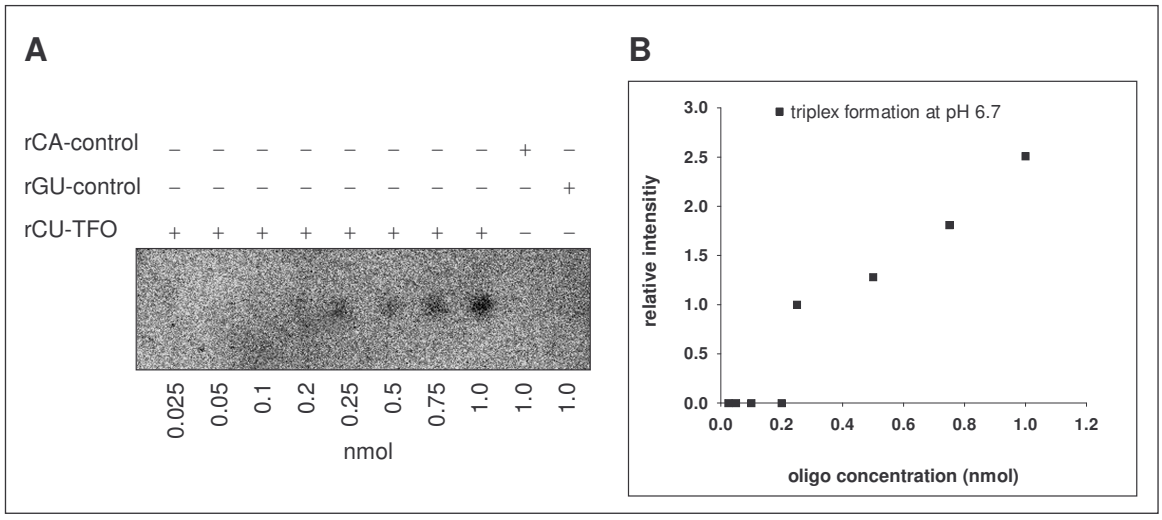

Figure 4-11. Participation of the pyrimidine rCU-TFO in triplex formation at pH 6.7. (**A**): The synthetic 19 nt oligonucleotides rCU-TFO, rGU-control and rCA control (0.025-1.0 nmol) were electrophoretically fractionated through a 6% polyacrylamide gel containing 7 M urea and blotted to a nylon membrane. Hybridisation with the radioactive labelled 39 bp MCP-1 promoter duplex (~3 x 10^{-3} nmol) was carried out overnight at 30°C. Hybridisation and stringency washes were performed at pH 6.7. (**B**): Concentration dependent binding of rCU-TFO to the duplex is shown.

Figure 4-11 A demonstrates the predicted and specific detection of triplex-forming rCU-TFO by triplex blotting with a minimum of 0.25 nmol transferred RNA at pH 6.7. rCA-control and rGU-control were not detected by the labelled double-stranded probe even at the highest concentration (1 nmol), suggesting that these RNA species are not able to form triplex structures. Concentration dependent binding of the rCU-TFO at pH 6.7 is shown in Figure 4-11 B. The concentration of the 39 bp MCP-1 promoter was calculated to be 3 x 10^{-3} nmol. Under these conditions binding of the duplex DNA to the rCU-TFO could be observed at an 83.3 fold molar excess of the TFO in comparison to the duplex DNA. Notably, binding of the duplex DNA to the rCU-TFO was more pronounced at low pH 5.5 (data not shown) These results are in agreement with other investigations (see “Discussion”), as triplex formation involving the pyrimidine binding motif is dependent on cytosine protonation and therefore more likely to occur at low pH. At pH 5.5 binding of the duplex to 0.25 nmol rCU-TFO was 19 times stronger than binding at pH 6.7. Nevertheless, the data clearly show that there is a strong triplex formation at pH 6.7 close to the physiological intracellular pH range. To underline binding specificity employing the pyrimidine motif an oligoribonucleotide with a single mismatch (19CU_M) was tested.

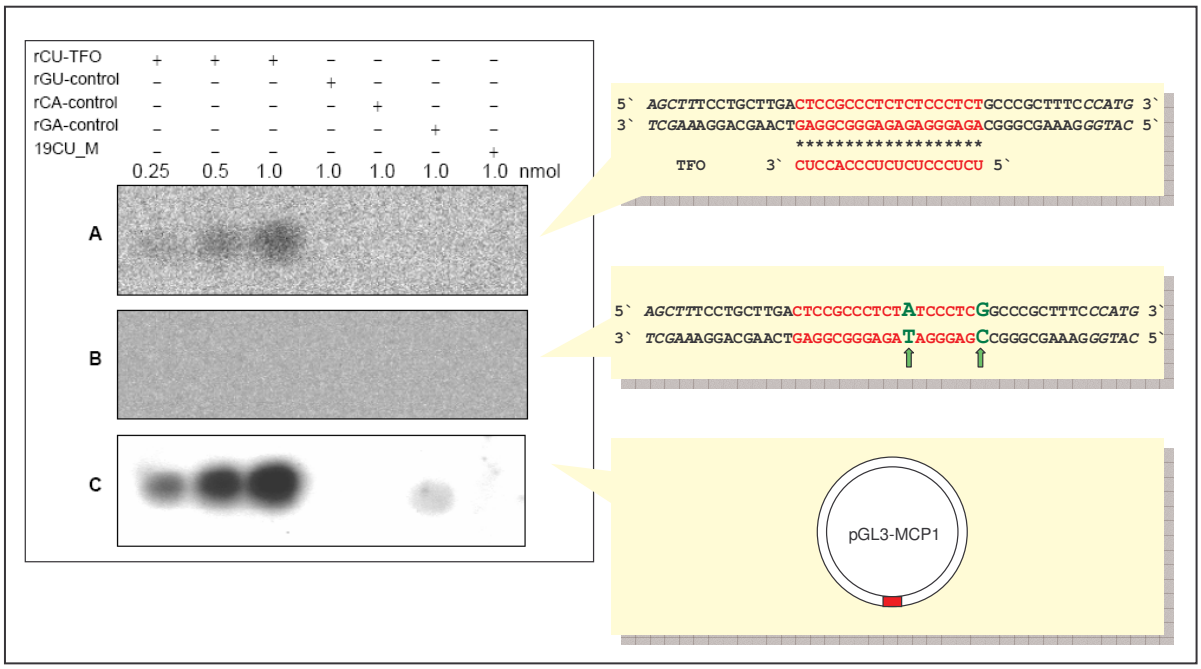

Figure 4-12. Specific binding of the 19 nt rCU-TFO to the MCP-1 promoter duplex. (**A**): Synthetic 19 nt oligoribonucleotides (0.25-1.0 nmol) were electrophoretically fractionated through a 6% polyacrylamide gel containing 7 M urea and blotted to a nylon membrane. Hybridisation with the radioactive labelled 39 bp MCP-1 promoter (~3 x 10^{-3} nmol) was carried out overnight at 37°C. Hybridisation and stringency washes were performed at pH 5.5. (**B**): Hybridisation was performed as described but with a MCP-1 promoter duplex containing 2 mismatches at position 1 and 8 of the TFO binding site. (**C**): Blots were stripped for 1 h at 70°C in 0.5 x NAE (50 mM sodium acetate, 0.5 mM pH 7.5) and re-probed with the linearised plasmid pGL3 control containing the 39 bp MCP-1 promoter sequence as described above.

In Figure 4-12 A it was demonstrated that the duplex DNA did not bind to 1.0 nmol 19CU_M, confirming the sequence dependent specificity of triplex formation in this experimental setup. No triplex formation occurred using the rGA-control, which represents an antiparallel, purine binding motif. As a further control it was demonstrated that a 39 bp MCP-1 duplex with two mismatches exhibited no interaction with any of the shown oligos (Figure 4-12 B). In a following experiment it could be excluded that the observed binding was due to non-sequence-specific interactions of the rCU-TFO with the duplex DNA. In principle it would be possible that binding occurs through D-loop formation with partial melting of the 39 bp target duplex DNA. Therefore, a circular double-stranded plasmid containing the 39 bp MCP-1 promoter duplex as a target was used for hybridisation in triplex blotting experiments, which drastically reduces the likelihood of D-loop formation. Figure 4-12 C confirms that a specific binding of the 19 nt rCU-TFO to the plasmid encoded target duplex occurred, whereas the control 19CU_M with one mismatch failed to bind to the target. Interestingly, in this experimental setting (pH 5.5) a weak binding of the antiparallel rGA-control to the target duplex was observed, indicating a marginal binding affinity. These results are summarised in Table 4-1.

Table 4-1. Summary triplex formation

oligo	sequence	properties	motif	triplex formation
rCU-TFO	5`UCUCCCUCUCUCCCACCUC		paralell, pyrimidine binding motif	yes
19CU_M	5`UCACCCUCUCUCCCACCUC	1 mismatch	paralell, pyrimidine binding motif	no
rGA-control	5`GAGGUGGGAGAGAGGGAGA		antiparalell, purine binding motif	weak binding
rGU-control	5`GUGGUGGGUGUGUGGGUGU		antiparalell, purine binding motif	no
rCA-control	5`CACACACCCAACCACACCC	scrambled	none	no

duplex	sequence	properties	triplex formation
MCP-1	5`*AGCTT*TCCTGCTTGA**CTCCGCCCTCTCTCCCTCT**GCCCGCTTTC*CCATG* 3` 3`*TCGAA*AGGACGAACT**GAGGCGGGAGAGAGGGAGA**CGGGCGAAAG*GGTAC* 5`		yes
MCP-1_2M	5`*AGCTT*TCCTGCTTGA**CTCCGCCCTCTATCCCTCG**GCCCGCTTTC*CCATG* 3` 3`*TCGAA*AGGACGAACT**GAGGCGGGAGATAGGGAGC**CGGGCGAAAG*GGTAC* 5`	2 mismatches	no

Summary of the analysed oligoribonucleotides and duplexes in triplex blotting experiments. Participation of the different synthetic 19 nt oligos in triplex formation, the 39 bp MCP-1 promoter duplex, and the duplex-containing 2 mismatches. Positions of mismatches are underlined.

4.2.2 Intracellular expression of TFO in HEK 293 cells

After demonstrating that the synthetic rCU-TFO binds in a sequence-specific fashion to the MCP-1 promoter, the presence of the three different intracellular generated RNA oligonucleotides in the stable transfected cell lines was verified. Because on the one hand the interfering CU-TFO had to be present in the nuclei to exert its function and on the other hand the template for the hygromycin resistance protein had to reach cytosol, nuclear RNA and total RNA containing the cytosolic fraction were separately isolated from each cell line carrying the vectors TVHygro-CU, TVHygro-GU or TVHygro-CA. Isolated RNA was reverse transcribed and subjected to PCR (Figure 4-13).

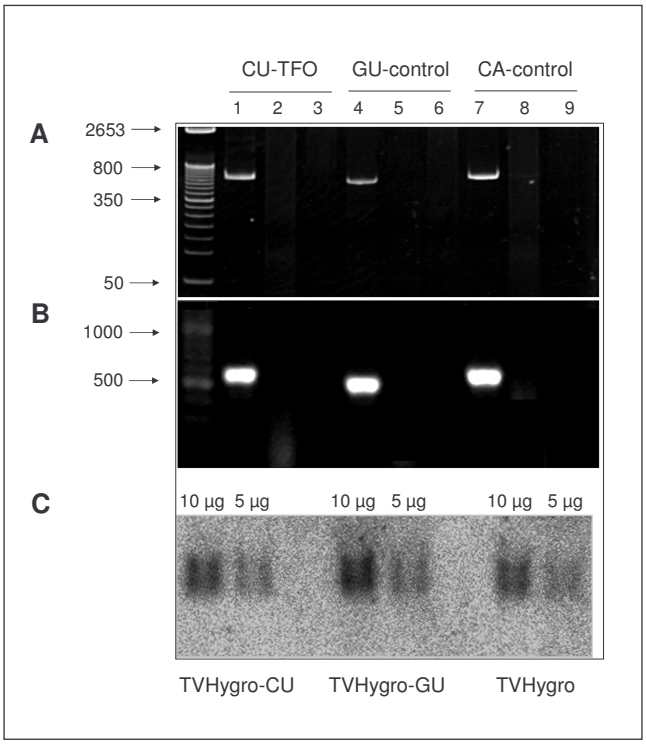

Figure 4-13. Presence of CU-TFO, GU-control and CA-control in the nuclei of stable transfected HEK 293 cells. (**A**): RNA from cell nuclei was isolated as described in "Materials and Methods" from each cell line TVHygro-CU, TVHygro-GU and TVHygro-CA and reverse transcribed. RT-PCR was performed using a specific upstream primer located in the 19 nt TFO and control-RNA coding sequence, respectively, and a downstream primer located in the hygromycin resistance gene. The calculated length of the amplified products were 578 bp (CU-TFO and CA-control) and 522 bp (GU-control). RT-PCR products were electrophoretically fractionated through a 12.5% native polyacrylamide gel. (**B**): Total RNA was isolated from each cell line and reverse transcribed. RT-PCR was carried out as described and products were electrophoretically fractionated through a 1% agarose gel. Lane 1: product CU-TFO, lane 4: product GU-control, lane 7: product CA-control. Lane 2, 5 and 8: Control reactions without reverse transcription to exclude DNA contamination. Lane 3: Control reactions with primer pair combination specific for GU-control. Lane 6 and 9: Control reactions with primer pair combination specific for CU-TFO. (**C**): For Northern blot analysis, 5 or 10 µg RNA per lane were electrophoresed through a formaldehyde-agarose gel and transferred to a nylon membrane. Hybridisation was performed using a radio-labelled, denatured cDNA-probe specific for the hygromycin resistance gene RNA.

Because the TFO and control sequence, respectively, were transcribed in line with the hygromycin resistance gene as one fusion transcript, the RT-PCR was performed using specific upstream primers for the 19 nt CU-, GU- or CA-RNA coding sequences and a downstream primer located within the hygromycin resistance gene. These primer pair combinations should result in an amplified product of 578 bp in TVHygro-CU and -CA cell lines and of 522 bp in TVHygro-GU cell lines, because different restriction enzymes were used for the cloning (see "Materials and Methods"). Figure 4-13 A shows that the expected specific RNA sequence was present in each cell line (lane 1, 4 and 7) in the nuclei. Additionally, Figure 4-13 B confirms this finding when total RNA containing the cytosolic fraction was used as PCR template. Control reactions were performed without reverse transcription to exclude DNA contamination (lane 2, 5 and 8). To confirm the exclusive presence of the CU-TFO generated in TVHygro-CU cell lines and the control-RNA generated in TVHygro-CA and -GU cell lines, control reactions were performed using the primer pair for CU-TFO detection with the two control-RNA templates, and the primer pair for the control-RNA for the CU-TFO extract. Excluding vector cross-contamination no PCR product was detectable in the respective samples (see lane 3, lanes 6 and 9, respectively). The different RNA species are synthesised in equal amounts in each cell line as shown by Northern blot analysis using a specific 522 bp antisense probe for the hygromycin resistance gene mRNA (Figure 4-13 C).

4.2.3 Binding of the TFO/ hygromycin fusion transcript to the MCP-1 promoter

The predicted CU-TFO produced inside HEK 293 cells is a fusion transcript of the 19 nt triplex forming sequence and the messenger RNA of the hygromycin resistance gene. Therefore, an *in vitro* experiment was established to demonstrate that not only the synthetic 19 nt CU-TFO but also the large single-stranded RNA fusion transcript containing the CU-TFO binds to the MCP-1 promoter duplex in a sequence-specific manner. The RNA transcripts of different vectors TVHygro (without insert), TVHygro-CU, -CA and –GU were generated by *in vitro* transcription using T7 polymerase. Transcripts in the length of about 1.1 kb contained the TFO or control sequence plus the hygromycin resistance gene mRNA. Binding of the fusion transcript to its MCP-1 target sequence was characterised *in vitro* with the set-up of a novel magnetic capture technique. The principle of these experiments is shown in Figure 4-14.

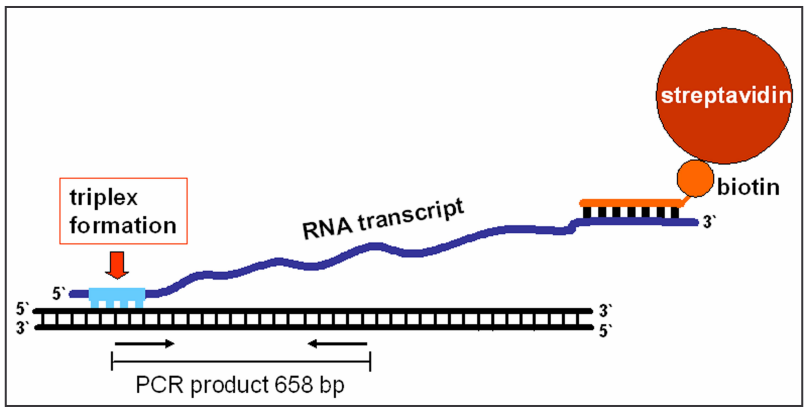

Figure 4-14. Capture assay for the evaluation of specific TFO binding to the MCP-1 promoter fragment. The 39 bp MCP-1 promoter fragment containing the TFO binding site was cloned into a plasmid and could be captured using a biotin/streptavidin-based mechanism. The captured target-plasmid was identified by PCR amplification. To compare the relative amount of bound plasmid to the TFO or control transcripts, a semi-quantitative PCR was performed.

4.2.3.1 In vitro transcription of the 1.1 kb TFO/hygromycin fusion transcript

Vector fragments containing the TFO or control sequences and part of the hygromycin resistance gene were amplified by PCR (Figure 4-15 A). PCR products included the T7 promoter sequence and were used for *in vitro* transcription using T7 polymerase. In Figure 4-15 B it is shown that the *in vitro* transcription resulted in intact RNA transcripts in the length of about 1.1 kb.

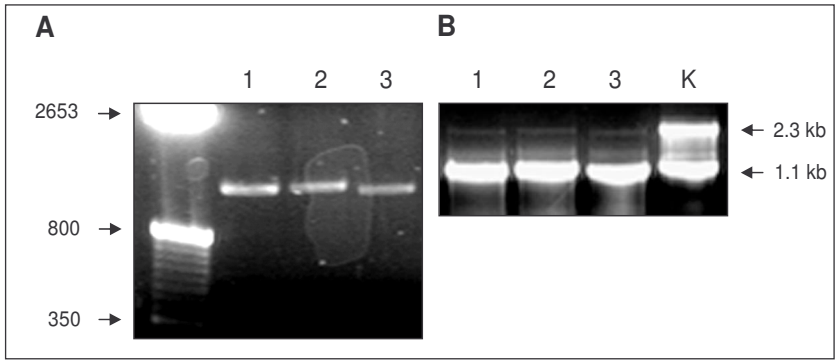

Figure 4-15. *In vitro* transcription of the vector encoded CU-TFO or control sequences. Vector sequences including the T7 promoter sequence were amplified by PCR and used as templates for *in vitro* transcription. Correct sizes of the PCR products and the transcribed RNA were proven by electrophoresis on 1% agarose gels. The sizes of the different PCR products for *in vitro* transcription are shown in (**A**); empty vector 1212 bp (lane 1), vector coding CU-TFO 1219 bp (lane 2), and vector coding GU-control 1181 bp (lane 3) (**B**): Estimated sizes of transcribed RNA due to the transcriptional start site at the T7 promoter; 1142 bp (empty vector, lane 1), 1149 bp (CU-TFO, lane 2) and 1111 bp (GU-control, lane 3). K= *in vitro* transcribed control template provided by the supplier produces two transcripts of 2.3 and 1.1 kb in size.

For magnetic capture the RNA transcripts were annealed to a complementary biotinylated oligonucleotide of 30 nt. This oligonucleotide was positioned at the 3' end of the RNA transcript, whereas the 19 nt TFO binding site was located at the 5' end. Hybridisation was performed for 1 h at RT. Annealing of the oligonucleotide to the RNA transcript was confirmed by gel electrophoresis, analysing the hybridisation complex and the biotinylated oligonucleotide alone, respectively. In Figure 4-16, lane 1 and 2, it is demonstrated that almost the complete amount of oligonucleotide was bound to the complementary part of the RNA, indicating that in the subsequent experiments intact and correctly biotinylated RNA transcripts were used.

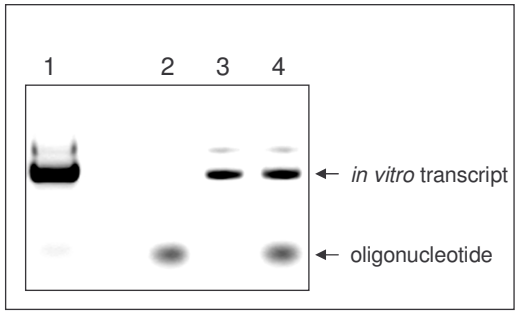

Figure 4-16. Labelling of the *in vitro* transcribed RNA with a biotinylated oligonucleotide. Annealing of the biotinylated oligonucleotide to *in vitro* transcribed RNA was confirmed by gel electrophoresis through a 1% agarose gel. Lane 1: 57 pmol (~20 µg) *in vitro* transcribed RNA were denatured for 5 min at 90°C and mixed with 57 pmol of biotinylated oligonucleotide in annealing buffer (100 mM potassium acetate, 30 mM HEPES, 2 mM magnesium acetate, pH 7.4) and incubated for 1 h at room temperature. Lane 2: 57 pmol of biotinylated oligonucleotide without RNA. Lane 3: 1 µg of the *in vitro* transcript. Lane 4: 1 µg of RNA transcript plus 57 pmol of biotinylated oligonucleotide without annealing reaction.

4.2.3.2 Semi-quantitative PCR

To compare the relative amount of bound plasmid containing the 39 bp MCP-1 promoter fragment to the TFO or control transcripts, a semi-quantitative PCR was established. Therefore, PCR was performed with 15-34 cycles, using 1.1 ng of the plasmid as a template (Figure 4-17). For product amplification two different primer pairs have been used: primer pair I contained an upstream primer which was set at the MCP-1 promoter target site and a downstream primer which was specific for the pGL3 vector, leading to a PCR product of 658 bp in length. The upstream primer was chosen to detect only recombinant vectors with the MCP-1 insert and not the wild-type vector without the target sequence. Primer pair II contained the same downstream primer but the upstream primer was vector-specific as well and did not include the MCP-1 promoter target site, leading to a product of 520 bp.

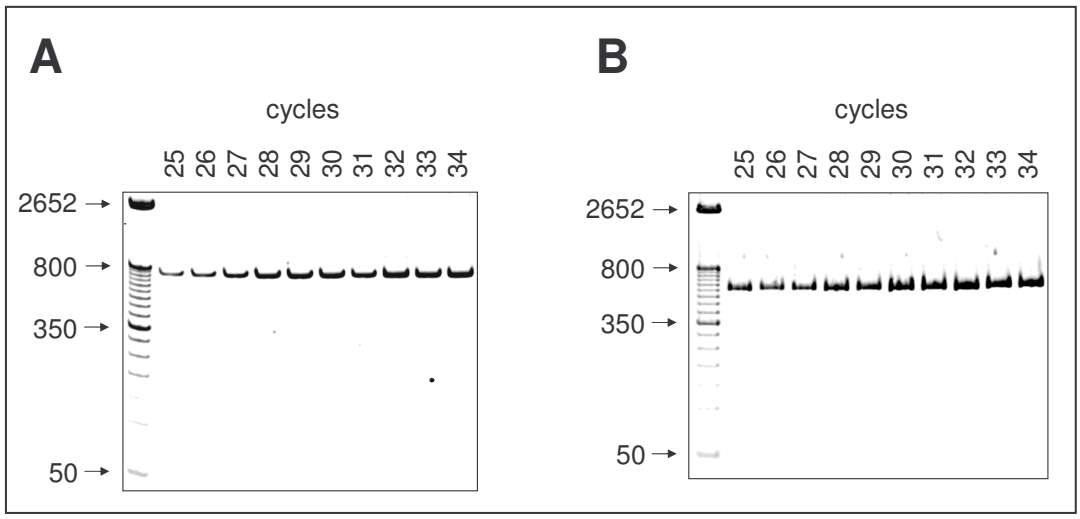

Figure 4-17. Amplification of the vector pGL3 control containing the 39 bp MCP-1 promoter fragment. PCR was performed using Platinum *Taq* DNA polymerase. Cycler conditions: 94°C for 2 min followed by 15-34 cycles of 94°C for 30 sec, 55°C for 30 sec and 72°C for 1 min. The following oligonucleotide primers were used at a 200 nM final concentration. (**A**): Primer pair I with upstream primer 5'AAGCTTTCCTGCTTGACTCC and downstream primer 5'AGACCAGTAGATCCAGAGGA, leading to a PCR product of 658 bp. (**B**): Primer pair II with upstream primer 5'AGAGATACGCCCTGGTTCCT and downstream primer 5'AGACCAGTAGATCCAGAGGA, leading to a PCR product of 520 bp.

A series of PCRs was carried out to determine the linear amplification range as a function of the number of cycles. In theory, DNA amplification is an infinite logarithmic process. But, DNA amplification at higher cycle numbers begins to slow down. This may be due to lower *Taq* polymerase activity, availability of substrates, or saturation of PCR products. The plateau phase can be visualised and quantified densitometrically after gel electrophoresis of the PCR products taken from different cycle numbers.

Here, amplification was linear between 25 and 28 cycles for both primer pairs. Thus, for the following experiments 25 cycles were chosen (Figure 4-18). PCR was performed with increasing amounts of template from 1.4 pg to 1.4 ng to ensure that the amplification remained in the linear phase and does not extend to the plateau phase. The products were then analysed by densitometry. These control experiments showed that the chosen conditions resulted in linear amplification for both primer pairs.

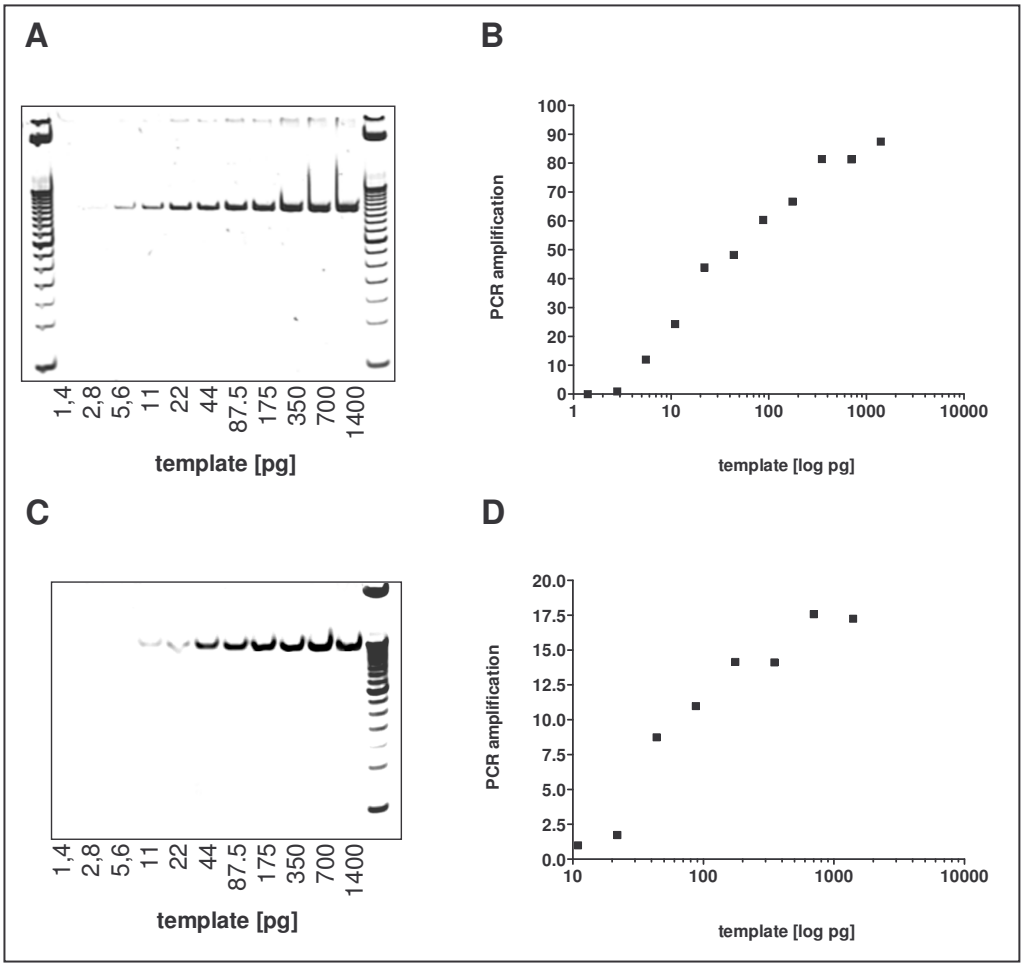

Figure 4-18. Semi-quantitative PCR. PCR was performed with 25 cycles and increasing amounts template as indicated. (**A**): PCR with primer pair I leading to a product of 520 bp in length; the respective densitometry is shown in (**B**). (**C, D**): PCR with primer pair II leading to a product of 658 bp in length.

4.2.3.3 Magnetic capture of triplex complexes

As a next step, the ability of the TFO/ fusion transcript to selectively bind to its MCP-1 target sequence was tested. Before each experiment, the amount and the quality of the control and TFO transcripts, respectively, were checked by gel electrophoresis to confirm that equal amounts of RNA were used (Figure 4-19 A). Then, the transcribed RNA (control and TFO) was annealed to the biotinylated oligonucleotide at equimolar amounts and incubated with the MCP-1 target sequence integrated within the pGL3 plasmid for 1 h. The results in Figure 4-12 C already demonstrated that the synthetic 19 nt CU-TFO was able to recognise and bind to the vector embedded MCP-1 target duplex in a sequence-specific manner via triplex formation. Here, the triplex complexes or control reactions were captured via the annealed and biotinylated RNA onto streptavidin coated magnetic beads and applied to separation columns in a magnetic field. To remove unbound RNA and plasmid, four washing steps were performed using the triplex binding buffer and in a final step the complexes were

eluted. Each fraction was saved for RNA analysis on a gel. In Figure 4-19 B one typical example of the washing and elution fractions during the magnetic separation is shown.

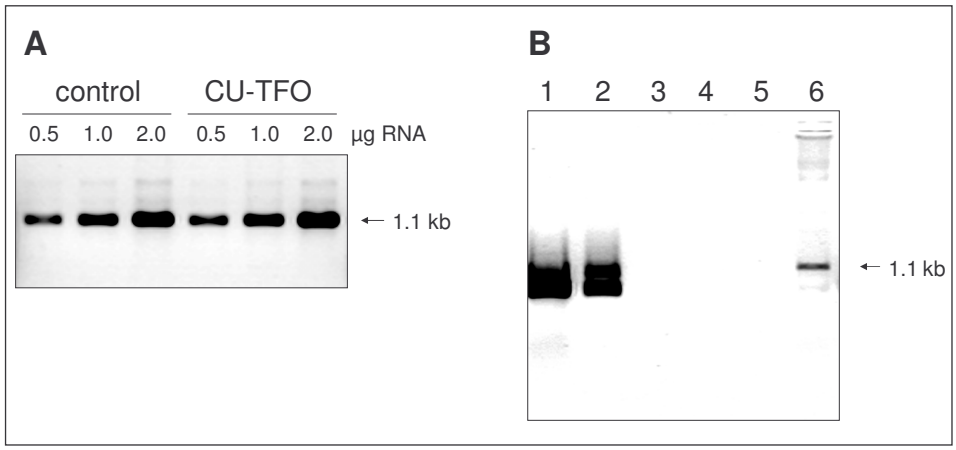

Figure 4-19. Stability of the magnetically labelled RNA during the separation steps. (**A**): Concentration and quality of the *in vitro* transcripts containing the control or CU-TFO sequence were analysed by electrophoresis through a 1% agarose gel before each individual experiment. (**B**): The biotinylated RNA transcripts were incubated with the plasmid pGL3 control containing the 39 bp MCP-1 promoter duplex to allow triplex formation. The RNA was magnetically labelled using streptavidin micro beads and the binding reaction was applied on top of the column. The magnetically labelled triplex complexes are retained on the column. All washing and elution fractions were saved and 40 µl of each fraction were subjected to electrophoresis through a 1% agarose gel. 1: binding reaction, flow-through; 2-5: wash; 6: eluate.

The entire unbound RNA was removed in the flow through and the first washing step (lanes 1 and 2), whereas the captured RNA-plasmid complexes remained on the column during further washing steps (lanes 3-5). At the elution step (lane 6) the RNA was released again and represented the amount of specifically bound RNA to the streptavidin beads. The relative amount of RNA in the elution step of the TFO and control samples, respectively, was quantified densitometrically. To allow quantitative comparison of bound plasmid to TFO and control transcripts, the template volume for PCR analysis was normalised to the amount of RNA present in the elution fraction. The relative amount of bound plasmid to the RNA transcripts was quantified by PCR, leading to a PCR product of 520 bp (primer pair II). When samples that had not been subjected to magnetic capture were used for PCR, the signals which could be observed in the TFO and in the control portion were equal (Figure 4-20, left panel). This result underlined that the same amount of plasmid was present in each reaction and that the plasmid was intact before magnetic separation. After magnetic separation, there was a stronger binding of MCP-1 target to the TFO rather than to the control detectable (right panel, lane 1).

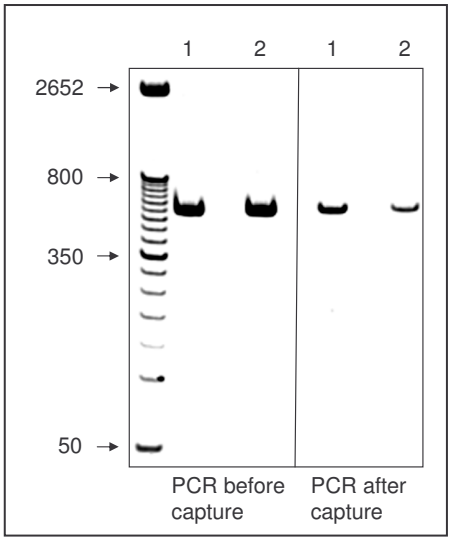

Figure 4-20. Capture assay for the evaluation of specific binding of the 1.1 kb TFO/hygromycin fusion transcript to vector encoded MCP-1 promoter target duplex. Plasmid pGL3 containing the 39 bp MCP-1 promoter target sequence was treated with biotinylated CU-TFO transcript (lane 1) or with biotinylated GU-control transcript (lane 2). After incubation aliquots of each sample were: (i) saved for control of intact plasmid present in each reaction and successful PCR amplification ("before capture", left panel), and (ii) subjected to magnetic separation ("after capture", right panel). Streptavidin-coated magnetic beads bind to the biotinylated RNA transcripts and allow magnetic capture of triplex complexes. The captured DNA was detected by PCR with pGL3 specific primers leading to a PCR product of 520 b.

Another primer pair was used to verify the enhanced binding of the plasmid containing the MCP-1 promoter sequence to the TFO. The upstream primer was set at the MCP-1 promoter target site and the downstream primer was specific for the pGL3 vector leading to a PCR product of 658 bp in length (primer pair I), and similar results were obtained. Figure 4-21 A demonstrates a stronger binding of the plasmid to the 1.1 kb TFO transcript rather than to the control transcript, resulting in a stronger PCR amplification (lanes 2 and 3). In lane 1 the reaction was performed without a biotinylated RNA transcript, and no PCR fragment was detected. The latter finding allows excluding non-specific, biotin-independent binding of the plasmid to the magnetic beads during the separation step, which would produce false positive PCR results. When summarizing results of three independent experiments, the binding of the TFO transcript to the plasmid containing the MCP-1 promoter target was three times stronger in comparison to the binding of control transcripts (Figure 4-21 B).

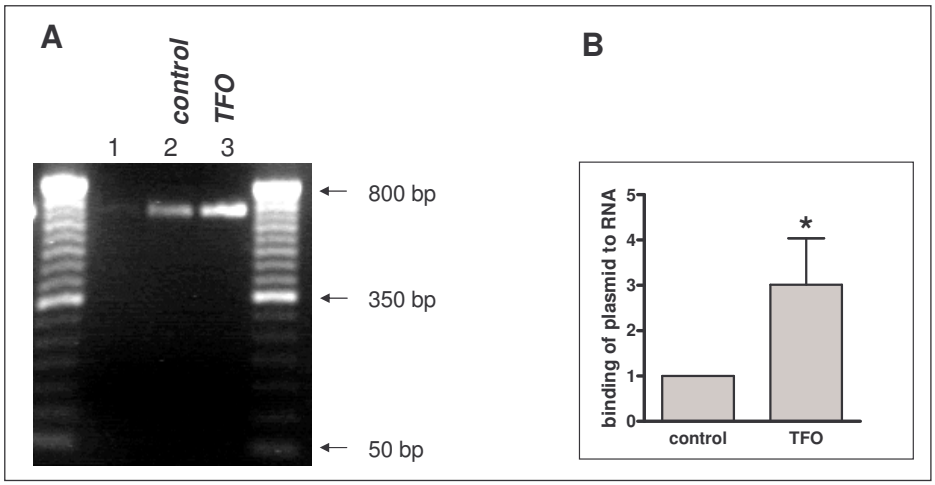

Figure 4-21. Plasmid encoded target duplex binds to the 1.1 kb CU-TFO transcript. (**A**): The amount of plasmid bound to the transcribed RNA (control or TFO) in each elution fraction was compared by PCR and a 658 bp fragment of the plasmid carrying the triplex target site was amplified. Plasmid encoded target DNA was treated without biotinylated RNA (lane 1), with control-RNA containing the 19 nt GU sequence (lane 2), or with the RNA transcript containing the CU-TFO sequence (lane 3). (**B**): The relative amount of bound plasmid to the TFO or control was quantified densitometrically. Binding was demonstrated in three independent experiments, using different *in vitro* transcribed controls without insert or with GU or CA sequences, respectively. The error bar indicates the SD and * significance level of $p<0.05$ as determined by unpaired student t test.

4.2.4 Sequence-specific inhibition of MCP-1 protein synthesis

Following these control experiments the effects of intracellular generated CU-TFO versus control-RNA on endogenous MCP-1 gene expression were analysed. Specifically the question whether the TFO-based antigene strategy is both limited to the target gene and effective also with different known stimuli of MCP-1 protein expression should be answered. Non-stimulated HEK 293 cells produced low basal amounts of MCP-1 in culture. As shown before protein secretion could be induced by pro-inflammatory cytokines like TNF-α and IFN-γ in these cells. HEK 293 cell lines TVHygro-CU, releasing CU-TFO, and control cell lines, releasing control-RNA (GU-control, CA-control or RNA without insert derived from vector TVHygro) were plated in 24-well plates at a density of $1.5x10^5$ cells/well and cultured for 24 h in the absence or presence of 500 U/ml TNF-α. In a series of 13 independent experiments with six different stable transfected cell lines generating intranuclear CU-TFOs a mean inhibition by 76 ± 10.2% of MCP-1 protein secretion was measured after stimulation with TNF-α alone as compared to measurements in two control cell lines (n=7). The basal MCP-1 protein secretion in unstimulated TVHygro-CU cell lines was reduced by 58 ± 13.1% (n=13, six cell lines) in comparison to non-stimulated control cell lines (Figure 4-22).

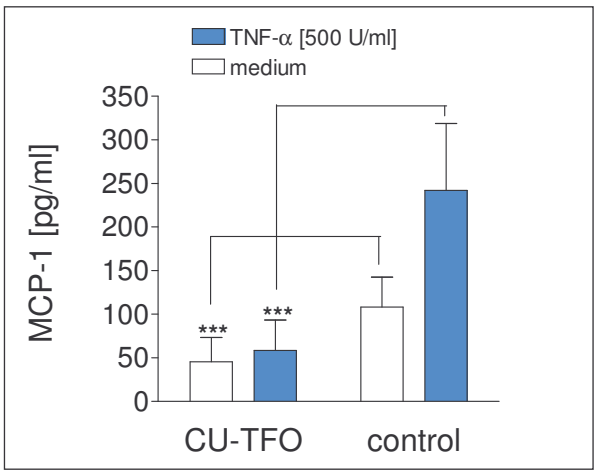

Figure 4-22. Inhibition of MCP-1 expression by intracellular generated CU-TFO in HEK 293 cells. Stable transfected HEK 293 cells lines generating CU-TFO, GU-control and CA-control, respectively, were plated in 24-well plates at a density of $1.5x10^5$ cells/well and cultured for 24 h in the absence or presence of 500 U/ml TNF-α. At the end of incubation time culture supernatants were harvested and MCP-1 concentrations determined by ELISA. The means of 13 independent measurements of 6 different CU-TFO generating cell lines and 7 independent measurements of 2 different control-RNA generating cell lines are shown. The error bars indicate the SD and *** significance level of $p<0.001$ as determined by unpaired student t test.

To further confirm that the inhibition of MCP-1 protein secretion indeed represents a gene specific effect, respective HEK 293 cell lines were plated in 24-well plates at different cell densities of $9x10^4$, $1.5x10^5$, and $3x10^5$ cells/well and cultured for 24 h in the absence or presence of 500 U/ml TNF-α. In addition to MCP-1 the release of the chemokine IL-8 was determined by ELISA. Also in this experimental series a marked reduction of MCP-1 protein secretion by up to 85% became apparent in the TNF-α stimulated TVHygro-CU transfected cell line when compared to the control vector transfected cell line (Figure 4-23 A). Analysing these supernatants for IL-8 protein secretion by ELISA no inhibition of IL-8 protein secretion could be shown in CU-TFO releasing cells, indicating that there was a sequence-specific inhibitory effect of CU-TFO only at the MCP-1 promoter site, whereas IL-8 as suitable TNF-α inducible control gene was not affected at all (Figure 4-23 B).

Extending these results IFN-γ induced MCP-1 expression was inhibited by 83% in CU-TFO releasing cell lines. Combined stimulation with IFN-γ and TNF-α resulted in an enhanced MCP-1 protein secretion in HEK 293 cell lines in comparison to single cytokine stimulation suggesting an additive effect. MCP-1 protein secretion was inhibited by up to 88% in co-stimulated CU-TFO generating cells in comparison to control cells (Figure 4-24).

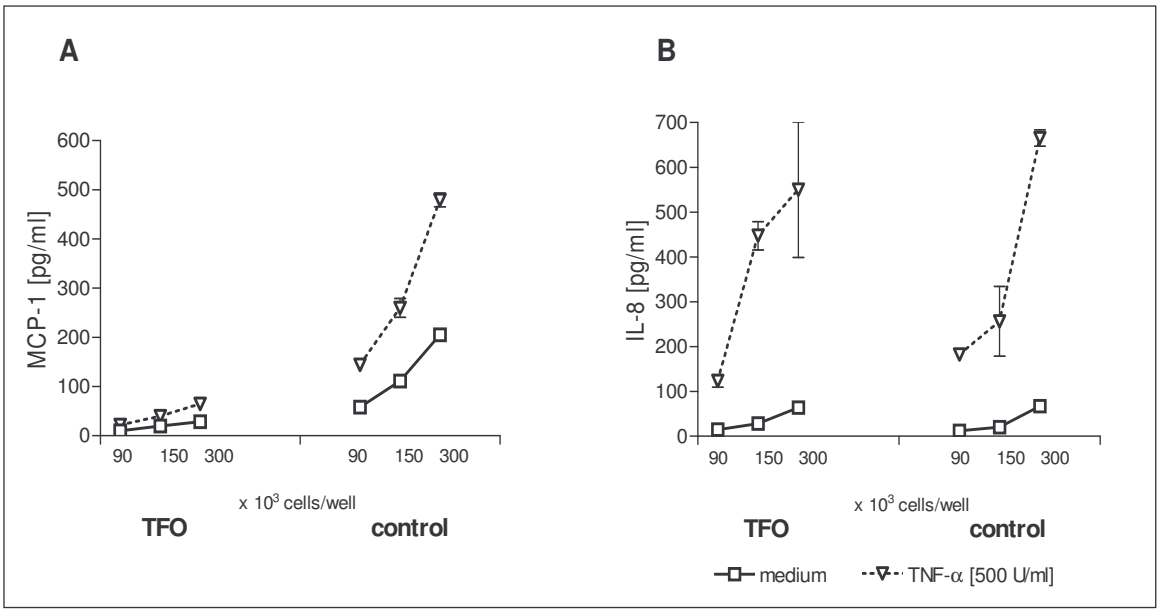

Figure 4-23. Sequence-specific inhibition of MCP-1 protein secretion. Stable transfected HEK 293 cells generating CU-TFO and control-RNA, respectively, were plated in 24-well plates at densities of $9.x10^4$, $1.5x10^5$and $3.x10^5$ cells/well and cultured for 24 h in the absence or presence of 500 U/ml TNF-α. At the end of incubation time culture supernatants were harvested and MCP-1 (**A**) and IL-8 concentrations (**B**) determined by ELISA. One experiment representative of three independent experiments is shown; the error bars indicate SD.

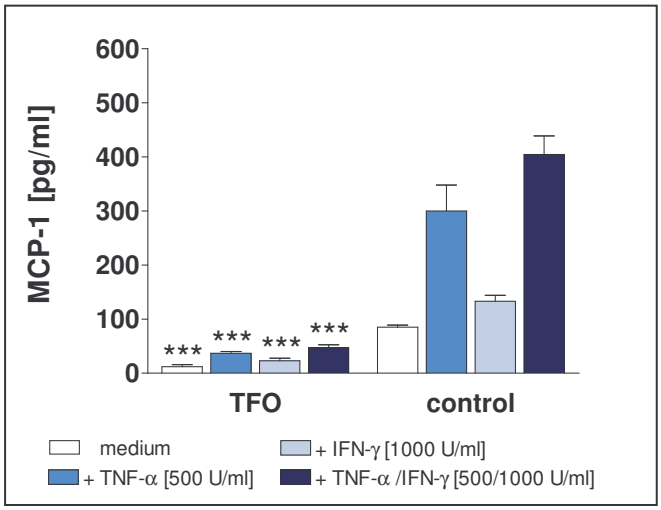

Figure 4-24. Sequence-specific inhibition of MCP-1 protein secretion. Stable transfected HEK 293 cells lines generating CU-TFO or control-RNA were plated in 24-well plates at a density of $3.x10^5$ cells/well and cultured for 24 h in the presence of 500 U/ml TNF-α, 1000 U/ml IFN-γ or TNF-α and IFN-γ together as indicated. At the end of incubation time culture supernatants were harvested and MCP-1 and IL-8 concentrations determined by ELISA. One experiment of three with similar results is shown. The error bars indicate the SD and *** significance level of $p<0.001$ as determined by unpaired student t test.

4.3 Transient transfection with siRNA

Short RNAs regulate gene expression in many species. Some are generated from any double-stranded RNA and degrade complementary RNAs; others are encoded by genes and repress specific mRNAs. RNA interference (RNAi) depends on the formation of double-stranded RNA (dsRNA) whose antisense strand is complementary to the transcript of a targeted gene. Two distinct steps are involved. In the first, the enzyme Dicer cleaves long dsRNA into short interfering RNA (siRNA) molecules in the length of 21-23 bp. In the second, a multi-component RNA-induced silencing complex (RISC) uses siRNA to guide the sequence-specific cleavage of the RNA transcripts of the targeted gene.
Here, the siRNA approach was tested as another strategy to inhibit expression of the pro-inflammatory chemokines MCP-1 and RANTES. Two different methods were pursuit, describing transient transfection with a) vector derived and b) synthetic siRNA. siRNA sequences were screened using a commercial siRNA target finder.
Two vector derived siRNAs against RANTES and MCP-1 were created and several cell lines were transiently transfected. Sense and antisense strands have been paired in a manner to have a UU 3' overhang. The 21 bp siRNA against murine RANTES (NM_013653) was located at position 205 in the target mRNA sequence with a GC content of 47.6%, and the siRNA (21 bp) against human MCP-1 (NM_002982) was located at position 180 in the target mRNA sequence with a GC content of 38.1%.

4.3.1 Vector system for expression of siRNA in mammalian cells

The vector pSUPER (Figure 4-25) is a mammalian expression vector that directs intracellular synthesis of siRNA like transcripts. The vector uses the polymerase-III H1-RNA gene promoter, as it produces a small RNA transcript lacking a polyadenosine tail and has a well-defined start of transcription and a termination signal consisting of five thymidines in a row. The cleavage of the transcript at the termination site is taking place after the second uridine (Baer et al. 1990), yielding a transcript with the ends resembling synthetic siRNAs, which also contain two 3' overhanging T or U nucleotides. A gene-specific insert was designed containing a unique 19-nt sequence derived from the target transcript and was cloned into the *Hind*III and *Bgl*II restriction sites of the vector. The 19-nt target appears in both sense and antisense orientation, separated by a 9-nt spacer sequence. The resulting transcript is predicted to fold back on itself to form a 19 bp stem-loop structure. Analysis indicated that the stem loop precursor transcript was quickly cleaved in the cell to produce a functional siRNA (Brummelkamp et al. 2002).

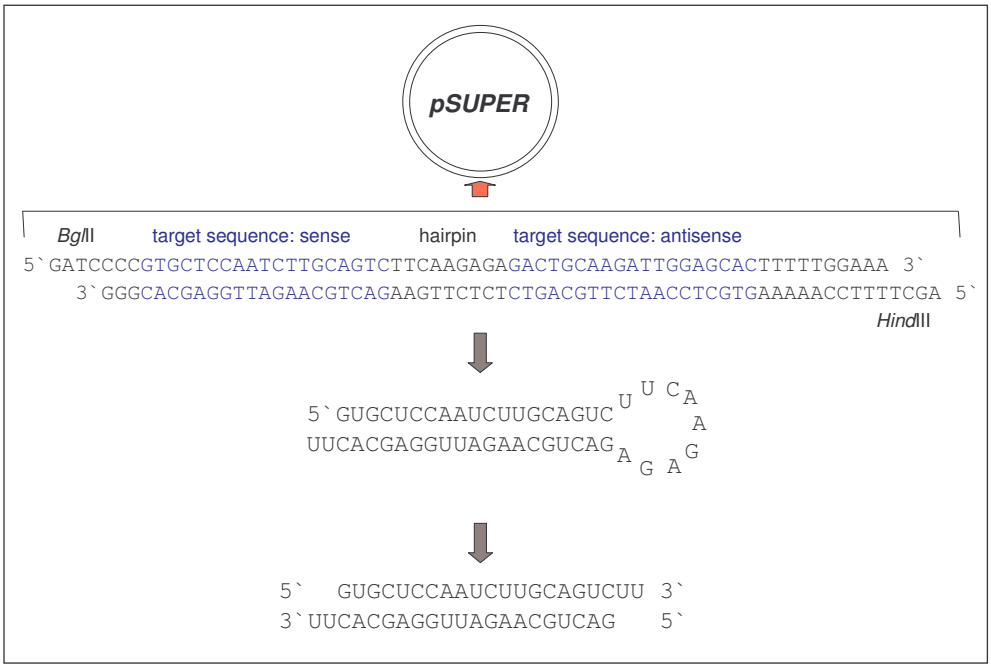

Figure 4-25. Transcription of 64 nt oligonucleotide to hairpin RNA, subsequently processed to functional siRNA. The pSUPER vector is based on a pBlueScript KS-phagemid vector, a 3176 bp DNA vector with ampicillin resistance. pSUPER also features the H1-RNA promoter for RNA transcription under the control of the polymerase-III expression system.

4.3.1.1 Design of siRNA vectors targeting RANTES and MCP-1 mRNA

Two different vectors were constructed directing the synthesis of double-stranded siRNA against RANTES and MCP-1; sequences are shown in Figure 4-26.

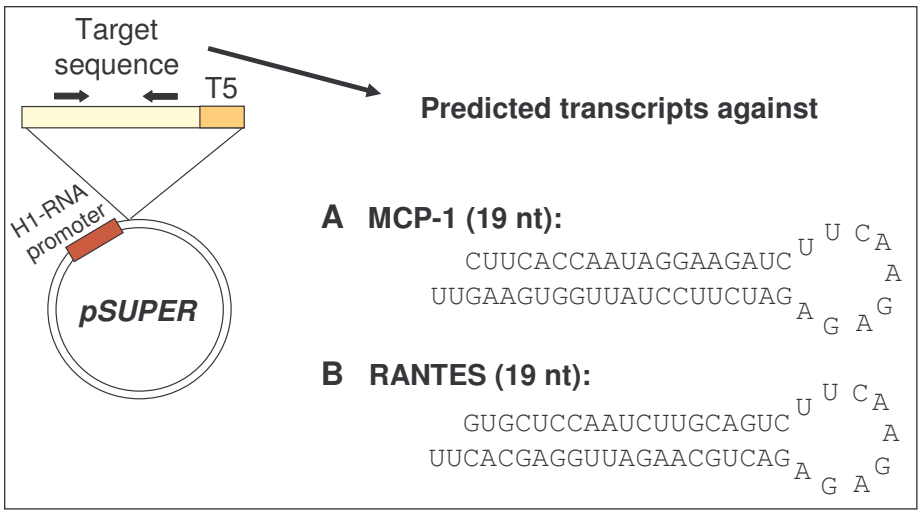

Figure 4-26. Schematic drawing of the pSUPER vector and the predicted secondary structures of the transcripts. Different vectors were constructed to generate double-stranded siRNA targeting (**A**) the human MCP-1 mRNA and (**B**) the murine RANTES mRNA.

After ligation and transformation into competent E. coli the presence of positive clones was checked by restriction digestion with *Eco*RI and *Hind*III. Positive clones should have inserts of about 290 bp in length (Figure 4-27 A). Upon ligation, the *Bgl*II site is destroyed to allow a better selection of positive clones. Recombinant plasmids containing the inserts were not linearised when digested with *Bgl*II, whereas the wild type vector was linearised (Figure 4-27 B). But: The MCP-1 siRNA insert contains an additional *Bgl*II restriction site (AGATCT); therefore the recombinant vector was linearised like the empty vector after digestion with *Bgl*II (Figure 4-27 B, lanes 1, 2 and 9). Endotoxin-free maxi plasmid preparations were performed, and before transfecting mammalian cells with the different constructs the presence of the correct inserts was confirmed by DNA sequencing using T7 and T3 primers.

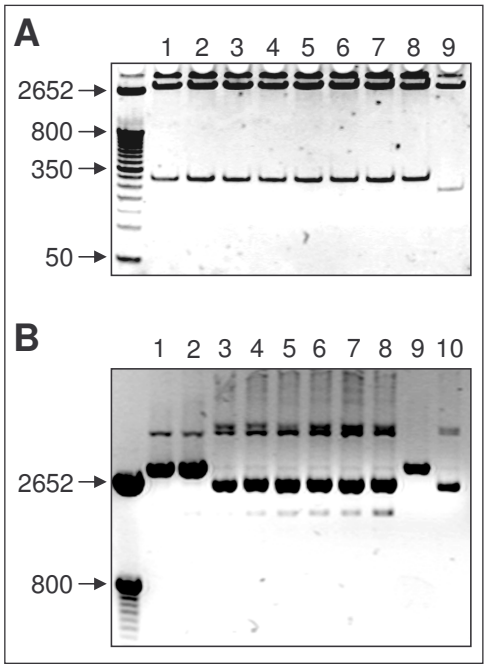

Figure 4-27. Cloning of vectors expressing siRNA: presence of positive clones. The 64 nt oligonucleotides containing the coding sequences for siRNA against the human MCP-1 or murine RANTES were annealed and ligated into the pSUPER vector. After transformation of recombinant pSUPER vector into competent cells (DH5α), several single colonies were picked, grown in LB amp+ broth for an additional cycle and minipreps were performed. (**A**): The presence of positive clones was analysed by digestion with HindIII and EcoRI. Positive clones should have inserts approximately 290 bp in length. An empty vector has an insert of approximately 227 bp. (**B**): Linearisation of the plasmids with *Bgl*II. Lane 1-2: vector with siRNA-insert against MCP-1; lane 3-8: vector with siRNA-insert against RANTES; lane 9: wild type vector; lane 10: wild type vector without restriction.

4.3.1.2 Transfection of mammalian cells with pSUPER

The ability of vector encoded siRNA to inhibit endogenous RANTES was tested in b-end3 cells and Th1 cells. Th1 cells were transfected with 0.5 µg of the pSUPER vector. To examine sequence-specificity, a vector harbouring the siRNA targeting human MCP-1 mRNA was tested as well, which should have no effect in the murine Th1 cells (Figure 4-28).

Murine brain microvascular endothelial cells have been transfected with 0.2 to 1 µg of the siRNA vector, and the unrelated siRNA sequence against MCP-1 served as a control (Figure 4-29). But, transient transfection of these constructs failed to suppress RANTES gene expression.

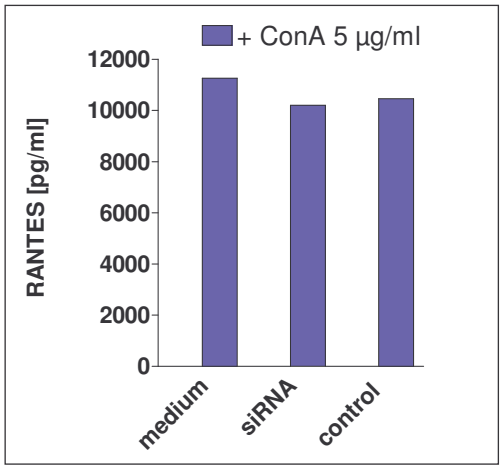

Figure 4-28. Treatment of Th1 cells with siRNA. Th1 cells were plated in 6-well plates at a density of 1 x 10^6 cells/well and transfected with 0.5 µg of the vector pSUPER, which contained either a siRNA sequence against murine RANTES or an unrelated siRNA sequence against human MCP-1 which served as a control. After 18 h the cells were left unstimulated or treated with 5 µg/ml ConA for additional 24 h. Following the incubation time, the culture media were harvested and the concentration of secreted RANTES was determined by ELISA. One experiment of two with similar results is shown.

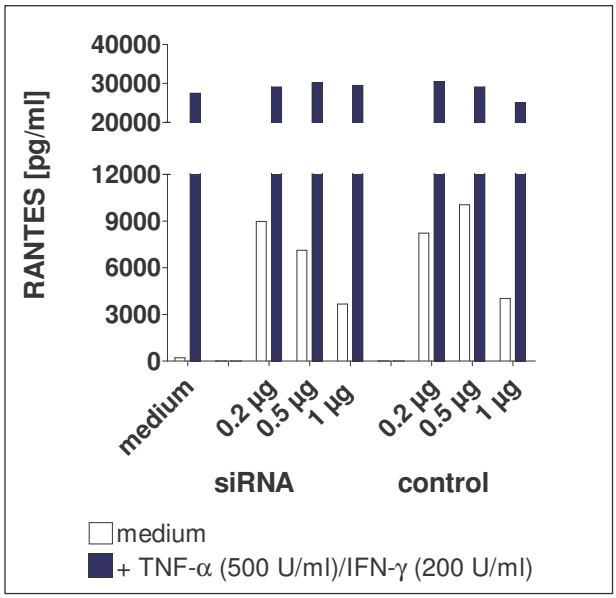

Figure 4-29. Treatment of brain microvascular endothelial cells with siRNA. B-end3 cells were plated in 6-well plates at a density of 600,000 cells/well and transfected with different concentrations of the vector pSUPER, which contained either a siRNA sequence against murine RANTES or an unrelated siRNA sequence against the human MCP-1 which served as a control. After 18 h the cells were left unstimulated or treated 500 U/ml TNF-α and 200 U/ml IFN-γ for additional 24 h. Following the incubation time, the culture media were harvested and the concentration of secreted RANTES was determined by ELISA. One experiment of three with similar results is shown.

But, interestingly, in b-end3 cells basal RANTES expression was increased by vector derived siRNA treatment in comparison to basal expression in the medium control. Induction caused by plasmid transfection was up to 45-fold. There seemed to be no correlation between the induction and the concentration of transfected vector. Enhancement was not visible any more after treatment with TNF-α and IFN-γ. Additionally to the stimuli used there is no effect of the siRNA detectable.

Furthermore HEK 293 cells were transfected with vector encoded siRNA against the human MCP-1. An empty vector without RNA sequence served as a control. Inhibition due to the siRNA was measured in stimulated and unstimulated cells (Figure 4-30). In TNF-α stimulated cells MCP-1 protein synthesis was decreased by 35 ± 11% after siRNA transfection. Cells transfected with the empty vector (no RNA transcript) revealed a decrease of MCP-1 protein synthesis by 18 ± 7%. These result demonstrate that the vector itself has an effect in HEK 293 cells, leading to a slight inhibition of gene expression, but inhibition was more pronounced by the vector derived MCP-1 siRNA.

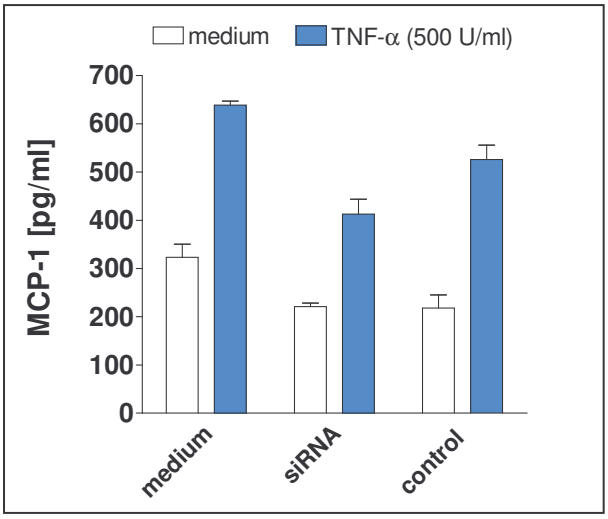

Figure 4-30. Transfection of HEK 293 cells with siRNA against MCP-1. HEK 293 cells plated in 6-well plates at a density of 600,000 cells/well were transfected with 2 µg of vector pSUPER which contained a siRNA against human MCP-1. An empty vector without siRNA sequence served as a control. After 18 h the cells were left unstimulated or treated with 500 U/ml TNF-α for additional 24 h. Following the incubation time, the culture media were harvested and the concentration of secreted MCP-1 was determined by ELISA. Cell culture was performed in duplicates; the error bars indicate the SEM.

4.3.2 Transfection with synthetic siRNA targeting MCP-1 and RANTES

Additionally, transient transfections with synthetic siRNA were performed. Selected 21 bp sequences were the same as described and used in the pSUPER RNAi system. The siRNA against MCP-1 and RANTES were purchased as single 21 nt RNA strands (sense and antisense), therefore they had to be annealed first to obtain double-stranded siRNA for transfection. Figure 4-31 shows the conversion from single to double strands after annealing and confirms that the siRNA was not degraded before transfection.

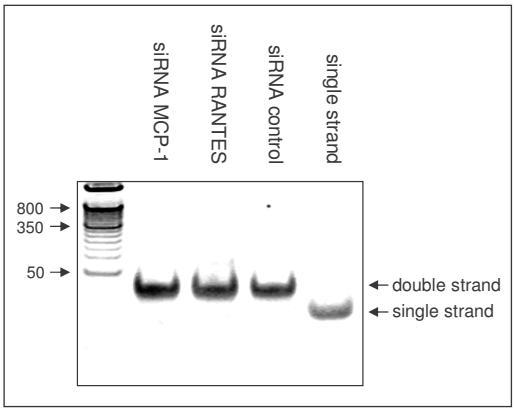

Figure 4-31. Annealing of single-stranded siRNAs to a double-stranded siRNA. Single strands were mixed in equimolar amounts in annealing buffer composed of 100 mM potassium acetate, 30 mM HEPES, and 2 mM magnesium acetate, pH 7.4 and incubated at 95°C for 5 min, followed by a slow cool-down to room temperature at a rate of 1°C/min. Quantitative annealing of the single strands to double strands was confirmed by native polyacrylamide gel electrophoresis through 12.5% gels, analysing 1 µg RNA per lane.

In a following experiment it was tested whether the siRNA against murine RANTES was functional in cells to inhibit RANTES gene expression (Figure 4-32).

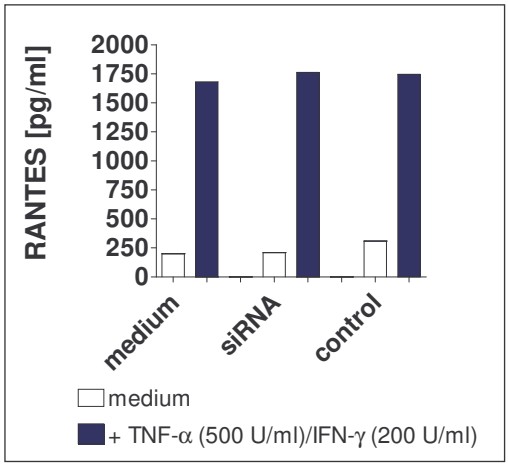

Figure 4-32. Transfection of microvascular brain endothelial cells with siRNA against RANTES. B-end3 cells plated in 6-well plates at a density of 600,000 cells/well were transfected with 2 µg siRNA (150 nM) against murine RANTES. An unrelated siRNA sequence against human MCP-1 served as a control. After 18 h the cells were left unstimulated or treated with 500 U/ml TNF-α and 200 U/ml IFN-γ for additional 24 h.

B-end3 cells were transfected with 2 µg of intact siRNA (~150 nM). An unrelated double-stranded RNA sequence with a length of 21 bp served as a control to rule out unspecific effects. After transfection the siRNA effects have been measured on protein level using ELISA. As a result, siRNA treatment did not lead to an inhibition of RANTES gene expression in b-end3 cells. No difference was visible using the siRNA or control sequence in comparison to the medium control. RANTES expression was inducible by TNF-α and IFN-γ treatment, but the expression rate was not changed by the siRNA in stimulated and unstimulated cells, respectively.

The siRNA against human MCP-1 was tested in HEK 293 cells. Effects on basal and TNF-α induced MCP-1 expression were examined (Figure 4-33). As described above, an unrelated RNA sequence was used as a control. After transfection of 2 µg siRNA (~150 nM), the MCP-1 expression was reduced about 30% in unstimulated cells and 23% in TNF-α stimulated cells. Conversely, the control RNA resulted in a decreased MCP-1 protein synthesis as well (37% in unstimulated and 15% in stimulated cells), indicating that the inhibitory effect was not sequence-specific but treatment resulted in a general slight decrease of protein synthesis.

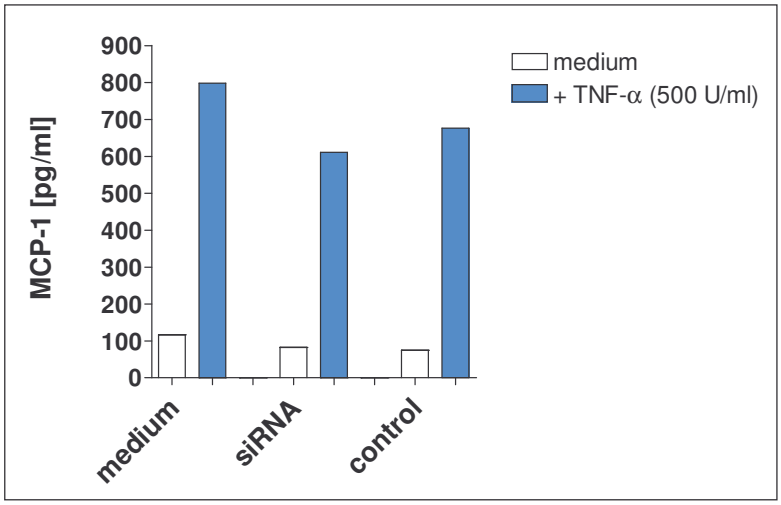

Figure 4-33. Transfection of HEK 293 cells with siRNA against MCP-1. HEK 293 cells plated in 6-well plates at a density of 600,000 cells/well were transfected with 2 µg siRNA (150 nM) against human MCP-1. A scrambled siRNA sequence served as an unrelated control. After 18 h the cells were left unstimulated or treated with 500 U/ml TNF-α for additional 24 h. Following the incubation time, the culture media was harvested and the concentration of secreted MCP-1 was determined by ELISA.

In a subsequent experiment a validated siRNA sequence targeting the MCP-1 mRNA was tested (for details of the sequence see “Materials and Methods, Table 3-22). According to the supplier’s information (Ambion), the siRNA was confirmed in HeLa cells. Validation results were expressed as the relative amount of target mRNA remaining (9.78% + 2.35/-1.03) compared to that of cells transfected with negative control.

Here, HEK 293 cells were transfected with 100 nM of the siRNA and incubated with TNF-α afterwards (Figure 4-34). In four independent experiments MCP-1 protein secretion was reduced by 62.3 ± 10.3%.

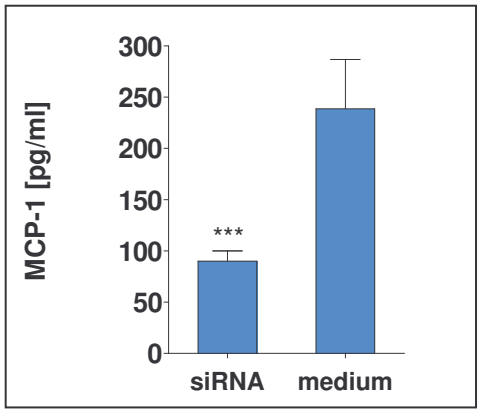

Figure 4-34. Transfection of HEK 293 cells with a validated siRNA sequence targeting MCP-1 mRNA. HEK 293 cells plated in 6-well plates at a density of 600,000 cells/well were transfected with 100 nM siRNA against human MCP-1. After 18 h the cells were treated with 500 U/ml TNF-α for additional 24 h. Following the incubation time, the culture media was harvested and the concentration of secreted MCP-1 was determined by ELISA. Cell culture was performed in duplicates, and the mean of four independent experiments is shown. The error bars indicate the SD and *** significance level of p=0.0009 as determined by unpaired student t test.

4.4 Generation of lentiviral vectors

The resistance of cells to transfection of siRNA and TFOs may limit their successful use *in vitro* and *in vivo*. To overcome these limitations, lentiviral vectors can be used as efficient and stable gene delivery tools in mammalian cells. Gene transfer vectors derived from lentiviruses, such as HIV-1, are potentially important tools in clinical gene therapy due to their ability to transduce several types of target cells independently of their proliferation status both *ex vivo* and *in vivo*. Lentiviral vectors are replication-defective viral particles made by the core proteins and enzymes of a lentivirus, and the envelope of a different virus. Here, the production of lentiviral vectors by transient transfection of HEK 239T cells is described. Vector plasmids, including the transfer construct ("SEW"), packaging construct ("pCMV Δ8.91"), and envelope plasmid ("pMD2.VSV.G") were kindly provided by Dr. Manuel Grez, Georg-Speyer-Haus, Frankfurt, and production of lentiviral VSV-G pseudotyped vectors was performed in S2-laboratories of the Georg-Speyer-Haus.
The following results show the cloning of recombinant transfer vectors and the transient transfection of lentiviral vector plasmids into a HEK 293T cell line for packaging lentiviral vector genomes into infectious lentiviral particles. For the determination of infectious particles per ml (transducing units per ml; TU/ml), the supernatants were titrated on HEK 293T cells and analysed using FACS. Finally, Th1 cells were transduced with infectious lentiviral particles and transduction efficacy was measured by FACS.

4.4.1 Recombinant lentiviral vector plasmids

The expression constructs used for lentiviral production were maintained in the form of bacterial plasmids and could be transfected into mammalian cells to produce replication defective virus stocks. The transfer vector SEW contains a coding sequence for the enhanced green fluorescent protein (eGFP).
Four different recombinant SEW transfer vectors have been constructed. Therefore, the expression cassette of the vector pSUPER (chapter 4.3.1) containing the H1 promoter was amplified using T7 and T3 primers. Each primer contained a 5' *Sna*BI restriction site for blunt end ligation into the *Sna*BI linearised SEW. The principle of the cloning is shown in Figure 4-35. The following constructs derived from pSUPER were cloned into SEW: a) expression cassettes coding for the 21 bp siRNA against MCP-1 and RANTES, respectively (see chapter 4.3.1.1), b) an expression cassette coding for the 19 nt single-stranded CU-TFO against MCP-1 with no stem loop formation, c) an expression cassettes without coding insert sequence (Figure 4-35 B-E).

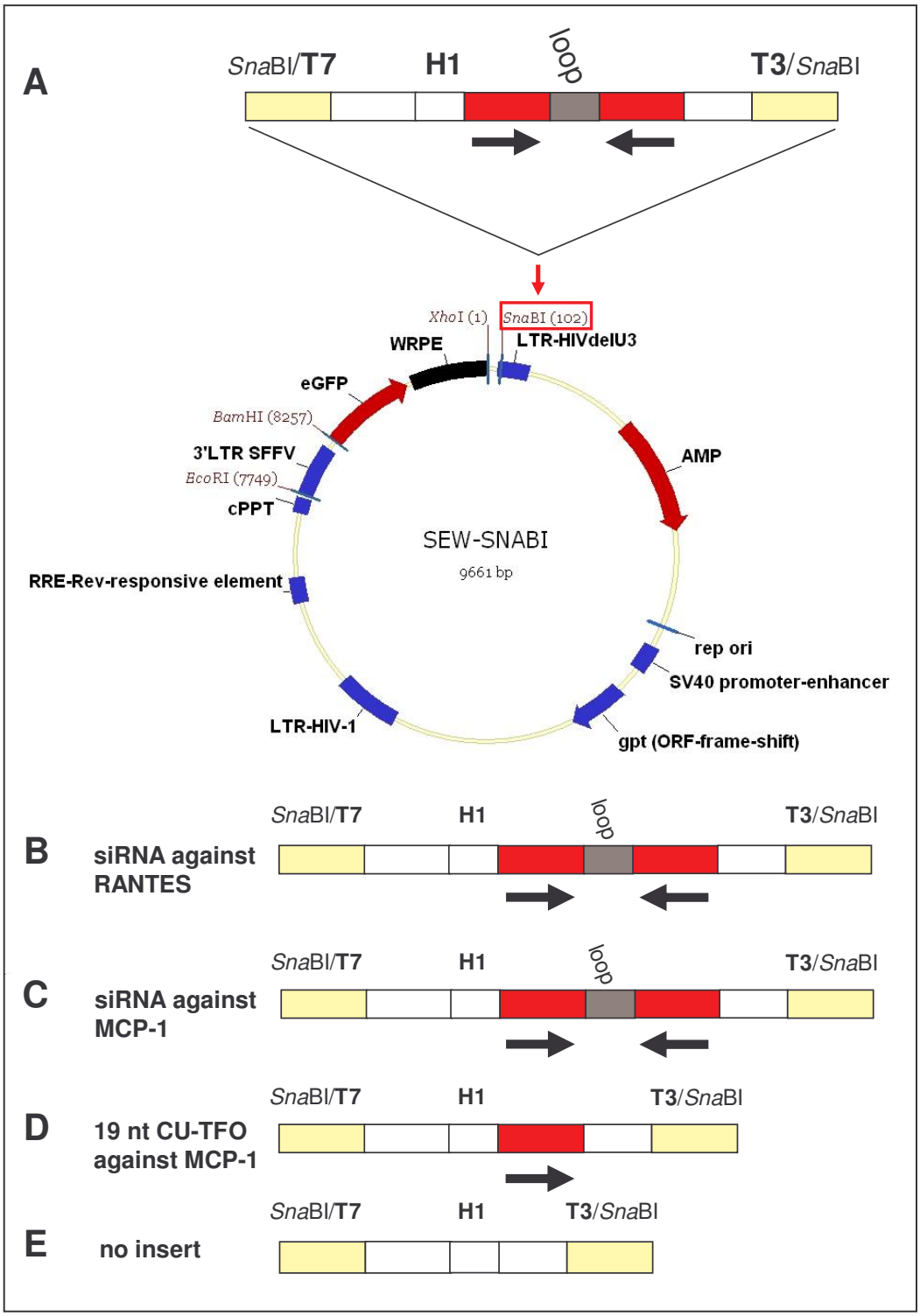

Figure 4-35. Cloning of the transfer vector SEW. (**A**): The siRNA expression cassette from the vector pSUPER including the H1 promoter was PCR amplified using T7 and T3 primers which contained *Sna*BI restriction sites. PCR products were digested with *Sna*BI and ligated into the *Sna*BI linearised transfer vector SEW. (**B-E**) shows the four different constructs cloned into SEW; the siRNA or TFO coding sequences are signed in red.

Correct ligation of the different expression cassettes into SEW was confirmed by restriction digestion of the recombinant vectors with *Sna*BI and PCR amplification using T7 and T3 primers. Restriction digestion of the constructs containing coding sequences for siRNA against RANTES and MCP-1 resulted in fragments of 448 bp (Figure 4-36, right panel). PCR amplification of the sequences resulted in products of 458 bp (Figure 4-36, left panel).

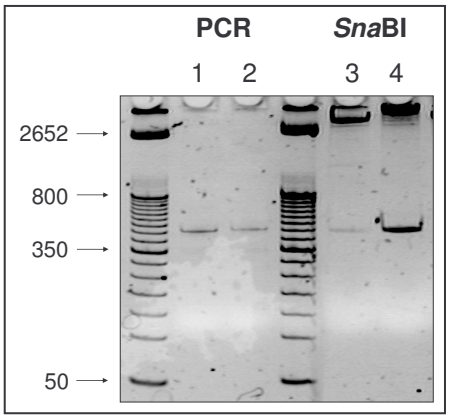

Figure 4-36. Recombinant vector SEW containing siRNA coding sequences against RANTES and MCP-1. Lanes 1 and 3: MCP-1 siRNA, lanes 2 and 4: RANTES siRNA. Controls were performed using PCR and restriction digestion.

Restriction digestion of the construct containing coding sequences for the 19 nt CU-TFO against MCP-1 resulted in fragments of 420 bp (Figure 4-37, right panel); PCR amplification resulted in a product of 430 bp (Figure 4-37, left panel).

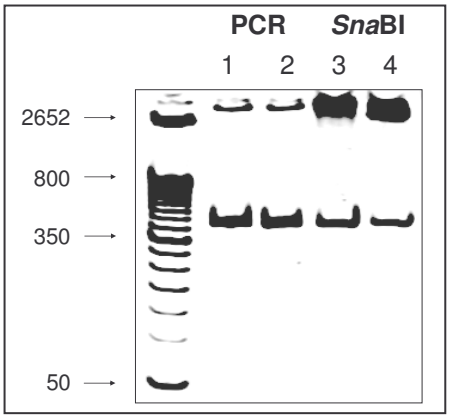

Figure 4-37. Recombinant vector SEW containing TFO coding sequences against MCP-1, 2 clones (I and II). Lanes 1 and 3: TFO clone I, lanes 2 and 4: TFO clone II. Controls were performed using PCR and restriction digestion.

An expression cassette without insert was cloned into the SEW vector. PCR amplification resulted in a product of 394 bp (Figure 4-37).
Additionally, correct inserts of all the four constructs described were confirmed by DNA sequencing.

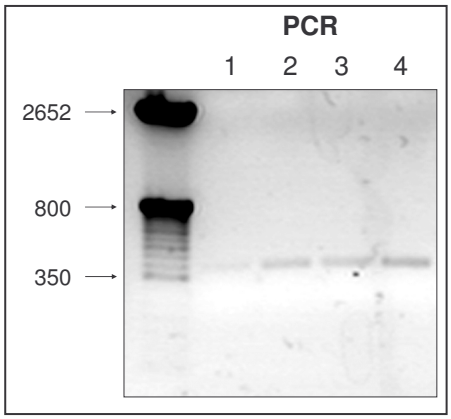

Figure 4-38. Recombinant vector SEW containing the expression cassette from the vector pSUPER without insert, 4 clones. Controls were performed using PCR amplification with T7 and T3 primers.

In the following experiments the production of infectious lentiviral particles is described. The recombinant SEW transfer vector containing the expression cassette without insert was used for transfection of HEK 293T cells.

4.4.2 Production of lentiviral VSV-G pseudotyped vectors

HEK 293T cells were co-transfected with 10 µg lentivirus construct SEW (see Figure 4-35 E), 6.5 µg packaging plasmid pCMV Δ8.91 and 3.5 µg VSV.G-expressing plasmid pMD2.VSV.G using the calcium phosphate DNA precipitation method, and two transfections were performed in parallel.

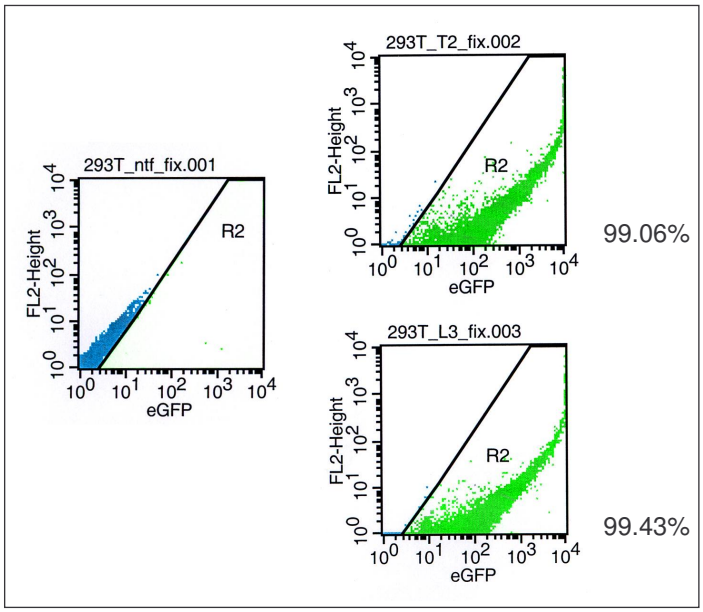

Figure 4-39. Transient transfection of HEK 293T cells. Transfection efficiencies were determined by analysis of eGFP expression with untransfected cells as negative controls (in blue).

Microscopy of the cells revealed a very small granular precipitate of the calcium phosphate-DNA complexes, initially floating above the cell layer and after incubation in the 37°C incubator overnight, visible on the bottom of the plate in the spaces between the cells. The calcium phosphate-DNA precipitate was allowed to stay on the cells for 14-16 h, after which the medium was replaced with fresh medium for vector collection to begin. Cell supernatants were collected 24 and 48 h after changing the medium. The supernatants were filtered and stored in aliquots at -80°C. Transfection efficiency was determined after 48 h by FACS analysis (Figure 4-39) and was higher than 99%.

4.4.3 Titration of lentiviral vectors

Relative concentrations of vectors were measured as a titre. The vector titre was determined as the number of complete particles that were able to transduce cells. The titre of infectious particles in the supernatant can be determined by FACS, if the vectors contain cell surface markers or reporter genes like GFP.

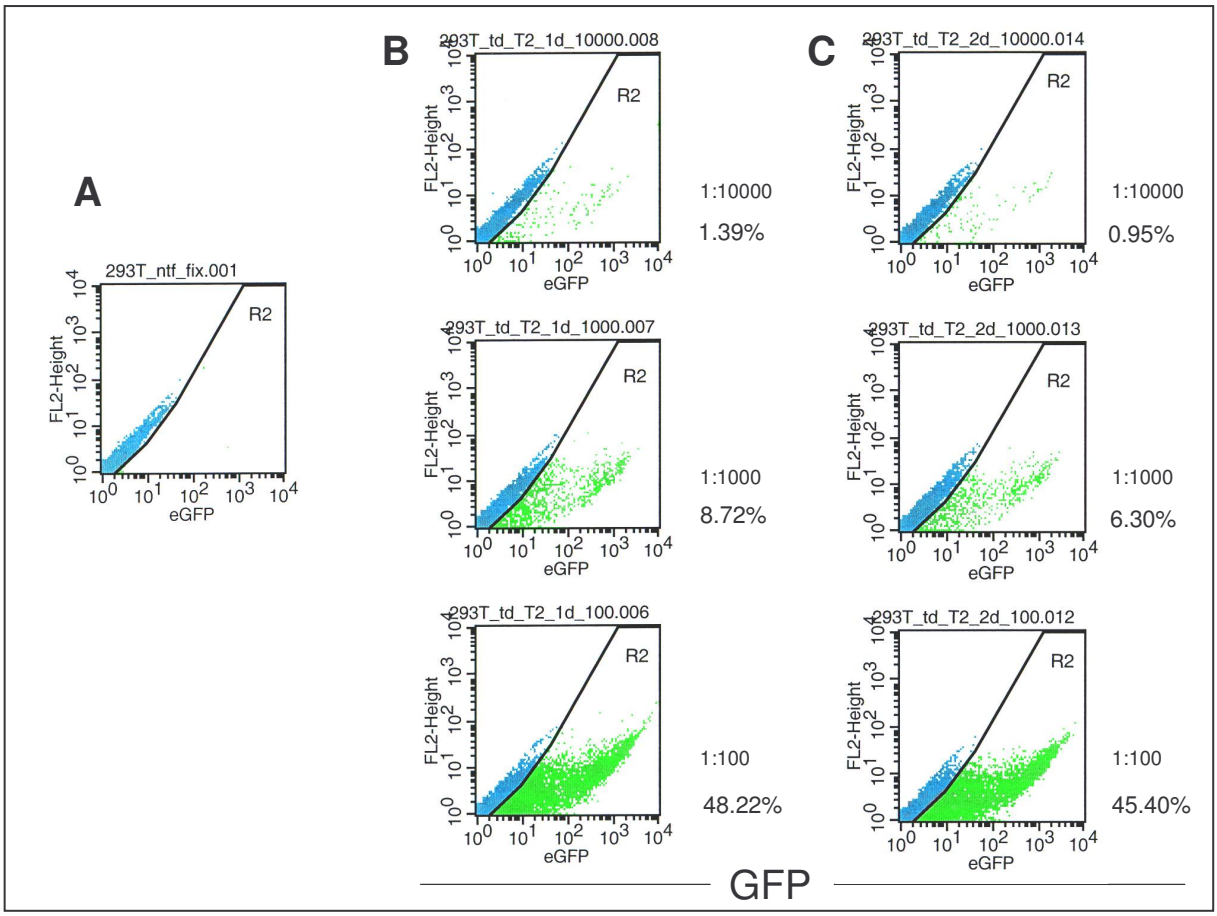

Figure 4-40. Titration of lentiviral vectors. (**A**): Cells expressing eGFP were measured by FACS analysis. Non-transduced cells served as negative controls. HEK 293T cells were transduced with different dilutions of viral supernatants collected after 24 (**B**) and 48 h (**C**).

HEK 293T cells were transduced with different dilutions of the viral samples collected after 24 and 48 h (final dilutions 10^{-2} to 10^{-4}). The day after transduction the medium was changed and cells were grown for additional 2-3 days. The titre was performed by FACS measuring the percentage of cells expressing eGFP in the total population. In Figure 4-40 one of two transductions of HEK 293T cells is shown. The titre is expressed in TU/ml and calculated as follows:

Titre [transducing units/ml] = 2 x seeded cell number x dilution factor x (positive transduced cells [%] / 100 [%])

The portion of positive transduced cells should be between 5% and 20% to be in the linear range of dilutions. The results are summarised in Table 4-2.

Table 4-2. Titration of lentiviral vectors

Viral stocks		Dilution	[%] eGFP	Cell number	Titre [TU/ml]
Transduction 1	24 h	10^{-3}	8.72	1×10^5	1.7×10^7
(Figure 4-40)	48 h	10^{-3}	6.30	1×10^5	1.3×10^7
Transduction 2	24 h	10^{-3}	5.85	1×10^5	1.2×10^7
(data not shown)	48 h	10^{-3}	4.82	1×10^5	9.6×10^6

Dilutions of the viral stocks of 10^{-3} appeared to be best and were chosen for calculation of viral titres. In comparison of the supernatants collected after 24 and 48 h the titre was slightly decreased after 48 h. Titres ranged from 10^6 to 10^7 TU/ml.

4.4.4 Transduction of Th1 cells

After determination of viral titres on HEK 293T cells, Th1 cells were transduced with the lentiviral particles.

The multiplicity of infection (MOI) describes the average number of viral particles that infect a single cell in a specific experiment and may serve as a parameter for the prediction of gene transfer events. For transduction, viral samples collected after 24 h with titres of 1.7×10^7 and 1.2×10^7 were used. Percentage of cells expressing eGFP was measured 7 days after transduction by FACS analysis.

The average transduction efficiency (n = 2) at a MOI of 0.5 was 25.92%, at a MOI of 5 = 67.46% and at a MOI of 50 = 81.76% (Figure 4-41).

Furthermore, positively transduced Th1 cells were visualised by fluorescence microscopy (Figure 4-42). EGFP expression occurred in almost all cells three weeks after transduction.

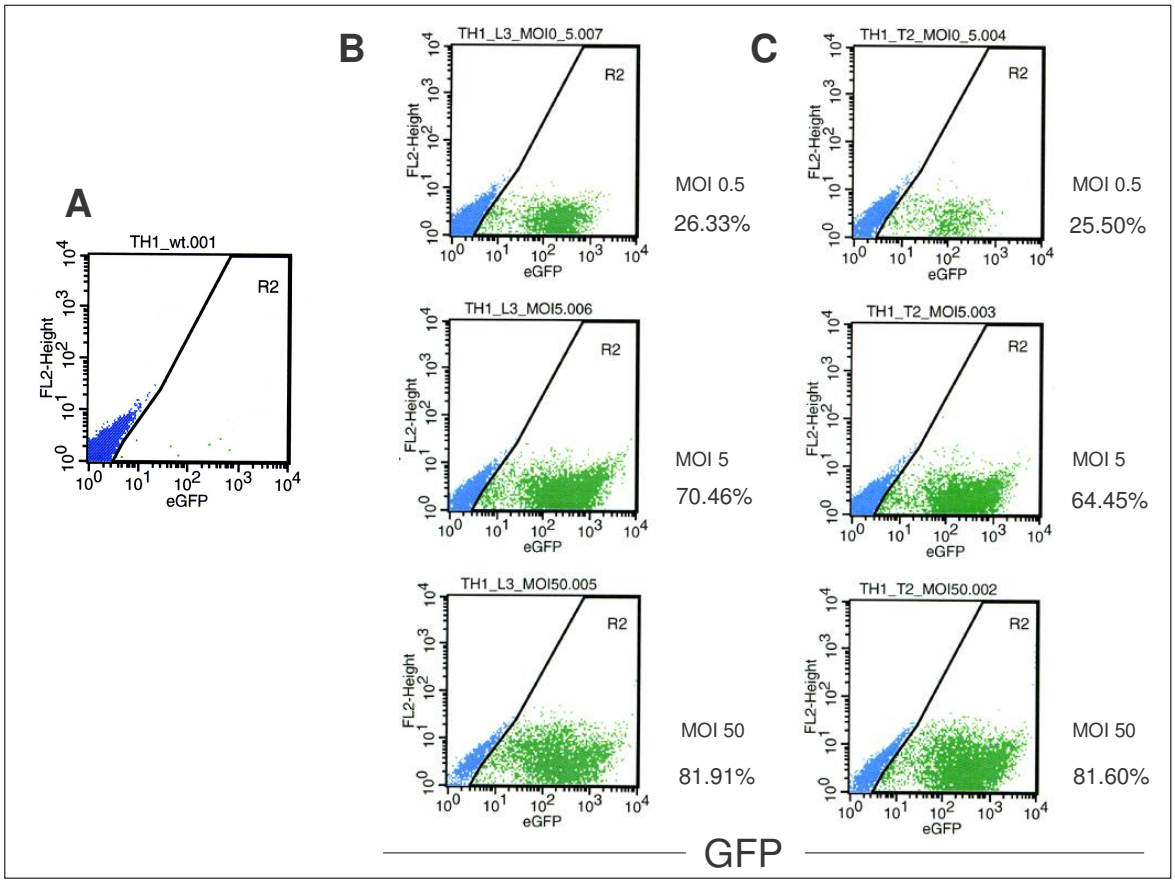

Figure 4-41. Expression of eGFP in transduced Th1 cells. Cells expressing eGFP at MOI between 0.5 and 50 were measured by FACS analysis. (**A**): Non-transduced cells served as negative controls. Transduction of Th1 cells was performed in duplicate (**B** and **C**).

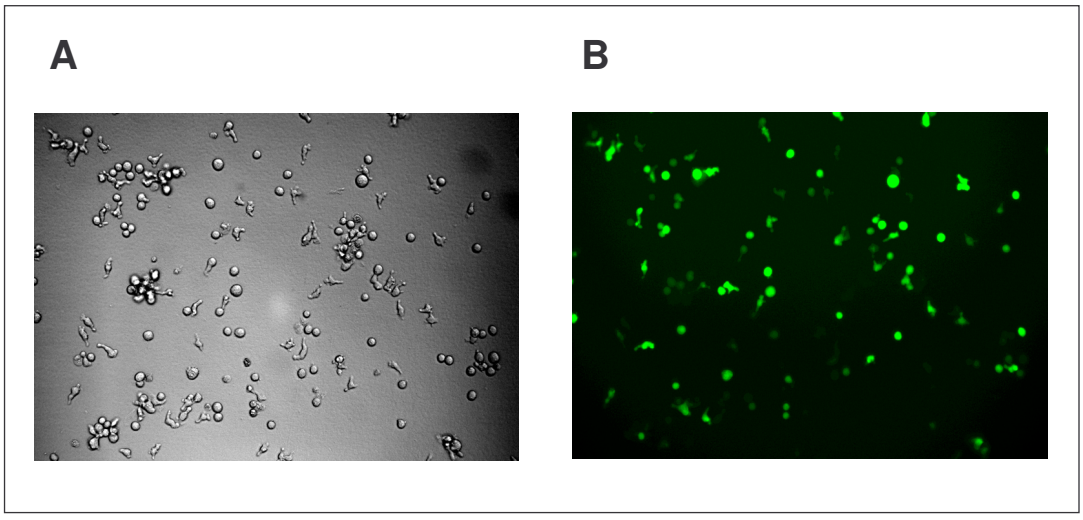

Figure 4-42. Phenotype of transduced Th1 cells. Three weeks after transduction with SEW (MOI 50) cells were examined for eGFP expression by fluorescence microscopy.

5 Discussion

5.1 The antigene strategy and RNA interference

The specific interference with gene expression has wide-ranging applications in experimental biology and is an attractive approach to the development of therapeutics. Numerous gene therapy strategies are under development, some of which use nucleic-acid based molecules to inhibit gene expression at either the transcriptional (e.g. triple helix-forming oligonucleotides) or post-transcriptional level (e.g. antisense oligonucleotides, siRNA).

5.1.1 TFOs targeting the chemokines MCP-1 and RANTES

Triple helix formation offers a direct means of selectively manipulating gene expression in cells. Synthetic triple helix-forming oligonucleotides (TFOs) bind with high affinity and specificity to the purine strand in the major groove of homopurine/homopyrimidine sequences in double-stranded DNA. TFOs have proofed effective in various gene strategies in living cells and in animals (Casey and Glazer 2001). Triplex formation can disrupt the regulation of gene expression at several points. Triplex formation was demonstrated to interfere with sequence-specific binding of transcription factors both *in vitro* and in cultured cells (Liu et al. 2001), and in addition it was shown to inhibit DNA replication when directed against DNA polymerase binding sites (Hacia et al. 1994a). Triplex mediated inhibition of transcription may be achieved by interfering with transcription initiation or transcription elongation.
Purine-rich tracts are frequently found in gene promoter regions and TFOs directed to these regulatory sites have been shown to selectively reduce transcription of the targeted genes, likely by blocking binding of transcriptional activators and/or formation of initiation complexes (Winters 2000). Triplex mediated modulation of transcription has potential application in therapy since it can be used, for example, to reduce levels of proteins thought to be important in disease processes. TFOs can also be molecular tools for studying gene expression and function.

In this study a triplex approach was investigated as a means of down-regulating expression of the proinflammatory chemokines MCP-1 and RANTES, which both play a crucial role in various diseases. The RANTES target was a 28 bp homopurine/homopyrimidine sequence at the promoter of the gene that appeared suitable for triplex mediated gene targeting with respect to the targeted DNA double-strand sequence. A GT-TFO, directed to this sequence, was able to bind to the target DNA in a sequence-specific manner according to the antiparallel purine triplex binding motif. Analysis of the binding properties of the RANTES

TFO showed that it bound with high affinity. This was consistent with previous reports showing that antiparallel GT-rich oligonucleotides were able to form stable triplex DNA at low concentrations and physiological pH and temperature (Catapano et al. 2000; Durland et al. 1991). The high binding affinity of the RANTES TFO was probably due to the perfect homopurine/homopyrimidine composition of the target sequence. Any pyrimidine interruption in the purine strand would possibly decrease stability of the triple helix and lower TFO binding affinity. Triplex formation was already detectable at a TFO concentration of 40 nM. Despite its high affinity, binding of the RANTES TFO required exact pairing with the target sequence according to the triplex DNA code. A control oligonucleotide with the same length but a scrambled base composition did not form a triplex DNA, even at the highest concentration (16 µM).

Subsequently it was tested whether the RANTES TFO exhibited any functional anti-transcriptional activity in cells. Convincing evidence of triplex formation on chromosomal targets has been reported previously (Faria et al. 2000; Wang et al. 1996). In the present study, binding of the 28 nt TFO to the promoter target sequences could be shown in a cell-free system *in vitro*, but the TFO did not functionally inhibit endogenous RANTES gene expression in two different cell systems tested. The TFO contained a phosphorothioate modification at each end to increase its intracellular stability. However, the RANTES TFO appeared to be not effective on the endogenous gene, which might be due to various factors. Accessibility of a chromosomal target site might be restricted to and depend on the transcriptional state of the gene. Faria (Faria et al. 2000) reported significant variability in gene expression levels in single cells over time and markedly different temporal responses to a TFO among individual cells in an unsynchronised cell population.

The use of synthetic TFOs *in vivo* might be limited by their susceptibility to endogenous nucleases or inefficient cellular uptake. Thus, the possible restricted accessibility of the endogenous RANTES gene promoter combined with heterogeneity of cellular and nuclear uptake of the TFO among cells may have contributed to the apparently poor efficacy of the TFO in inhibiting the endogenous gene.

Furthermore, the RANTES TFO is G-rich and contains several Gs in a row (5'TTT GTT GGT GGG GGT GGG GGT GGG GGT G 3'). Triplex formation in the purine binding motif often requires a high divalent cation concentration, and the third strand, which is G-rich, might tend to self-association into unfavourable structures in the presence of intracellular concentration of K^+. Such complexes reduce the ability of TFOs to bind to its intended target (Cheng and Van Dyke 1993; Olivas and Maher, III 1995a). This tendency led to the design of guanine analogues unable to form G-quartets but still having the potential to establish one or more hydrogen bonds with a C-G base pair (Olivas and Maher, III 1995b; Rao et al. 1995). Purine

oligonucleotides also have the potential to form another competing structure, a G-A parallel duplex, which can also interfere with triplex formation (Noonberg et al. 1995a).
Another target was the human MCP-1. A TFO target site consisting of 19 bp was identified in the promoter region at bp -66 to -48. The TFO target site in the MCP-1 promoter includes the binding site for the transcription factor SP-1 and partially overlaps a putative AP-1 binding site; both are sites which been implicated in the regulation of MCP-1. A 19 nt TFO based on the antiparallel purine motif was designed according to the known rules; T opposite A:T pairs G opposite G:C pairs. T was placed opposite the G-C inversion, because this base was previously shown to be tolerated opposite C:G pairs in triple helix motifs without adverse effect on the binding affinity of the TFO (Durland et al. 1994; Marchand et al. 2000).
To assess the ability of the TFO to form triple helices with the target site in the MCP-1 promoter, gel mobility shift assays were performed. The aim was to develop a TFO that could be tested in biological systems, therefore oligonucleotides contained a 3' and 5' phosphorothioate modification since it confers resistance to nuclease degradation. The 5', 3' phosphorothioated GT oligonucleotide was found to form stable triple helical complexes with the duplex DNA. According to the literature, phosphorothioated TFOs are able to bind specifically to the duplex DNA with only a slightly reduced affinity compared with the unmodified phosphodiester TFOs (Hacia et al. 1994b; Lacoste et al. 1997; Marchand et al. 2000). But, phosphorothioated TFOs have been found to form triplex DNA more efficiently than their phosphodiester counterparts in the presence of intracellular concentrations of potassium ions (Tu et al. 1995), suggesting that phosphorothioated TFOs may be advantageous for binding *in vivo*.
The observed interaction was sequence-specific, because a scrambled control oligonucleotide did not bind to the MCP-1 promoter fragment. To further confirm sequence-specificity, the TFO and control were incubated with a RANTES promoter sequences as a control duplex DNA. No binding occurred using this unrelated target sequence.

A next aim was to test whether the TFO can inhibit expression of MCP-1 in cultured cells. MCP-1 is a member of the CC chemokine family and is expressed in vascular endothelial cells, vascular smooth muscle cells, monocytes, fibroblasts, and several cancer cell lines. MCP-1 can be induced by a variety of mediators including PDGF, IL-1β, TNF-α, VEGF, LPS and IFN-γ (Murao et al. 2000; Thibeault et al. 2001). In this study it was further demonstrated that it is possible to use the TFO to partially inhibit MCP-1 expression in HEK 293 cells. Incubation of the cells with 2.0 µM TFO inhibited TNF-α stimulated MCP-1 protein secretion about 25% in comparison to the scrambled control oligonucleotide, as determined by ELISA.
In a previous study Marchand (Marchand et al. 2000) demonstrated via gel shift assays that the same 19 nt purine TFO binds to the SP-1 site of the MCP-1 gene promoter, but not to the

SP-1 region of the IL-6 gene as a control target. Binding experiments with nuclear extract proteins from HEK 293 cells, including the transcription factor SP-1, have shown that binding of the TFO replaces binding of nuclear proteins to the target duplex DNA, indicating that the binding of oligonucleotides or protein to the target are competing reactions. The *in vitro* findings support the hypothesis that triplex formation at the MCP-1 promoter can serve as a mechanism for transcriptional repression by replacing or preventing the binding of necessary transcription factors. In cell culture experiments, Marchand et al. used a TFO which contained phosphorothioate modifications at each oligonucleotide in comparison to a 5', 3' phosphorothioated TFO which was used in this study, and they could show 45% inhibition of TNF-α induced MCP-1 expression in comparison to 25% inhibition demonstrated here. These results suggest that a complete phosphorothioate modification of the oligonucleotide might be more effective than only a partial one in cell culture experiments. Notably, the inhibitory effect of the TFO was hardly visible in the unstimulated cells and more pronounced in TNF-α stimulated cells. This observation might be related to differences in the accessibility of the target sequence due to transcriptional activation. The TFO must overcome possible steric hindrance by the chromatin structure, which can undergo major changes upon up-regulation of transcription. The hypothesis that the TFO target region in the MCP-1 gene can change accessibility under cytokine stimulation is supported by a study that showed that IFN-γ induced signalling resulted in changes in the genomic footprinting pattern of the MCP-1 promoter SP-1 site in astrocytoma cells (Zhou et al. 1998).

In the present study it could be shown that transcription inhibition by a TFO targeting the MCP-1 promoter was sequence-specific and triplex mediated. Although the overall efficacy of inhibition demonstrated with the purine GT-TFO was only moderate, specific DNA binding molecules may prove useful for the development of therapeutics and as tools the for further understanding of DNA associated functions in the cellular context. TFOs can be used as sequence-specific DNA ligands and they can affect cellular processes such as transcription. The ability to block the synthesis of a chemokine *in vivo* during in inflammatory reaction might have a beneficial effect on the course of the disease. A substantial increase in the intracellular efficacy of triplex-induced effects will be achieved by chemical modifications of the oligonucleotide that could improve triplex stability, or by optimised delivery methods enhancing cellular uptake of the oligonucleotide. A successful solution to improve delivery systems is the *in vivo* generation of the TFO, as described in chapter 5.2.

5.1.2 RNA interference

RNA interference (RNAi) is a post-transcriptional process triggered by the introduction of double-stranded RNA which leads to gene silencing in a sequence-specific manner. RNAi has been reported to naturally occur in organisms as diverse as nematodes, trypanosomes, plants and fungi. Introduction of double-stranded RNA into the cells leads to sequence-specific destruction of endogenous RNAs that are complementary to the dsRNA (Hammond et al. 2000; Nykanen et al. 2001). During RNA interference, long dsRNA molecules are processed into 19 to 23 nt RNAs known as small interfering RNAs (siRNA) that serve as guides for enzymatic cleavage of complementary RNAs. In addition, siRNAs can function as primers for an RNA-dependent RNA polymerase that synthesises additional dsRNA, which in turn is processed into siRNAs, amplifying the effects of the original siRNAs.
Tuschl and co-workers observed that transfection of synthetic 21 nt siRNA duplexes into mammalian cells effectively interfered with mRNA translation in a sequence-specific manner (Elbashir et al. 2001; Harborth et al. 2001). These siRNA duplexes are too short to trigger non-specific dsRNA responses, but they still cause destruction of complementary RNA sequences (Hutvagner et al. 2001).
In this study, different strategies have been tested to destruct the targeted mRNA of the human MCP-1 and murine RANTES in various cell lines. One approach was the production of siRNA from a transfected expression vector (pSUPER) containing the polymerase-III H1-RNA gene promoter. The vector produces a small RNA transcript lacking a polyadenosine tail and has a well-defined start of transcription and a termination signal consisting of five thymidines in a row. The cleavage of the transcript at the termination site is taking place after the second uridine (Baer et al. 1990) yielding a transcript with the ends resembling synthetic siRNAs, which also contain two 3' overhanging T or U nucleotides. The vector pSUPER was used to suppress endogenous MCP-1 translation in HEK 293 cells. An empty vector without RNA sequence served as a control. Inhibition due to the siRNA was measured in stimulated and unstimulated cells. In TNF-α stimulated cells MCP-1 protein synthesis was decreased by 35 ± 11% after siRNA transfection. Cells transfected with the empty vector (no RNA transcript) revealed a decrease of MCP-1 protein synthesis by 18 ± 7%. These result demonstrate that the vector itself has an effect in HEK 293 cells, leading to a slight inhibition of gene expression, but inhibition was more pronounced by the vector derived MCP-1 siRNA. Transfection experiments were performed using the same sequence as a synthetic double-stranded siRNA. This led to similar results, but the inhibitory effect of the siRNA was even less pronounced (30% inhibition in unstimulated cells and 23% in TNF-α stimulated cells). Additionally, another synthetic siRNA sequence was tested, which was ordered from the manufacturer as a validated siRNA targeting the human MCP-1. Using this sequence, the

TNF-α induced MCP-1 protein secretion could be successfully inhibited about 62.3 ± 10.3% in HEK 293 cells, indicating that the siRNAs are functional in these cells to suppress chemokine expression. It would be very interesting and worthwhile to transcribe this siRNA from the vector pSUPER and analyse its efficacy in direct comparison to the TFO-RNA (see below).

The siRNA approach targeting murine RANTES in TH1 cells and b-end3 cells revealed no inhibition of endogenous gene expression. But, in this study only one siRNA sequence was tested, which seems to have no functional relevance in the tested cell lines. It would be necessary to test several different siRNA sequences with respect to their ability to inhibit RANTES gene expression.

5.2 Intracellular generation of a TFO targeting endogenous MCP-1

Triple helix-forming oligonucleotides bind to the duplex DNA in a sequence-specific manner. By forming a local triple helix structure, e.g. in the promoter, they are able to inhibit transcription of the target gene. In this study the *in vivo* generation of a TFO targeting the human MCP-1 is described. A pyrimidine triplex forming RNA sequence generated within HEK 293 cells by specific expression vectors was effective in inhibiting the transcription of the human MCP-1 gene. The 19 bp target sequence is located in the promoter region of this gene and encompasses binding sites for the transcription factors SP-1 and AP-1.

Specific binding of the 19 nt CU-TFO to the MCP-1 promoter target site was shown *in vitro* at pH 6.7, and additionally it was proven that the 1.1 kb TFO/ hygromycin fusion transcript binds to the MCP-1 promoter duplex at pH 7. This was demonstrated by a newly developed technique measuring the relative binding of the plasmid encoded MCP-1 promoter duplex to the TFO/hygromycin fusion transcript in comparison to control transcripts via magnetic separation of the triplex complexes. As shown, the binding of the specific TFO/ hygromycin fusion transcript to the plasmid embedded MCP-1 promoter duplex was three times more efficient than the binding of control-RNA. The TFO or control transcripts were present in the cytosol and nucleus, the site of triplex formation, as shown by RT-PCR. Finally, a highly effective and specific inhibition of MCP-1 protein secretion was detectable as compared to IL-8 in cytokine stimulated cells which express the CU-TFO unlike cell lines carrying control vectors. These results proof that the triplex formation we observed in cell-free experiments was readily transferable to intact target cells by using RNA TFO expressing vectors and led to a functional blockade of the target gene (Kautz et al. 2005).

The potential of ribonucleotide sequences to form triplexes is supported by several *in vitro* studies (Escude et al. 1993; Han and Dervan 1993; Roberts and Crothers 1992). Triplex formation with RNA oligonucleotides and double-stranded DNA may provide a means of controlling gene expression from specific promoters and/or creating more selective DNA cleaving agents. Triple-helical complexes have been shown to inhibit gene expression when introduced into eukaryotic cells. Thus, oligonucleotides that bind duplex DNA via triple helix formation have potential as gene specific repressors. Conventional triple helix formation in the pyrimidine motif allows the design of RNA oligonucleotides that can recognise cognate sequences in duplex DNA: However, mildly acidic conditions are often required for strong binding. In addition, the pyrimidine recognition sequence must be optimally represented within a longer RNA transcript when produced *in vivo* (McDonald and Maher, III 1995).

5.2.1 The pyrimidine binding motif

Pyrimidine-rich triplex forming oligoribonucleotides have a considerable higher binding affinity to the duplex DNA in comparison to their triplex forming DNA oligonucleotide counterparts as described by Roberts (Roberts and Crothers 1992). They observed a markedly higher stability for triplexes in which the third strand was RNA. The observed variability in the complexes must be due to the chemical differences between RNA and DNA; the 2'OH and the thymine methyl groups, respectively. They emphasised that the stability of the triplex with an RNA third strand + DNA duplex points to novel strategies and opens the possibility of an *in vivo* role of these structures. But triplex formation alongside the pyrimidine binding motif typically requires mildly acidic conditions to protonate cytosines. Several potential cytosine analogues like 8-oxoadenine derivatives exist which can overcome the need for cytosine protonation (Chan and Glazer 1997; Miller et al. 1992). On the other hand, Soukup (Soukup et al. 1996) selected RNA transcripts which all contained a pyrimidine recognition sequence and were able to bind to the target duplex between pH 6.5 and pH 7.4. RNAs have been selected for binding to a homopurine/homopyrimidine duplex DNA sequence under pH conditions that ranged from slightly acidic to neutral. They found that all RNAs appeared to form conventional triple helices with the DNA target sequence via a pyrimidine recognition sequence within the longer RNA molecule. Furthermore, pyrimidine recognition sequences within longer RNAs may be subject to important context effects because of their secondary structures that may modulate their binding affinities.

Noonberg (Noonberg et al. 1994a) suggested that the high concentration of a triplex RNA oligonucleotide, which is generated in the nucleus in vast excess over its DNA duplex target, may drive triplex binding to a critical element on a gene promoter, and block subsequent gene expression. To circumvent the problems extracellular degradation, cellular uptake, and intracellular sequestration they described a system for producing large quantities of short, sequence-specific RNA oligonucleotides for use in gene regulation strategies.

The pH within the cell is different for various organelles, and compartments of the biosynthetic pathway are described to have a neutral pH, endosomes are slightly acidic (pH 6.2) and lysosomes range between pH 4.8 and 5.2 (Weisz 2003). Llopis (Llopis et al. 1998) detected a pH of 6.58 for the trans-Golgi network, a major sorting site for newly synthesised molecules. In triplex blotting experiments described below a pH of 5.5 was chosen to perform experiments with the control oligonucleotide (single mismatch) and mismatched duplex DNA under optimal conditions for the pyrimidine motif. A possible unspecific effect was excluded in that way. As lined out the magnetic bead capture assay was performed at a pH of 7.0 with

positive evidence for a specific interaction of the long mRNA containing the CU-RNA TFO. These data together with the expected pH of 6.8 to 7.2 in the respective subcellular compartments and the highly specific functional effect underline that pH conditions did not interfere with triplex formation using the pyrimidine binding motif inside the cells.

Few studies have been published which excluded the possibility that purine oligoribonucleotides form triplex structures with duplex DNA (Escude et al. 1993; Semerad and Maher, III 1994; Skoog and Maher, III 1993), but more recently Cogoi (Cogoi et al. 2000) convincingly demonstrated triplex formation using CU-, GU- as well as GA-oligoribonucleotides. Based on these promising results there is a growing interest to develop methods to produce repressor RNA transcripts inside the target cell *in vivo* (Cogoi et al. 2000; Noonberg et al. 1994a; Rininsland et al. 1997). Another strategy was discussed by Datta (Datta and Glazer 2001). They tested a vector system for the production of single-stranded DNA to serve as a TFO in mouse cells and assayed TFO induced recombination, but no inhibition on endogenous gene expression was measured. Rininsland (Rininsland et al. 1997) described the specific suppression of IGF-1 receptor gene expression in rat glioblastoma cells in culture as well as in animals by using a plasmid-encoded homopurine (AG) RNA effector sequence. They showed that this RNA TFO formed a triple helix with the target DNA, whereas a homopyrimidine RNA sequence had no effect. Shevelev (Shevelev et al. 1997) demonstrated tumour growth inhibition in an animal model employing a eukaryotic expression vector encoding a purine GA-TFO corresponding to the IGF I gene. Additionally, an antiparallel GA oligoribonucleotide binding to the rat α1(I) procollagen promoter inhibits procollagen gene transcription (Ririe and Guntaka 1998). Here, the authors demonstrated formation of a triplex structure by an antiparallel RNA oligonucleotide corresponding to the 21 bp polypurine/polypyrimidine stretch from -141 to -162 of the rat α1(I) procollagen promoter with a K_d of 0.1-0.2 µM, and triplex formation was observed under physiological conditions. *In vitro* transcription run-off experiments showed that triplex formation results in inhibited transcription of the rat α1(I) procollagen gene.

Over all, while these studies suggested that triplex formation inside the cell nuclei led to the observed inhibitory effect, no clear experimental proof has been delivered. The data presented in this study, however, clearly show that the CU-sequence was capable of triplex formation with the target duplex at the human MCP-1 promoter not only with a short target duplex in triplex blots but moreover even when expressed within a large transcript and with the target duplex embedded in a complete plasmid.

5.2.2 Sequence-specific binding of the TFO to the MCP-1 target sequence

In this study the binding of a 19 nt CU oligoribonucleotide to the MCP-1 promoter duplex and the formation of a triplex structure was verified by triplex blotting, a technique first described by Noonberg (Noonberg et al. 1994b). This technique is designed to detect RNA species capable of triplex formation with radio-labelled duplex DNA probes. Triplex blotting offers a new approach for screening potential RNA sequences for triplex formation with double-stranded DNA targets, for comparing relative binding affinities of various triplex-forming RNAs and confirming the specificity of triplex formation of a DNA target probe. Using this technique, specific binding of the synthetic 19 nt CU-TFO to the 39 bp MCP-1 promoter target at pH 6.7 was shown. While a mismatch at position 15 (C/G inversion) was tolerated well in the triple helix motif without adverse effects on TFO binding, no triplex formation was observed using an oligoribonucleotide with CA base composition in a scrambled order (rCA-control) or using an oligoribonucleotide in the purine binding motif (rGU-control). The CU-TFO was able to bind to the short 39 bp duplex DNA, but binding might occur through D-loop formation with partial melting of the target duplex. Therefore a plasmid containing the triplex site as a target was used for hybridisation in a subsequent experiment since it should be less favourable to a DNA opening phenomenon. Using this target in triplex blotting experiments a specific binding of the 19 nt CU-TFO to the plasmid encoded MCP-1 promoter duplex DNA was seen. However, only a weak binding of the GA-sequence to the plasmid encoded MCP-1 promoter target duplex occurred, indicating a stronger binding affinity of the CU-sequence to the target. Binding of the GA-sequence did not occur using the short 39 bp target.

Because the TFO sequence contains a symmetric sequence in the length of 11 nt (5’ ucuCCCUCUCUCCCaccuc 3’), a short double helix might form between CU-RNA and the GA-rich strand of the MCP-1 promoter instead of a triplex structure. Therefore, the binding capacity of a TFO sequence containing only one mismatch which did not interrupt the symmetric structure (5’ uc<u>a</u>CCCUCUCUCCCaccuc 3’, mismatch underlined) was tested. Here, an antisense double helix might be still possible but triplex formation should be less favourable. The data clearly show that no binding occurred using this kind of control, indicating that the observed binding indeed must represent triplex formation. Another control employed consisted of a duplex DNA containing two mismatches, which did not bind to the TFO. This finding is a strong argument that the binding of the RNA TFO shown herein is not a result of unspecific duplex/oligo interaction.

According to the literature, the binding affinity is stronger at low pH because of cytosine protonation. However, the data clearly indicate that under the chosen conditions triplex

formation in the pyrimidine binding motif occurred at pH 6.7, which is close to the physiological pH. Moreover, the magnetic capture assay, involving the TFO fusion transcript, raised additional evidence for triplex formation at pH 7.0 and showed three fold stronger binding of the TFO to the target in comparison to controls.

The effector molecule which is produced in stable transfected HEK 293 cells is a fusion transcript of the CU TFO sequence tethered to the messenger RNA of the hygromycin resistance gene. Therefore it is critical to demonstrate the triplex forming ability of the TFO/hygromycin fusion transcript rather than the synthetic 19 nt CU-TFO alone. A new assay for the detection of TFO/hygromycin fusion transcripts binding to the MCP-1 target sequence was established to evaluate whether the fusion transcript is able to interact with the MCP-1 target duplex DNA in a sequence-specific and in a triplex mediated manner. Triplex complexes could be captured using a biotin/streptavidin-based mechanism and identified by PCR amplification of a portion of the captured fragment. To prepare for the magnetic separation of triplex complexes, the *in vitro* transcribed single-stranded TFO/hygromycin fusion transcript was annealed to a biotinylated oligonucleotide. The aim was to clearly demonstrate that the 1.1 kb fusion transcript recognises in a sequence-specific manner the double-stranded 39 bp MCP-1 promoter target sequence which was integrated into a plasmid. In the final step, triplex complexes were captured via magnetic separation using magnetic streptavidin coated beads which bind to the biotinylated RNA/DNA complexes and a magnetic separator. This technique of magnetic capture of triplex complexes has been used successfully before by Besch (Besch et al. 2002). They performed a capture assay for the evaluation the specific TFO binding to genomic DNA, using a psoralen- and biotin-modified TFO which was UV cross-linked to a 16 bp target sequence of the ICAM-1 gene. Quantification of bound duplex DNA was done by PCR. Adapting this technique to the situation described in this study a biotinylated RNA strand was annealed to the TFO and control fusion transcripts, respectively, and the interaction with a plasmid containing the 39 bp MCP-1 promoter target duplex was tested.
The relative amount of bound plasmid was quantified using a semi-quantitative PCR with 25 cycles, where product amplification was shown to be in a linear range. In this experimental setting the binding of the TFO fusion transcript to the plasmid was three times stronger in comparison to the controls, meaning a fusion transcript containing the 19 nt GU or CA sequence or no insert. Notably, these experiments were performed at pH 7.0 indicating that triplex formation in the pyrimidine binding motif is likely to happen at physiologic pH. Some problems might occur in this experimental set up, like differences in the grade of degradation of the RNA fusion transcript in the control- and TFO samples or even unspecific binding of the plasmid to RNA or the streptavidin microbeads, which might easily lead to false results.

To minimise these problems, RNase inhibitor was included in all steps and the integrity of the RNA was tested before each experiment to ensure that equal amounts of the fusion transcripts (TFO or control) were used. Next, the relative amount of intact RNA in the elution fractions after four washing steps was quantified densitometrically and then normalised to compare the quantity of bound plasmid. Bound plasmid to RNA was analysed by PCR with the template volume calculated according to the amount of RNA present in the elution fractions. An unspecific binding of the controls to the RNA could be observed in the shown experiments, but summarised, the binding of the TFO was three times stronger. By using the magnetic capture technique, Besch et al. observed 23% binding of the control to the ICAM-1 duplex target, when the binding of the TFO to the duplex was set to 100%. In the experiments described here, there was no PCR amplification when the experiments were performed without biotinylated RNA, indicating that the “background” might be due to unspecific RNA/plasmid interaction but not to unspecific plasmid and streptavidin interaction. Together with the significant results of the triplex blotting experiments one can conclude that the stronger binding of the TFO fusion transcript to the plasmid is a result of triplex formation involving the pyrimidine 19 nt CU sequence. Finally, this experiment was done to underline that triplex formation might be the correct mechanism of action in the cells being responsible for the marked inhibition of MCP-1 expression. There is no publication demonstrating the binding of an intracellular generated RNA-TFO to the endogenous target duplex in a triplex mediated manner leading to an inhibitory effect. For example, Rininsland (Rininsland et al. 1997) used a large GA-TFO fusion transcript expressed intracellular and showed convincing data in cell culture experiments and in animal models as well, but there was no functional analysis of triplex formation in the cell nucleus. Last but not least one cannot exclude that binding reaction in the cell nucleus is far more complex and difficult to reproduce *in vitro*, taking into account that the secondary structure of the RNA or mRNA binding proteins and the chromosomal structure of the MCP-1 gene after stimulation might be important.

5.2.3 Inhibition of endogenous MCP-1 gene expression

With respect to the functional antigene activity, in this study a vector mediated synthesis of pyrimidine triplex-forming RNA species inside HEK 293 cells was successfully developed, leading to up to 88% inhibition of TNF-α and IFN-γ co-stimulated MCP-1 protein secretion. Vector constructs used for transfection to generate stable cell lines had to cross the plasma membrane, move through the cytoplasm, and be transported into the nucleus before any transcription of their encoded genes can take place. The intracellular trafficking and cytoplasmic transport of plasmid DNA is reviewed by Zhou (Zhou et al. 2004)

Transcription of the TFO coding sequence was driven together with the hygromycin resistance gene as one fusion transcript from the constitutive CMV promoter. The presence of each of the intracellular generated CU-, GU-, and CA-RNA sequences in the nucleus and the cytosolic fraction was confirmed by RT-PCR, leading to the conclusion that the vector constructs successfully entered the nucleus. Furthermore, the transcript was sufficiently stable given that the RNA translocated into the cytosol, where it was translated into protein and enabled stable transfected HEK 293 cells to be cultured under continued hygromycin selection pressure. The evidence of transcription and the cell culture conditions show that the vector constructs reached the nucleus where the action of TFO binding to the endogenous MCP-1 promoter target sequences takes place. No quantitative experiments were performed to evaluate the exact copy numbers or concentration of expressed transcripts, which would be possible with nuclear run-off assays.

In direct comparison with the previous data this investigation convincingly shows that vector mediated delivery of triplex forming RNA sequences is much more efficient than adding DNA TFOs against the human MCP-1 extracellular, which lead to 45% inhibition of gene expression (Marchand et al. 2000). A 76 to 88% inhibition was reached herein with an intracellular generated CU triplex RNA sequence. To exclude the possibility that the TFO inhibited MCP-1 expression by interfering with TNF-α signalling, it was evaluated whether the TFO interfered with the expression of IL-8, which is also induced by TNF-α. In samples identical to those with the mentioned reduction of MCP-1, no reduction of IL-8 protein secretion was measured. Again, the control GU- and CA- sequences had neither an effect on IL-8 protein secretion nor on MCP-1 protein secretion. Binding of the CU-TFO to the MCP-1 RNA appeared to be unlikely, because there is no matching sequence in the MCP-1 RNA for stable duplex formation with the TFO; thus an “antisense” effect could also be excluded.

The inhibitory effect of the TFO is more pronounced in TNF-α stimulated HEK 293 cells in comparison to unstimulated cells (76% versus 53%, respectively), leading to the question of accessibility of chromosomal DNA targets to TFOs. Macris (Macris and Glazer 2003) detected binding of TFOs to a chromosomal site even in the absence of transcription when high concentrations of the TFO were used for transfection, demonstrating that transcription at a chromosomal site increased duplex site accessibility to the TFO. Comparably, the data suggest that induction of transcription enhanced TFO-binding to the MCP-1 promoter target site resulting in a stronger inhibitory effect of MCP-1 expression.

In summary, these data strongly suggest that a specific RNA TFO inhibited MCP-1 expression by a triplex mediated blockade of transcription, and moreover that this can be

achieved by transfectable shuttle systems. Unlike siRNAs and antisense oligonucleotides which have to deal with a high number of mRNA targets, triplex-forming oligonucleotides selectively inhibit expression of specific genes directly. Released from transfectable RNA vectors they only have to reach the two alleles of the gene which opens the perspective for a longer lasting pharmacologic effect. Recently developed siRNA generating vector systems are also suitable to generate RNA TFOs *in vivo*. Combining these improved expression vectors with the knowledge of hundreds of suitable TFO targets in the mammalian genome (Radeke HH and Bruno B, unpublished data) warrants that the intracellular TFO delivery technique may be developed to a successful gene therapeutic approach.

5.3 Lentiviral vectors

Several recently developed vector based strategies that contain stem-loop constructs encoding hairpin RNAs lead to the intracellular generation of siRNA like species (Brummelkamp et al. 2002; McCaffrey et al. 2002; Paul et al. 2002). Dicer cleavage of hairpin RNA can generate small dsRNA that silence expression of genes whose transcription are complementary to one of the two strands of the hairpin RNA. Most vector-based hairpin expression systems have demonstrated only transient knockdown of gene expression. More recently, inhibition of gene expression has been achieved using retroviral vector constructs that express hairpin RNAs within vector infected cells and produce long-term knockdown within cultured cell lines (Barton and Medzhitov 2002; Devroe and Silver 2002).
Rubinson (Rubinson et al. 2003) demonstrated that lentiviruses can be used to deliver siRNAs and reduce gene expression in cycling and non-cycling cells, as well as in chimeric and transgenic mice. They suggested that lentiviral expression vectors might be used therapeutically to silence disease causing genes, to render cells resistant to infectious organisms, and to facilitate the creation of tissues deficient in specific antigens as a source of transplant organs. Further modifications to lentiviral expression vectors, such as the inclusion of inducible or tissue-specific promoters, might extend the range of cells and situations in which they can induce RNA interference.

Although lentiviral vectors promise great utility for gene therapy, there might be some concern about their safety since HIV-1 is the etiologic agent of AIDS. One major concern is the generation of replication-competent virus during the production of vectors. The possibility for generating replication-competent virus through recombination was minimised by using a three plasmid expression system which consists of packaging, envelope, and transfer vector constructs (Follenzi and Naldini 2002). Furthermore, all accessory genes can be eliminated from a packaging construct without losing the ability to transduce non-dividing cells. Another modification is the construction of a self inactivating (SIN) vector in which the viral enhancer and promoter sequences have been deleted (Follenzi and Naldini 2002; Vigna and Naldini 2000). Concerning biosafety, a self-inactivating vector diminishes the risk of oncogene activation by promoter insertion and alleviates substantially the risk of vector mobilisation and recombination with wild-type virus (Bukovsky et al. 1999). Additionally, the replacement of the U3 region of the 5' long terminal repeat with the cytomegalovirus (CMV) promoter resulted in tat-independent transcription with no decreases in viral titre. SIN vectors combined with this hybrid 5' LTR further reduce the possibility of recombination because there is no complete U3 sequence in the virus production system (Miyoshi et al. 1998).

In principle, lentiviral vectors capable of generating siRNA might be modified and used for the *in vivo* synthesis of specific TFO-like transcripts in several cell lines. Of course one has to take into account that the place of action of TFOs and siRNAs is different (nucleus versus cytosol), and siRNA producing vectors might be optimised for the rapid translocation of the transcript into the cytosol, which would be disadvantageous for the TFO technology. But, lentiviral vectors have been demonstrated to achieve high levels of transduction and gene expression *in vivo* after a single exposure to viral supernatant and therefore they are highly effective for gene transfer to several cells and possibly suitable for the TFO technique.

In this study the cloning of recombinant transfer vectors and the transient transfection of lentiviral vector plasmids into a HEK 293T cell line for packaging lentiviral vector genomes into infectious lentiviral particles were performed. The transfer vector pHR'SIN-cPPT-SEW ("SEW") was used, which contained the spleen focus forming virus (SFFV) long terminal repeat sequences, and the woodchuck hepatitis virus posttranscriptional element (WPRE) to enhance the level of transcription (Demaison et al. 2002). By including the central polypurine tract (cPPT) sequence of HIV-1, high levels of transduction could be achieved.
Here, Th1 cells were transduced with infectious lentiviral particles and transduction efficacy was measured. Th1 have been shown to be difficult to transfect using synthetic TFOs or double-stranded siRNAs. But a transduction efficacy higher than 82% could be achieved using the lentiviral vector SEW, opening optimal possibilities for the TFO or siRNA approach.

6 Outlook

In the present study gene and sequence-specific inhibition of MCP-1 transcription was shown due to interference of intracellular generated single-stranded RNA (CU-TFO) with an overlapping SP-1/AP-1 target. CU-TFO inhibited MCP-1 protein release about 76 to 88% in comparison to intracellular generated control oligonucleotides which did not show any activity. IL-8 as a control target gene was not affected by CU-TFO. The data proof effective and specific inhibition of MCP-1 expression by TFOs generated by transfectable shuttle vectors opening the possibility of *in vivo* gene therapeutic application of the TFO technique. Another successful approach was the use of synthetic siRNA to inhibit MCP-1 protein secretion in TNF-α stimulated HEK 293 cells about 62%.

To date, the successes achieved with TFOs in cell cultures and animal models indicate that TFOs constitute a new class of molecules potentially useful in therapy. But, in order to think about clinical applications with these compounds, their delivery to cells must be improved. Before reaching the level of clinical trials, the TFOs have to be improved in their capacity to penetrate the cells and target the DNA in a sequence-specific manner. When they will be properly delivered to the tissues, TFOs may become strong anti-gene drugs to treat several types of diseases, in particular those in which a partial reduction of the level of protein is sufficient to improve the phenotype of the disease.

To achieve this goal, lentiviruses might be used to deliver TFOs or siRNA to specific tissues or cells in order to suppress expression of the targeted gene. For the siRNA approach, the sequence of the synthetic siRNA targeting MCP-1 can be cloned with the appropriate expression cassette into the lentiviral transfer vector SEW using the sequences 5'GAT CCC C*GG ATT CCA TGG ACC ACC TG*T TCA AGA GA*C AGG TGG TCC ATG GAA TCC* TTT TTG GAA A and 5'AGC TTT TCC AAA AA*G GAT TCC ATG GAC CAC CTG* TCT CTT GAA *CAG GTG GTC CAT GGA ATC C*GG G, where the siRNA sequence is presented in sense and antisense orientation to build a stem-loop structure.

For the TFO technology different cloning strategies are possible. The successful 19 nt TFO sequence targeting the human MCP-1 can be represented as a single copy, or the recognition sequence might be represented in larger a RNA in several copies in a row, as presented by McDonald (McDonald and Maher, III 1995). Alternatively, the TFO sequence might be embedded in larger RNA fusion transcript as described in the present study. Finally, different cells of interest can be transduced with the resulting constructs, and strategies to suppress gene expression using siRNAs or TFOs might be compared or even combined. It should be helpful to generate different TFO sequences, because secondary structure of the RNA might have influence on the intracellular processes and binding affinities. The further development of oligonucleotide-based reagents with improved binding affinities and delivery

systems could be an alternative therapeutic strategy to modulate gene expression not only of proinflammatory chemokines.

7 Literature

Akkina RK, Walton RM, Chen ML, Li QX, Planelles V, Chen IS (1996) High-efficiency gene transfer into CD34+ cells with a human immunodeficiency virus type 1-based retroviral vector pseudotyped with vesicular stomatitis virus envelope glycoprotein G. J. Virol. 70:2581-5

Anders HJ, Vielhauer V, Kretzler M, Cohen CD, Segerer S, Luckow B, Weller L, Grone HJ, Schlöndorff D (2001) Chemokine and chemokine receptor expression during initiation and resolution of immune complex glomerulonephritis. J. Am. Soc. Nephrol. 12:919-31

Anfossi G, Gewirtz AM, Calabretta B (1989) An oligomer complementary to c-myb-encoded mRNA inhibits proliferation of human myeloid leukemia cell lines. Proc. Natl. Acad. Sci. U. S. A 86:3379-83

Appay V, Dunbar PR, Cerundolo V, McMichael A, Czaplewski L, Rowland-Jones S (2000) RANTES activates antigen-specific cytotoxic T lymphocytes in a mitogen-like manner through cell surface aggregation. Int. Immunol 12:1173-82

Appay V, Rowland-Jones SL (2001) RANTES: a versatile and controversial chemokine. Trends Immunol 22:83-7

Arimondo PB, Bailly C, Boutorine AS, Moreau P, Prudhomme M, Sun JS, Garestier T, Helene C (2001) Triple helix-forming oligonucleotides conjugated to indolocarbazole poisons direct topoisomerase I-mediated DNA cleavage to a specific site. Bioconjug. Chem. 12:501-9

Arimondo PB, Boutorine A, Baldeyrou B, Bailly C, Kuwahara M, Hecht SM, Sun JS, Garestier T, Helene C (2002) Design and optimization of camptothecin conjugates of triple helix-forming oligonucleotides for sequence-specific DNA cleavage by topoisomerase I. J. Biol. Chem. 277:3132-40

Bacon KB, Premack BA, Gardner P, Schall TJ (1995) Activation of dual T cell signaling pathways by the chemokine RANTES. Science 269:1727-30

Baer M, Nilsen TW, Costigan C, Altman S (1990) Structure and transcription of a human gene for H1 RNA, the RNA component of human RNase P. Nucleic Acids Res. 18:97-103

Baggiolini M, Loetscher P (2000) Chemokines in inflammation and immunity. Immunol Today 21:418-20

Barton GM, Medzhitov R (2002) Retroviral delivery of small interfering RNA into primary cells. Proc. Natl. Acad. Sci. U. S. A 99:14943-5

Basye J, Trent JO, Gao D, Ebbinghaus SW (2001) Triplex formation by morpholino oligodeoxyribonucleotides in the HER-2/neu promoter requires the pyrimidine motif. Nucleic Acids Res. 29:4873-80

Bates PJ, Reddoch JF, Hansakul P, Arrow A, Dale R, Miller DM (2002) Biosensor detection of triplex formation by modified oligonucleotides. Anal. Biochem. 307:235-43

Becker S, Reed W, Henderson FW, Noah TL (1997) RSV infection of human airway epithelial cells causes production of the beta-chemokine RANTES. Am. J. Physiol 272:L512-L520

Belperio JA, Keane MP, Arenberg DA, Addison CL, Ehlert JE, Burdick MD, Strieter RM (2000) CXC chemokines in angiogenesis. J. Leukoc. Biol. 68:1-8

Bernstein E, Denli AM, Hannon GJ (2001) The rest is silence. RNA. 7:1509-21

Besch R, Giovannangeli C, Kammerbauer C, Degitz K (2002) Specific inhibition of ICAM-1 expression mediated by gene targeting with Triplex-forming oligonucleotides. J. Biol. Chem. 277:32473-9

Bogdanov VY, Poon M, Taubman MB (1998) Platelet-derived growth factor-specific regulation of the JE promoter in rat aortic smooth muscle cells. J. Biol. Chem. 273:24932-8

Brown Z, Robson RL, Westwick J (1996) Regulation and expression of chemokines: potential role in glomerulonephritis. J. Leukoc. Biol. 59:75-80

Brummelkamp TR, Bernards R, Agami R (2002) A system for stable expression of short interfering RNAs in mammalian cells. Science 296:550-3

Buchini S, Leumann CJ (2003) Recent improvements in antigene technology. Curr. Opin. Chem. Biol. 7:717-26

Bukovsky AA, Song JP, Naldini L (1999) Interaction of human immunodeficiency virus-derived vectors with wild-type virus in transduced cells. J. Virol. 73:7087-92

Carbone GM, McGuffie E, Napoli S, Flanagan CE, Dembech C, Negri U, Arcamone F, Capobianco ML, Catapano CV (2004) DNA binding and antigene activity of a daunomycin-conjugated triplex-forming oligonucleotide targeting the P2 promoter of the human c-myc gene. Nucleic Acids Res. 32:2396-410

Carbone GM, McGuffie EM, Collier A, Catapano CV (2003) Selective inhibition of transcription of the Ets2 gene in prostate cancer cells by a triplex-forming oligonucleotide. Nucleic Acids Res. 31:833-43

Carr MW, Roth SJ, Luther E, Rose SS, Springer TA (1994) Monocyte chemoattractant protein 1 acts as a T-lymphocyte chemoattractant. Proc. Natl. Acad. Sci. U. S. A 91:3652-6

Casey BP, Glazer PM (2001) Gene targeting via triple-helix formation. Prog. Nucleic Acid Res. Mol. Biol. 67:163-92

Cassidy RA, Kondo NS, Miller PS (2000) Triplex formation by psoralen-conjugated chimeric oligonucleoside methylphosphonates. Biochemistry 39:8683-91

Catapano CV, McGuffie EM, Pacheco D, Carbone GM (2000) Inhibition of gene expression and cell proliferation by triple helix-forming oligonucleotides directed to the c-myc gene. Biochemistry 39:5126-38

Chan PP, Glazer PM (1997) Triplex DNA: fundamentals, advances, and potential applications for gene therapy. J. Mol. Med. 75:267-82

Chang TL, Gordon CJ, Roscic-Mrkic B, Power C, Proudfoot AE, Moore JP, Trkola A (2002) Interaction of the CC-chemokine RANTES with glycosaminoglycans activates a p44/p42 mitogen-activated protein kinase-dependent signaling pathway and enhances human immunodeficiency virus type 1 infectivity. J. Virol. 76:2245-54

Charo IF, Peters W (2003) Chemokine receptor 2 (CCR2) in atherosclerosis, infectious diseases, and regulation of T-cell polarization. Microcirculation. 10:259-64

Chen G, Oh S, Monia BP, Stacey DW (1996) Antisense oligonucleotides demonstrate a dominant role of c-Ki-RAS proteins in regulating the proliferation of diploid human fibroblasts. J. Biol. Chem. 271:28259-65

Chen Y, Ji YJ, Roxby R, Conrad C (2000) In vivo expression of single-stranded DNA in mammalian cells with DNA enzyme sequences targeted to C-raf. Antisense Nucleic Acid Drug Dev. 10:415-22

Cheng AJ, Van Dyke MW (1993) Monovalent cation effects on intermolecular purine-purine-pyrimidine triple-helix formation. Nucleic Acids Res. 21:5630-5

Cheng AJ, Van Dyke MW (1994) Oligodeoxyribonucleotide length and sequence effects on intermolecular purine-purine-pyrimidine triple-helix formation. Nucleic Acids Res. 22:4742-7

Chuang CF, Meyerowitz EM (2000) Specific and heritable genetic interference by double-stranded RNA in Arabidopsis thaliana. Proc. Natl. Acad. Sci. U. S. A 97:4985-90

Cioffi CL, Garay M, Johnston JF, McGraw K, Boggs RT, Hreniuk D, Monia BP (1997) Selective inhibition of A-Raf and C-Raf mRNA expression by antisense oligodeoxynucleotides in rat vascular smooth muscle cells: role of A-Raf and C-Raf in serum-induced proliferation. Mol. Pharmacol. 51:383-9

Cioffi CL, Monia BP (2000) Evaluation of biological role of c-Jun N-terminal kinase using an antisense approach. Methods Enzymol. 314:363-78

Cogoi S, Rapozzi V, Quadrifoglio F, Xodo L (2001) Anti-gene effect in live cells of AG motif triplex-forming oligonucleotides containing an increasing number of phosphorothioate linkages. Biochemistry 40:1135-43

Cogoi S, Suraci C, Del Terra E, Diviacco S, van der MG, van Boom J, Quadrifoglio F, Xodo L (2000) Downregulation of c-Ki-ras promoter activity by triplex-forming oligonucleotides endogenously generated in human 293 cells. Antisense Nucleic Acid Drug Dev. 10:283-95

Coletta I, Soldo L, Polentarutti N, Mancini F, Guglielmotti A, Pinza M, Mantovani A, Milanese C (2000) Selective induction of MCP-1 in human mesangial cells by the IL-6/sIL-6R complex. Exp. Nephrol. 8:37-43

Conti P, Barbacane RC, Reale M (1999) Chemokines in inflammatory states. Allergy Asthma Proc. 20:205-8

Cravens PD, Lipsky PE (2002) Dendritic cells, chemokine receptors and autoimmune inflammatory diseases. Immunol Cell Biol. 80:497-505

Czaplewski LG, McKeating J, Craven CJ, Higgins LD, Appay V, Brown A, Dudgeon T, Howard LA, Meyers T, Owen J, Palan SR, Tan P, Wilson G, Woods NR, Heyworth CM, Lord BI, Brotherton D, Christison R, Craig S, Cribbes S, Edwards RM, Evans SJ, Gilbert R, Morgan P, Hunter MG, . (1999) Identification of amino acid residues critical for aggregation of human CC chemokines macrophage inflammatory protein (MIP)-1alpha, MIP-1beta, and RANTES. Characterization of active disaggregated chemokine variants. J. Biol. Chem. 274:16077-84

Dairaghi DJ, Franz-Bacon K, Callas E, Cupp J, Schall TJ, Tamraz SA, Boehme SA, Taylor N, Bacon KB (1998) Macrophage Inflammatory Protein-1beta Induces Migration and Activation of Human Thymocytes. Blood 91:2905-13

Danoff TM, Lalley PA, Chang YS, Heeger PS, Neilson EG (1994) Cloning, genomic organization, and chromosomal localization of the Scya5 gene encoding the murine chemokine RANTES. J. Immunol 152:1182-9

Datta HJ, Chan PP, Vasquez KM, Gupta RC, Glazer PM (2001) Triplex-induced recombination in human cell-free extracts. Dependence on XPA and HsRad51. J. Biol. Chem. 276:18018-23

Datta HJ, Glazer PM (2001) Intracellular generation of single-stranded DNA for chromosomal triplex formation and induced recombination. Nucleic Acids Res. 29:5140-7

Deglon N, Tseng JL, Bensadoun JC, Zurn AD, Arsenijevic Y, Pereira dA, Zufferey R, Trono D, Aebischer P (2000) Self-inactivating lentiviral vectors with enhanced transgene expression as potential gene transfer system in Parkinson's disease. Hum. Gene Ther. 11:179-90

del Pozo MA, Sanchez-Mateos P, Nieto M, Sanchez-Madrid F (1995) Chemokines regulate cellular polarization and adhesion receptor redistribution during lymphocyte interaction with endothelium and extracellular matrix. Involvement of cAMP signaling pathway. J. Cell Biol. 131:495-508

Demaison C, Parsley K, Brouns G, Scherr M, Battmer K, Kinnon C, Grez M, Thrasher AJ (2002) High-level transduction and gene expression in hematopoietic repopulating cells using a human immunodeficiency [correction of imunodeficiency] virus type 1-based lentiviral vector containing an internal spleen focus forming virus promoter. Hum. Gene Ther. 13:803-13

Devergne O, Marfaing-Koka A, Schall TJ, Leger-Ravet MB, Sadick M, Peuchmaur M, Crevon MC, Kim KJ, Schall TT, Kim T, . (1994) Production of the RANTES chemokine in delayed-type hypersensitivity reactions: involvement of macrophages and endothelial cells. J. Exp. Med. 179:1689-94

Devroe E, Silver PA (2002) Retrovirus-delivered siRNA. BMC. Biotechnol. 2:15

Dragic T, Litwin V, Allaway GP, Martin SR, Huang Y, Nagashima KA, Cayanan C, Maddon PJ, Koup RA, Moore JP, Paxton WA (1996) HIV-1 entry into CD4+ cells is mediated by the chemokine receptor CC-CKR-5. Nature 381:667-73

Durland RH, Kessler DJ, Gunnell S, Duvic M, Pettitt BM, Hogan ME (1991) Binding of triple helix forming oligonucleotides to sites in gene promoters. Biochemistry 30:9246-55

Durland RH, Rao TS, Revankar GR, Tinsley JH, Myrick MA, Seth DM, Rayford J, Singh P, Jayaraman K (1994) Binding of T and T analogs to CG base pairs in antiparallel triplexes. Nucleic Acids Res. 22:3233-40

Earnshaw DJ, Gait MJ (1997) Progress toward the structure and therapeutic use of the hairpin ribozyme. Antisense Nucleic Acid Drug Dev. 7:403-11

Ebnet K, Simon MM, Shaw S (1996) Regulation of chemokine gene expression in human endothelial cells by proinflammatory cytokines and Borrelia burgdorferi. Ann. N. Y. Acad. Sci. 797:107-17

Elbashir SM, Harborth J, Lendeckel W, Yalcin A, Weber K, Tuschl T (2001) Duplexes of 21-nucleotide RNAs mediate RNA interference in cultured mammalian cells. Nature 411:494-8

Escude C, Francois JC, Sun JS, Ott G, Sprinzl M, Garestier T, Helene C (1993) Stability of triple helices containing RNA and DNA strands: experimental and molecular modeling studies. Nucleic Acids Res. 21:5547-53

Escude C, Giovannangeli C, Sun JS, Lloyd DH, Chen JK, Gryaznov SM, Garestier T, Helene C (1996) Stable triple helices formed by oligonucleotide N3'-->P5' phosphoramidates inhibit transcription elongation. Proc. Natl. Acad. Sci. U. S. A 93:4365-9

Faria M, Wood CD, Perrouault L, Nelson JS, Winter A, White MR, Helene C, Giovannangeli C (2000) Targeted inhibition of transcription elongation in cells mediated by triplex-forming oligonucleotides. Proc. Natl. Acad. Sci. U. S. A 97:3862-7

Farson D, Witt R, McGuinness R, Dull T, Kelly M, Song J, Radeke R, Bukovsky A, Consiglio A, Naldini L (2001) A new-generation stable inducible packaging cell line for lentiviral vectors. Hum. Gene Ther. 12:981-97

Felsenfeld G, Davies DR, Rich A (1957) Formation of a three-stranded polynucleotide molecule. J. Am. Chem. Soc. 79:2023-24

Feng L (2000) Role of chemokines in inflammation and immunoregulation. Immunol Res. 21:203-10

Fire A, Xu S, Montgomery MK, Kostas SA, Driver SE, Mello CC (1998) Potent and specific genetic interference by double-stranded RNA in Caenorhabditis elegans. Nature 391:806-11

Follenzi A, Ailles LE, Bakovic S, Geuna M, Naldini L (2000) Gene transfer by lentiviral vectors is limited by nuclear translocation and rescued by HIV-1 pol sequences. Nat. Genet. 25:217-22

Follenzi A, Naldini L (2002) Generation of HIV-1 derived lentiviral vectors. Methods Enzymol. 346:454-65

Frade JM, Mellado M, del Real G, Gutierrez-Ramos JC, Lind P, Martinez A (1997) Characterization of the CCR2 chemokine receptor: functional CCR2 receptor expression in B cells. J. Immunol 159:5576-84

Frank-Kamenetskii MD, Mirkin SM (1995) Triplex DNA structures. Annu. Rev Biochem. 64:65-95

Galindo M, Santiago B, Rivero M, Rullas J, Alcami J, Pablos JL (2001) Chemokine expression by systemic sclerosis fibroblasts: abnormal regulation of monocyte chemoattractant protein 1 expression. Arthritis Rheum. 44:1382-6

Gillitzer R, Goebeler M (2001) Chemokines in cutaneous wound healing. J. Leukoc. Biol. 69:513-21

Giovannangeli C, Diviacco S, Labrousse V, Gryaznov S, Charneau P, Helene C (1997) Accessibility of nuclear DNA to triplex-forming oligonucleotides: the integrated HIV-1 provirus as a target. Proc. Natl. Acad. Sci. U. S. A 94:79-84

Glabinski AR, Balasingam V, Tani M, Kunkel SL, Strieter RM, Yong VW, Ransohoff RM (1996) Chemokine monocyte chemoattractant protein-1 is expressed by astrocytes after mechanical injury to the brain. J. Immunol 156:4363-8

Grigoriev M, Praseuth D, Robin P, Hemar A, Saison-Behmoaras T, Dautry-Varsat A, Thuong NT, Helene C, Harel-Bellan A (1992) A triple helix-forming oligonucleotide-intercalator conjugate acts as a transcriptional repressor via inhibition of NF kappa B binding to interleukin-2 receptor alpha-regulatory sequence. J. Biol. Chem. 267:3389-95

Gunther EJ, Havre PA, Gasparro FP, Glazer PM (1996) Triplex-mediated, in vitro targeting of psoralen photoadducts within the genome of a transgenic mouse. Photochem. Photobiol. 63:207-12

Hacia JG, Dervan PB, Wold BJ (1994a) Inhibition of Klenow fragment DNA polymerase on double-helical templates by oligonucleotide-directed triple-helix formation. Biochemistry 33:6192-200

Hacia JG, Wold BJ, Dervan PB (1994b) Phosphorothioate oligonucleotide-directed triple helix formation. Biochemistry 33:5367-9

Hammond SM, Bernstein E, Beach D, Hannon GJ (2000) An RNA-directed nuclease mediates post-transcriptional gene silencing in Drosophila cells. Nature 404:293-6

Hampel KJ, Crosson P, Lee JS (1991) Polyamines favor DNA triplex formation at neutral pH. Biochemistry 30:4455-9

Han H, Dervan PB (1993) Sequence-specific recognition of double helical RNA and RNA.DNA by triple helix formation. Proc. Natl. Acad. Sci. U. S. A 90:3806-10

Han H, Dervan PB (1994) Different conformational families of pyrimidine.purine.pyrimidine triple helices depending on backbone composition. Nucleic Acids Res. 22:2837-44

Harborth J, Elbashir SM, Bechert K, Tuschl T, Weber K (2001) Identification of essential genes in cultured mammalian cells using small interfering RNAs. J. Cell Sci. 114:4557-65

Harkness KA, Sussman JD, Davies-Jones GA, Greenwood J, Woodroofe MN (2003) Cytokine regulation of MCP-1 expression in brain and retinal microvascular endothelial cells. J. Neuroimmunol. 142:1-9

Holt JT, Redner RL, Nienhuis AW (1988) An oligomer complementary to c-myc mRNA inhibits proliferation of HL-60 promyelocytic cells and induces differentiation. Mol. Cell Biol. 8:963-73

Hornung D, Ryan IP, Chao VA, Vigne JL, Schriock ED, Taylor RN (1997) Immunolocalization and regulation of the chemokine RANTES in human endometrial and endometriosis tissues and cells. J. Clin. Endocrinol. Metab 82:1621-8

Hutvagner G, McLachlan J, Pasquinelli AE, Balint E, Tuschl T, Zamore PD (2001) A cellular function for the RNA-interference enzyme Dicer in the maturation of the let-7 small temporal RNA. Science 293:834-8

Ilves H, Barske C, Junker U, Bohnlein E, Veres G (1996) Retroviral vectors designed for targeted expression of RNA polymerase III-driven transcripts: a comparative study. Gene 171:203-8

Imhof BA, Aurrand-Lions M (2004) Adhesion mechanisms regulating the migration of monocytes. Nat. Rev Immunol 4:432-44

Intody Z, Perkins BD, Wilson JH, Wensel TG (2000) Blocking transcription of the human rhodopsin gene by triplex-mediated DNA photocrosslinking. Nucleic Acids Res. 28:4283-90

Irie A, Anderegg B, Kashani-Sabet M, Ohkawa T, Suzuki T, Halks-Miller M, Curiel DT, Scanlon KJ (1999) Therapeutic efficacy of an adenovirus-mediated anti-H-ras ribozyme in experimental bladder cancer. Antisense Nucleic Acid Drug Dev. 9:341-9

Irie A, Kijima H, Ohkawa T, Bouffard DY, Suzuki T, Curcio LD, Holm PS, Sassani A, Scanlon KJ (1997) Anti-oncogene ribozymes for cancer gene therapy. Adv. Pharmacol. 40:207-57

Iwakuma T, Cui Y, Chang LJ (1999) Self-inactivating lentiviral vectors with U3 and U5 modifications. Virology 261:120-32

Jansen B, Schlagbauer-Wadl H, Brown BD, Bryan RN, van Elsas A, Muller M, Wolff K, Eichler HG, Pehamberger H (1998) bcl-2 antisense therapy chemosensitizes human melanoma in SCID mice. Nat. Med. 4:232-4

Jetter MC, Hobbs FW (1993) 7,8-Dihydro-8-oxoadenine as a replacement for cytosine in the third strand of triple helices. Triplex formation without hypochromicity. Biochemistry 32:3249-54

Johnston B, Butcher EC (2002) Chemokines in rapid leukocyte adhesion triggering and migration. Semin. Immunol 14:83-92

Joseph J, Kandala JC, Veerapanane D, Weber KT, Guntaka RV (1997) Antiparallel polypurine phosphorothioate oligonucleotides form stable triplexes with the rat alpha1(I) collagen gene promoter and inhibit transcription in cultured rat fibroblasts. Nucleic Acids Res. 25:2182-8

Juarez J, Bendall L, Bradstock K (2004) Chemokines and their receptors as therapeutic targets: the role of the SDF-1/CXCR4 axis. Curr. Pharm. Des 10:1245-59

Kautz K, Schwarz M, Radeke HH (2005) Interference with MCP-1 gene expression by vector generated triple helix-forming RNA oligonucleotides. Cell Mol. Life Sci. 62:362-76

Kelner GS, Kennedy J, Bacon KB, Kleyensteuber S, Largaespada DA, Jenkins NA, Copeland NG, Bazan JF, Moore KW, Schall TJ, . (1994) Lymphotactin: a cytokine that represents a new class of chemokine. Science 266:1395-9

Kim HG, Miller DM (1998) A novel triplex-forming oligonucleotide targeted to human cyclin D1 (bcl-1, proto-oncogene) promoter inhibits transcription in HeLa cells. Biochemistry 37:2666-72

Kochetkova M, Shannon MF (1996) DNA triplex formation selectively inhibits granulocyte-macrophage colony-stimulating factor gene expression in human T cells. J. Biol. Chem. 271:14438-44

Kondo Y, Koga S, Komata T, Kondo S (2000) Treatment of prostate cancer in vitro and in vivo with 2-5A-anti-telomerase RNA component. Oncogene 19:2205-11

Kraus J, Borner C, Giannini E, Hollt V (2003) The role of nuclear factor kappaB in tumor necrosis factor-regulated transcription of the human mu-opioid receptor gene. Mol. Pharmacol. 64:876-84

Lacoste J, Francois JC, Helene C (1997) Triple helix formation with purine-rich phosphorothioate-containing oligonucleotides covalently linked to an acridine derivative. Nucleic Acids Res. 25:1991-8

Lacroix L, Mergny JL, Leroy JL, Helene C (1996) Inability of RNA to form the i-motif: implications for triplex formation. Biochemistry 35:8715-22

Lee AH, Hong JH, Seo YS (2000) Tumour necrosis factor-alpha and interferon-gamma synergistically activate the RANTES promoter through nuclear factor kappaB and interferon regulatory factor 1 (IRF-1) transcription factors. Biochem. J. 350 Pt 1:131-8

Lee JS, Woodsworth ML, Latimer LJ, Morgan AR (1984) Poly(pyrimidine) . poly(purine) synthetic DNAs containing 5-methylcytosine form stable triplexes at neutral pH. Nucleic Acids Res. 12:6603-14

Leech SH, Olie RA, Gautschi O, Simoes-Wust AP, Tschopp S, Haner R, Hall J, Stahel RA, Zangemeister-Wittke U (2000) Induction of apoptosis in lung-cancer cells following bcl-xL anti-sense treatment. Int. J. Cancer 86:570-6

Lefkowitz RJ (2000) The superfamily of heptahelical receptors. Nat. Cell Biol. 2:E133-E136

Leitner D, Schroder W, Weisz K (2000) Influence of sequence-dependent cytosine protonation and methylation on DNA triplex stability. Biochemistry 39:5886-92

Li F, Ackermann EJ, Bennett CF, Rothermel AL, Plescia J, Tognin S, Villa A, Marchisio PC, Altieri DC (1999) Pleiotropic cell-division defects and apoptosis induced by interference with survivin function. Nat. Cell Biol. 1:461-6

Liu J, Xu R, Jin Y, Wang D (2001) Triplex targeting of human PDGF-B (c-sis, proto-oncogene) promoter specifically inhibits factors binding and PDGF-B transcription. Nucleic Acids Res. 29:783-91

Liu ZH, Chen SF, Zhou H, Chen HP, Li LS (2003) Glomerular expression of C-C chemokines in different types of human crescentic glomerulonephritis. Nephrol. Dial. Transplant. 18:1526-34

Llopis J, McCaffery JM, Miyawaki A, Farquhar MG, Tsien RY (1998) Measurement of cytosolic, mitochondrial, and Golgi pH in single living cells with green fluorescent proteins. Proc. Natl. Acad. Sci. U. S. A 95:6803-8

Loetscher P, Seitz M, Clark-Lewis I, Baggiolini M, Moser B (1994) Monocyte chemotactic proteins MCP-1, MCP-2, and MCP-3 are major attractants for human CD4+ and CD8+ T lymphocytes. FASEB J. 8:1055-60

Lucio-Cazana J, Nakayama K, Xu Q, Konta T, Moreno-Manzano V, Furusu A, Kitamura M (2001) Suppression of constitutive but not Il-1beta-inducible expression of monocyte chemoattractant protein-1 in mesangial cells by retinoic acids: intervention in the activator protein-1 pathway. J. Am. Soc. Nephrol. 12:688-94

Macris MA, Glazer PM (2003) Transcription dependence of chromosomal gene targeting by triplex-forming oligonucleotides. J. Biol. Chem. 278:3357-62

Maghazachi AA (2000) Intracellular signaling events at the leading edge of migrating cells. Int. J. Biochem. Cell Biol. 32:931-43

Mahon FX, Ripoche J, Pigeonnier V, Jazwiec B, Pigneux A, Moreau JF, Reiffers J (1995) Inhibition of chronic myelogenous leukemia cells harboring a BCR-ABL B3A2 junction by antisense oligonucleotides targeted at the B2A2 junction. Exp. Hematol. 23:1606-11

Mann R, Mulligan RC, Baltimore D (1983) Construction of a retrovirus packaging mutant and its use to produce helper-free defective retrovirus. Cell 33:153-9

Marchand P, Resch K, Radeke HH (2000) Selective inhibition of monocyte chemoattractant protein-1 gene expression in human embryonal kidney cells by specific triple helix-forming oligonucleotides. J. Immunol 164:2070-6

Marfaing-Koka A, Devergne O, Gorgone G, Portier A, Schall TJ, Galanaud P, Emilie D (1995) Regulation of the production of the RANTES chemokine by endothelial cells.

Synergistic induction by IFN-gamma plus TNF-alpha and inhibition by IL-4 and IL-13. J. Immunol 154:1870-8

Maune S, Berner I, Sticherling M, Kulke R, Bartels J, Schroder JM (1996) Fibroblasts but not epithelial cells obtained from human nasal mucosa produce the chemokine RANTES. Rhinology 34:210-4

McCaffrey AP, Meuse L, Pham TT, Conklin DS, Hannon GJ, Kay MA (2002) RNA interference in adult mice. Nature 418:38-9

McDonald CD, Maher LJ, III (1995) Recognition of duplex DNA by RNA polynucleotides. Nucleic Acids Res. 23:500-6

McGuffie EM, Pacheco D, Carbone GM, Catapano CV (2000) Antigene and antiproliferative effects of a c-myc-targeting phosphorothioate triple helix-forming oligonucleotide in human leukemia cells. Cancer Res. 60:3790-9

Mezhevaya K, Winters TA, Neumann RD (1999) Gene targeted DNA double-strand break induction by (125)I-labeled triplex-forming oligonucleotides is highly mutagenic following repair in human cells. Nucleic Acids Res. 27:4282-90

Miller AD, Miller DG, Garcia JV, Lynch CM (1993) Use of retroviral vectors for gene transfer and expression. Methods Enzymol. 217:581-99

Miller LJ, Kurtzman SH, Wang Y, Anderson KH, Lindquist RR, Kreutzer DL (1998) Expression of interleukin-8 receptors on tumor cells and vascular endothelial cells in human breast cancer tissue. Anticancer Res. 18:77-81

Miller PS, Bhan P, Cushman CD, Trapane TL (1992) Recognition of a guanine-cytosine base pair by 8-oxoadenine. Biochemistry 31:6788-93

Miller PS, Bi G, Kipp SA, Fok V, DeLong RK (1996) Triplex formation by a psoralen-conjugated oligodeoxyribonucleotide containing the base analog 8-oxo-adenine. Nucleic Acids Res. 24:730-6

Milligan G (2001) Oligomerisation of G-protein-coupled receptors. J. Cell Sci. 114:1265-71

Misquitta L, Paterson BM (1999) Targeted disruption of gene function in Drosophila by RNA interference (RNA-i): a role for nautilus in embryonic somatic muscle formation. Proc. Natl. Acad. Sci. U. S. A 96:1451-6

Miyoshi H, Blomer U, Takahashi M, Gage FH, Verma IM (1998) Development of a self-inactivating lentivirus vector. J. Virol. 72:8150-7

Mizuno T, Chou MY, Inouye M (1984) A unique mechanism regulating gene expression: translational inhibition by a complementary RNA transcript (micRNA). Proc. Natl. Acad. Sci. U. S. A 81:1966-70

Moore BB, Keane MP, Addison CL, Arenberg DA, Strieter RM (1998) CXC chemokine modulation of angiogenesis: the importance of balance between angiogenic and angiostatic members of the family. J. Investig. Med. 46:113-20

Murao K, Ohyama T, Imachi H, Ishida T, Cao WM, Namihira H, Sato M, Wong NC, Takahara J (2000) TNF-alpha stimulation of MCP-1 expression is mediated by the Akt/PKB signal transduction pathway in vascular endothelial cells. Biochem. Biophys. Res. Commun. 276:791-6

Murphy PM (1994) The molecular biology of leukocyte chemoattractant receptors. Annu. Rev Immunol 12:593-633

Murugesan G, Sandhya Rani MR, Gerber CE, Mukhopadhyay C, Ransohoff RM, Chisolm GM, Kottke-Marchant K (2003) Lysophosphatidylcholine regulates human microvascular endothelial cell expression of chemokines. J. Mol. Cell Cardiol. 35:1375-84

Nagatsugi F, Sasaki S, Miller PS, Seidman MM (2003) Site-specific mutagenesis by triple helix-forming oligonucleotides containing a reactive nucleoside analog. Nucleic Acids Res. 31:e31

Nakanishi M, Weber KT, Guntaka RV (1998) Triple helix formation with the promoter of human alpha1(I) procollagen gene by an antiparallel triplex-forming oligodeoxyribonucleotide. Nucleic Acids Res. 26:5218-22

Naldini L (1998) Lentiviruses as gene transfer agents for delivery to non-dividing cells. Curr. Opin. Biotechnol. 9:457-63

Naldini L, Blomer U, Gallay P, Ory D, Mulligan R, Gage FH, Verma IM, Trono D (1996) In vivo gene delivery and stable transduction of nondividing cells by a lentiviral vector. Science 272:263-7

Ni W, Kitamoto S, Ishibashi M, Usui M, Inoue S, Hiasa K, Zhao Q, Nishida K, Takeshita A, Egashira K (2004) Monocyte chemoattractant protein-1 is an essential inflammatory mediator in angiotensin II-induced progression of established atherosclerosis in hypercholesterolemic mice. Arterioscler. Thromb. Vasc. Biol. 24:534-9

Noonberg SB, Francois JC, Garestier T, Helene C (1995a) Effect of competing self-structure on triplex formation with purine-rich oligodeoxynucleotides containing GA repeats. Nucleic Acids Res. 23:1956-63

Noonberg SB, Francois JC, Praseuth D, Guieysse-Peugeot AL, Lacoste J, Garestier T, Helene C (1995b) Triplex formation with alpha anomers of purine-rich and pyrimidine-rich oligodeoxynucleotides. Nucleic Acids Res. 23:4042-9

Noonberg SB, Scott GK, Garovoy MR, Benz CC, Hunt CA (1994a) In vivo generation of highly abundant sequence-specific oligonucleotides for antisense and triplex gene regulation. Nucleic Acids Res. 22:2830-6

Noonberg SB, Scott GK, Hunt CA, Benz CC (1994b) Detection of triplex-forming RNA oligonucleotides by triplex blotting. Biotechniques 16:1070-2, 1074

Nunez ME, Noyes KT, Gianolio DA, McLaughlin LW, Barton JK (2000) Long-range guanine oxidation in DNA restriction fragments by a triplex-directed naphthalene diimide intercalator. Biochemistry 39:6190-9

Nykanen A, Haley B, Zamore PD (2001) ATP requirements and small interfering RNA structure in the RNA interference pathway. Cell 107:309-21

Okkenhaug K, Vanhaesebroeck B (2003) PI3K in lymphocyte development, differentiation and activation. Nat. Rev Immunol 3:317-30

Olie RA, Simoes-Wust AP, Baumann B, Leech SH, Fabbro D, Stahel RA, Zangemeister-Wittke U (2000) A novel antisense oligonucleotide targeting survivin expression induces apoptosis and sensitizes lung cancer cells to chemotherapy. Cancer Res. 60:2805-9

Olivas WM, Maher LJ, III (1995a) Competitive triplex/quadruplex equilibria involving guanine-rich oligonucleotides. Biochemistry 34:278-84

Olivas WM, Maher LJ, III (1995b) Overcoming potassium-mediated triplex inhibition. Nucleic Acids Res. 23:1936-41

Olszewska-Pazdrak B, Casola A, Saito T, Alam R, Crowe SE, Mei F, Ogra PL, Garofalo RP (1998) Cell-specific expression of RANTES, MCP-1, and MIP-1alpha by lower airway epithelial cells and eosinophils infected with respiratory syncytial virus. J. Virol. 72:4756-64

Ono A, Chen CN, Kan LS (1991) DNA triplex formation of oligonucleotide analogues consisting of linker groups and octamer segments that have opposite sugar-phosphate backbone polarities. Biochemistry 30:9914-2

Ono SJ, Nakamura T, Miyazaki D, Ohbayashi M, Dawson M, Toda M (2003) Chemokines: roles in leukocyte development, trafficking, and effector function. J. Allergy Clin. Immunol 111:1185-99

Oppenheim JJ, Murphy WJ, Chertox O, Schirrmacher V, Wang JM (1997) Prospects for cytokine and chemokine biotherapy. Clin. Cancer Res. 3:2682-6

Orson FM, Thomas DW, McShan WM, Kessler DJ, Hogan ME (1991) Oligonucleotide inhibition of IL2R alpha mRNA transcription by promoter region collinear triplex formation in lymphocytes. Nucleic Acids Res. 19:3435-41

Panyutin IV, Luu AN, Panyutin IG, Neumann RD (2001) Strand breaks in whole plasmid dna produced by the decay of (125)I in a triplex-forming oligonucleotide. Radiat. Res. 156:158-66

Paterson BM, Roberts BE, Kuff EL (1977) Structural gene identification and mapping by DNA-mRNA hybrid-arrested cell-free translation. Proc. Natl. Acad. Sci. U. S. A 74:4370-4

Pattison J, Nelson PJ, Huie P, von L, I, Farshid G, Sibley RK, Krensky AM (1994) RANTES chemokine expression in cell-mediated transplant rejection of the kidney. Lancet 343:209-11

Pattison JM, Nelson PJ, Huie P, Sibley RK, Krensky AM (1996) RANTES chemokine expression in transplant-associated accelerated atherosclerosis. J. Heart Lung Transplant. 15:1194-9

Paul CP, Good PD, Winer I, Engelke DR (2002) Effective expression of small interfering RNA in human cells. Nat. Biotechnol. 20:505-8

Ping D, Boekhoudt G, Boss JM (1999a) trans-Retinoic acid blocks platelet-derived growth factor-BB-induced expression of the murine monocyte chemoattractant-1 gene by blocking the assembly of a promoter proximal Sp1 binding site. J. Biol. Chem. 274:31909-16

Ping D, Boekhoudt GH, Rogers EM, Boss JM (1999b) Nuclear factor-kappa B p65 mediates the assembly and activation of the TNF-responsive element of the murine monocyte chemoattractant-1 gene. J. Immunol 162:727-34

Ping D, Jones PL, Boss JM (1996) TNF regulates the in vivo occupancy of both distal and proximal regulatory regions of the MCP-1/JE gene. Immunity. 4:455-69

Porumb H, Gousset H, Letellier R, Salle V, Briane D, Vassy J, Amor-Gueret M, Israel L, Taillandier E (1996) Temporary ex vivo inhibition of the expression of the human oncogene HER2 (NEU) by a triple helix-forming oligonucleotide. Cancer Res. 56:515-22

Postel EH, Flint SJ, Kessler DJ, Hogan ME (1991) Evidence that a triplex-forming oligodeoxyribonucleotide binds to the c-myc promoter in HeLa cells, thereby reducing c-myc mRNA levels. Proc. Natl. Acad. Sci. U. S. A 88:8227-31

Powell N, Humbert M, Durham SR, Assoufi B, Kay AB, Corrigan CJ (1996) Increased expression of mRNA encoding RANTES and MCP-3 in the bronchial mucosa in atopic asthma. Eur. Respir. J. 9:2454-60

Praseuth D, Guieysse AL, Helene C (1999) Triple helix formation and the antigene strategy for sequence-specific control of gene expression. Biochim. Biophys. Acta 1489:181-206

Proietto AI, O'Keeffe M, Gartlan K, Wright MD, Shortman K, Wu L, Lahoud MH (2004) Differential production of inflammatory chemokines by murine dendritic cell subsets. Immunobiology 209:163-72

Radeke HH, Janssen-Graalfs I, Sowa EN, Chouchakova N, Skokowa J, Loscher F, Schmidt RE, Heeringa P, Gessner JE (2002) Opposite regulation of type II and III receptors for immunoglobulin G in mouse glomerular mesangial cells and in the induction of anti-glomerular basement membrane (GBM) nephritis. J. Biol. Chem. 277:27535-44

Rao TS, Durland RH, Seth DM, Myrick MA, Bodepudi V, Revankar GR (1995) Incorporation of 2'-deoxy-6-thioguanosine into G-rich oligodeoxyribonucleotides inhibits G-tetrad formation and facilitates triplex formation. Biochemistry 34:765-72

Rathanaswami P, Hachicha M, Sadick M, Schall TJ, McColl SR (1993) Expression of the cytokine RANTES in human rheumatoid synovial fibroblasts. Differential regulation of RANTES and interleukin-8 genes by inflammatory cytokines. J. Biol. Chem. 268:5834-9

Ray A, Norden B (2000) Peptide nucleic acid (PNA): its medical and biotechnical applications and promise for the future. FASEB J. 14:1041-60

Reiser J, Harmison G, Kluepfel-Stahl S, Brady RO, Karlsson S, Schubert M (1996) Transduction of nondividing cells using pseudotyped defective high-titer HIV type 1 particles. Proc. Natl. Acad. Sci. U. S. A 93:15266-71

Rininsland F, Johnson TR, Chernicky CL, Schulze E, Burfeind P, Ilan J (1997) Suppression of insulin-like growth factor type I receptor by a triple-helix strategy inhibits IGF-I transcription and tumorigenic potential of rat C6 glioblastoma cells. Proc. Natl. Acad. Sci. U. S. A 94:5854-9

Ririe SS, Guntaka RV (1998) An RNA oligonucleotide corresponding to the polypyrimidine region of the rat alpha 1(I) procollagen promoter forms a stable triplex and inhibits transcription. Biochem. Biophys. Res. Commun. 249:218-21

Roberts RW, Crothers DM (1992) Stability and properties of double and triple helices: dramatic effects of RNA or DNA backbone composition. Science 258:1463-6

Rogers FA, Vasquez KM, Egholm M, Glazer PM (2002) Site-directed recombination via bifunctional PNA-DNA conjugates. Proc. Natl. Acad. Sci. U. S. A 99:16695-700

Rollins BJ, Yoshimura T, Leonard EJ, Pober JS (1990) Cytokine-activated human endothelial cells synthesize and secrete a monocyte chemoattractant, MCP-1/JE. Am. J. Pathol. 136:1229-33

Romagnani P, Beltrame C, Annunziato F, Lasagni L, Luconi M, Galli G, Cosmi L, Maggi E, Salvadori M, Pupilli C, Serio M (1999) Role for interactions between IP-10/Mig and CXCR3 in proliferative glomerulonephritis. J. Am. Soc. Nephrol. 10:2518-26

Roscic-Mrkic B, Fischer M, Leemann C, Manrique A, Gordon CJ, Moore JP, Proudfoot AE, Trkola A (2003) RANTES (CCL5) uses the proteoglycan CD44 as an auxiliary receptor to mediate cellular activation signals and HIV-1 enhancement. Blood 102:1169-77

Rose CE, Jr., Sung SS, Fu SM (2003) Significant involvement of CCL2 (MCP-1) in inflammatory disorders of the lung. Microcirculation. 10:273-88

Roth SJ, Carr MW, Springer TA (1995) C-C chemokines, but not the C-X-C chemokines interleukin-8 and interferon-gamma inducible protein-10, stimulate transendothelial chemotaxis of T lymphocytes. Eur. J. Immunol 25:3482-8

Rott D, Zhu J, Zhou YF, Burnett MS, Zalles-Ganley A, Epstein SE (2003) IL-6 is produced by splenocytes derived from CMV-infected mice in response to CMV antigens, and induces MCP-1 production by endothelial cells: a new mechanistic paradigm for infection-induced atherogenesis. Atherosclerosis 170:223-8

Rovin BH, Yoshiumura T, Tan L (1992) Cytokine-induced production of monocyte chemoattractant protein-1 by cultured human mesangial cells. J. Immunol 148:2148-53

Rubinson DA, Dillon CP, Kwiatkowski AV, Sievers C, Yang L, Kopinja J, Rooney DL, Ihrig MM, McManus MT, Gertler FB, Scott ML, Van Parijs L (2003) A lentivirus-based system to functionally silence genes in primary mammalian cells, stem cells and transgenic mice by RNA interference. Nat. Genet. 33:401-6

Saito T, Deskin RW, Casola A, Haeberle H, Olszewska B, Ernst PB, Alam R, Ogra PL, Garofalo R (1997) Respiratory syncytial virus induces selective production of the chemokine RANTES by upper airway epithelial cells. J. Infect. Dis. 175:497-504

Schwarz M, Radeke HH, Resch K, Uciechowski P (1997) Lymphocyte-derived cytokines induce sequential expression of monocyte- and T cell-specific chemokines in human mesangial cells. Kidney Int. 52:1521-31

Semerad CL, Maher LJ, III (1994) Exclusion of RNA strands from a purine motif triple helix. Nucleic Acids Res. 22:5321-5

Sharma HW, Narayanan R (1996) The NF-kappaB transcription factor in oncogenesis. Anticancer Res. 16:589-96

Sharma HW, Perez JR, Higgins-Sochaski K, Hsiao R, Narayanan R (1996) Transcription factor decoy approach to decipher the role of NF-kappa B in oncogenesis. Anticancer Res. 16:61-9

Sharp PA (2001) RNA interference--2001. Genes Dev. 15:485-90

Shen C, Buck A, Mehrke G, Polat B, Gross H, Bachem M, Reske S (2001) Triplex forming oligonucleotide targeted to 3'UTR downregulates the expression of the bcl-2 proto-oncogene in HeLa cells. Nucleic Acids Res. 29:622-8

Shevelev A, Burfeind P, Schulze E, Rininsland F, Johnson TR, Trojan J, Chernicky CL, Helene C, Ilan J, Ilan J (1997) Potential triple helix-mediated inhibition of IGF-I gene expression significantly reduces tumorigenicity of glioblastoma in an animal model. Cancer Gene Ther. 4:105-12

Shippy R, Lockner R, Farnsworth M, Hampel A (1999) The hairpin ribozyme. Discovery, mechanism, and development for gene therapy. Mol. Biotechnol. 12:117-29

Shukaliak JA, Dorovini-Zis K (2000) Expression of the beta-chemokines RANTES and MIP-1 beta by human brain microvessel endothelial cells in primary culture. J. Neuropathol. Exp. Neurol. 59:339-52

Simonini A, Moscucci M, Muller DW, Bates ER, Pagani FD, Burdick MD, Strieter RM (2000) IL-8 is an angiogenic factor in human coronary atherectomy tissue. Circulation 101:1519-26

Simons RW, Kleckner N (1983) Translational control of IS10 transposition. Cell 34:683-91

Skoog JU, Maher LJ, III (1993) Repression of bacteriophage promoters by DNA and RNA oligonucleotides. Nucleic Acids Res. 21:2131-8

Song J, Intody Z, Li M, Wilson JH (2004) Activation of gene expression by triplex-directed psoralen crosslinks. Gene 324:183-90

Soukup GA, Ellington AD, Maher LJ, III (1996) Selection of RNAs that bind to duplex DNA at neutral pH. J. Mol. Biol. 259:216-28

Sridhar P, Liu Y, Chin LD, Borja CE, Mann M, Skopicki HA, Freter RR (1999) Platelet-derived growth factor-stimulated expression of the MCP-1 immediate-early gene involves an inhibitory multiprotein complex. Mol. Cell Biol. 19:4219-30

Stellato C, Beck LA, Gorgone GA, Proud D, Schall TJ, Ono SJ, Lichtenstein LM, Schleimer RP (1995) Expression of the chemokine RANTES by a human bronchial epithelial cell line. Modulation by cytokines and glucocorticoids. J. Immunol 155:410-8

Stephenson ML, Zamecnik PC (1978) Inhibition of Rous sarcoma viral RNA translation by a specific oligodeoxyribonucleotide. Proc. Natl. Acad. Sci. U. S. A 75:285-8

Sun JS, Garestier T, Helene C (1996) Oligonucleotide directed triple helix formation. Curr. Opin. Struct. Biol. 6:327-33

Takasugi M, Guendouz A, Chassignol M, Decout JL, Lhomme J, Thuong NT, Helene C (1991) Sequence-specific photo-induced cross-linking of the two strands of double-helical DNA by a psoralen covalently linked to a triple helix-forming oligonucleotide. Proc. Natl. Acad. Sci. U. S. A 88:5602-6

Tamm I, Dorken B, Hartmann G (2001) Antisense therapy in oncology: new hope for an old idea? Lancet 358:489-97

Tesch GH, Schwarting A, Kinoshita K, Lan HY, Rollins BJ, Kelley VR (1999) Monocyte chemoattractant protein-1 promotes macrophage-mediated tubular injury, but not glomerular injury, in nephrotoxic serum nephritis. J. Clin. Invest 103:73-80

Thibeault I, Laflamme N, Rivest S (2001) Regulation of the gene encoding the monocyte chemoattractant protein 1 (MCP-1) in the mouse and rat brain in response to circulating LPS and proinflammatory cytokines. J. Comp Neurol. 434:461-77

Thomas T, Thomas TJ (1993) Selectivity of polyamines in triplex DNA stabilization. Biochemistry 32:14068-74

Thomas TJ, Faaland CA, Gallo MA, Thomas T (1995) Suppression of c-myc oncogene expression by a polyamine-complexed triplex forming oligonucleotide in MCF-7 breast cancer cells. Nucleic Acids Res. 23:3594-9

Torigoe H (2001) Promotion of triplex formation by N3'-->P5' phosphoramidate modification: thermodynamic and kinetic studies. Nucleic Acids Res. Suppl57-8

Tu GC, Cao QN, Israel Y (1995) Inhibition of gene expression by triple helix formation in hepatoma cells. J. Biol. Chem. 270:28402-7

Tuschl T, Zamore PD, Lehmann R, Bartel DP, Sharp PA (1999) Targeted mRNA degradation by double-stranded RNA in vitro. Genes Dev. 13:3191-7

Ueda A, Okuda K, Ohno S, Shirai A, Igarashi T, Matsunaga K, Fukushima J, Kawamoto S, Ishigatsubo Y, Okubo T (1994) NF-kappa B and Sp1 regulate transcription of the human monocyte chemoattractant protein-1 gene. J. Immunol 153:2052-63

Uguccioni M, D'Apuzzo M, Loetscher M, Dewald B, Baggiolini M (1995) Actions of the chemotactic cytokines MCP-1, MCP-2, MCP-3, RANTES, MIP-1 alpha and MIP-1 beta on human monocytes. Eur. J. Immunol 25:64-8

Umekawa T, Chegini N, Khan SR (2003) Increased expression of monocyte chemoattractant protein-1 (MCP-1) by renal epithelial cells in culture on exposure to calcium oxalate, phosphate and uric acid crystals. Nephrol. Dial. Transplant. 18:664-9

Vasquez KM, Dagle JM, Weeks DL, Glazer PM (2001a) Chromosome targeting at short polypurine sites by cationic triplex-forming oligonucleotides. J. Biol. Chem. 276:38536-41

Vasquez KM, Marburger K, Intody Z, Wilson JH (2001b) Manipulating the mammalian genome by homologous recombination. Proc. Natl. Acad. Sci. U. S. A 98:8403-10

Vasquez KM, Narayanan L, Glazer PM (2000) Specific mutations induced by triplex-forming oligonucleotides in mice. Science 290:530-3

Vigna E, Naldini L (2000) Lentiviral vectors: excellent tools for experimental gene transfer and promising candidates for gene therapy. J. Gene Med. 2:308-16

Wang G, Seidman MM, Glazer PM (1996) Mutagenesis in mammalian cells induced by triple helix formation and transcription-coupled repair. Science 271:802-5

Wang H, Zeng X, Oliver P, Le LP, Chen J, Chen L, Zhou W, Agrawal S, Zhang R (1999) MDM2 oncogene as a target for cancer therapy: An antisense approach. Int. J. Oncol. 15:653-60

Ward SG, Bacon K, Westwick J (1998) Chemokines and T lymphocytes: more than an attraction. Immunity. 9:1-11

Weber M, Uguccioni M, Ochensberger B, Baggiolini M, Clark-Lewis I, Dahinden CA (1995) Monocyte chemotactic protein MCP-2 activates human basophil and eosinophil leukocytes similar to MCP-3. J. Immunol 154:4166-72

Weisz OA (2003) Organelle acidification and disease. Traffic. 4:57-64

Wenzel U, Schneider A, Valente AJ, Abboud HE, Thaiss F, Helmchen UM, Stahl RA (1997) Monocyte chemoattractant protein-1 mediates monocyte/macrophage influx in anti-thymocyte antibody-induced glomerulonephritis. Kidney Int. 51:770-6

Wickstrom EL, Bacon TA, Gonzalez A, Freeman DL, Lyman GH, Wickstrom E (1988) Human promyelocytic leukemia HL-60 cell proliferation and c-myc protein expression are inhibited by an antisense pentadecadeoxynucleotide targeted against c-myc mRNA. Proc. Natl. Acad. Sci. U. S. A 85:1028-32

Winters TA (2000) Gene targeted agents: new opportunities for rational drug development. Curr. Opin. Mol. Ther. 2:670-81

Wong M, Fish EN (1998) RANTES and MIP-1alpha Activate Stats in T Cells. J. Biol. Chem. 273:309-14

Xiang G, Bogacki R, McLaughlin LW (1996) Use of a pyrimidine nucleoside that functions as a bidentate hydrogen bond donor for the recognition of isolated or contiguous G-C base pairs by oligonucleotide-directed triplex formation. Nucleic Acids Res. 24:1963-70

Xu XS, Glazer PM, Wang G (2000) Activation of human gamma-globin gene expression via triplex-forming oligonucleotide (TFO)-directed mutations in the gamma-globin gene 5' flanking region. Gene 242:219-28

Zamore PD (2001) RNA interference: listening to the sound of silence. Nat. Struct. Biol. 8:746-50

Zennou V, Petit C, Guetard D, Nerhbass U, Montagnier L, Charneau P (2000) HIV-1 genome nuclear import is mediated by a central DNA flap. Cell 101:173-85

Zhou R, Geiger RC, Dean DA (2004) Intracellular trafficking of nucleic acids. Expert Opin. Drug Deliv. 1(1): 127-40

Zhou ZH, Chaturvedi P, Han YL, Aras S, Li YS, Kolattukudy PE, Ping D, Boss JM, Ransohoff RM (1998) IFN-gamma induction of the human monocyte chemoattractant protein (hMCP)-1 gene in astrocytoma cells: functional interaction between an IFN-gamma-activated site and a GC-rich element. J. Immunol 160:3908-16

Zhou ZH, Han Y, Wei T, Aras S, Chaturvedi P, Tyler S, Rani MR, Ransohoff RM (2001) Regulation of monocyte chemoattractant protein (MCP)-1 transcription by interferon-gamma (IFN-gamma) in human astrocytoma cells: postinduction refractory state of the gene, governed by its upstream elements. FASEB J. 15:383-92

Zufferey R, Donello JE, Trono D, Hope TJ (1999) Woodchuck hepatitis virus posttranscriptional regulatory element enhances expression of transgenes delivered by retroviral vectors. J. Virol. 73:2886-92

Zufferey R, Dull T, Mandel RJ, Bukovsky A, Quiroz D, Naldini L, Trono D (1998) Self-inactivating lentivirus vector for safe and efficient in vivo gene delivery. J. Virol. 72:9873-80

8 Appendix

8.1 Abbreviations

A	Adenine
AP-1	Activating protein-1
APS	Ammonium peroxo-disulfate
bp	Basepairs
BSA	Bovine serum albumin
C	Cytosine
cAMP	Cyclic adenosine monophosphate
cDNA	Copy DNA, complementary DNA
CIP	Calf intestine phosphatase
CMV	Cytomegalovirus
ConA	Concanavalin A
cPPT	Central polypurine tract
DEPC	Diethyl pyrocarbonate
DMSO	Dimethyl sulfoxide
DNA	Desoxy ribonucleic acid
dNTP	Desoxynucleoside triphosphate
ds	Double-stranded
DTT	Dithiotreitol
E.coli	Escherichia coli
EDTA	Ethylendiaminetetraacetic acid
ELISA	Enzyme linked immunosorbent assay
ELR	Glutamic acid-leucine-arginine motif
EMSA	Electrophoretic mobility shift assay
ENA-78	Epithelial neutrophil activating factor-78
EtOH	Ethanol
FA	Formaldehyde
FACS	Fluorescence activated cell sorting
FAK	Focal adhesion kinase
FCS	Fetal calf serum
G	Guanine
GAGs	Glycosaminoglycans
GAS	Interferon gamma activated site
GFP, eGFP	(Enhanced) green fluorescent protein
GM-CSF	Granulocyte macrophage-colony stimulating factor
GPCR	G-protein coupled receptor
GRO-α	Growth related oncogene-α

HEK 293	Human embryonic kidney cells
HEPES	N-(2-Hydroxyethyl)piperazine-N'-ethanesulfonic acid
HIV	Human immunodeficiency virus
HPLC	High Performance Liquid Chromatography
ICAM-1	Intercellular adhesion molecule-1
IFN-γ	Interferon-γ
IGF-IR	Insuline-like growth factor I receptor
IL	Interleukin
IP-10	Interferon-inducible protein-10
IRF	Interferon regulatory factor
I-TAC	Interferon-inducible T cell alpha chemoattractant
JAK	Janus kinase
kb	Kilobase
kDa	Kilodalton
LB-medium	Luria Bertani-medium
LFA-1	Lymphocyte-function-associated antigen-1
LPS	Lipopolysaccharide
LTR	Long terminal repeat
MCP-1	Monocyte chemoattractant protein-1
MIG	Monokine induced by interferon-γ
MIP-1α	Macrophage inflammatory protein-1α
MoMuLV	Moloney murine leukemia virus
MOPS	3-(N-Morpholino)propanesulfonic acid
NEA	Non-essential amino acids
NF-κB	Nuclear factor κB
NP-40	Nonidet P-40
nt	Nucleotides
OD	Optical density
PBS	Phosphate buffered saline
PCR	Polymerase chain reaction
PDGF	Platelet derived growth factor
PF4	Platelet factor 4
PNA	Peptide nucleic acid
PNK	T4 poly-nucleotide kinase
PTK	Protein tyrosine kinase
RANTES	Regulated upon activation normal T cell expressed and secreted
RCR	Replication competent recombinants
RNA, mRNA	(Messenger) ribonucleic acid
RNAi	RNA interference
rpm	Rounds per minute
RSV	Rous sarcoma virus

RT-PCR	Reverse transcribed-polymerase chain reaction
SD	Standard deviation
SDF-1	Stromal cell-derived factor-1
SDS	Sodiumdodecyl sulfate
SEM	Standard error of the mean
SFFV	Spleen focus forming virus
SIN	Self-inactivating transfer vector
siRNA	Small interfering RNA
STAT	Signal transducer and activator of transcription
T	Thymine
TEMED	N,N,N',N' - tetramethylethylene diamine
TFO	Triple helix-forming oligonucleotide
TNF-α	Tumour necrosis factor-α
TPA	Tetradecanoyl phorbol acetate
tRNA	Transfer RNA
U	Units
UTR	Utranslated region
UV	Ultraviolet (light)
v/v	Volume per volume
VCAM-1	Vascular-cell adhesion molecule-1
VLA-4	Very late antigen 4
VSV	Vesicular stomatitis virus
w/v	Weight per volume
WPRE	Woodchuck hepatitis virus
wt	Wild type

8.2 Deutsche Zusammenfassung

Die Chemokine sind eine Unterfamilie der Zytokine mit starker chemotaktischer Aktivität und übernehmen bei der Positionierung von Zellen im Organismus wichtige Aufgaben. Chemokine sind strukturell verwandte Moleküle zwischen 8 und 14 kDa. Sie können an verschiedene Chemokinrezeptoren binden und vermitteln ihre Signale über G-Proteine. Man unterteilt die Chemokine funktionell in homöostatische (konstitutiv exprimierte) und inflammatorische (induzierbare) Chemokine. Im Falle einer Infektion mobilisieren sie Effektorzellen und leiten sie zu den Infektionsherden und ins lymphatische Gewebe. Darüber hinaus spielen Chemokine in der Organentwicklung, Wundheilung, Angiogenese, Angiostase, bei der homöostatischen Leukozytenrezirkulation und Immunregulation eine Rolle. MCP-1 (*monocyte chemoattractant protein-1*) ist ein Mitglied der CC-Chemokin Familie und lockt eine Vielzahl von Zelltypen wie Monozyten, T-Lymphozyten und Basophile zum Entzündungsherd. MCP-1 wird von verschiedenen Zellen wie Monozyten, Fibroblasten, vaskulären Endothelzellen und glatten Muskelzellen nach Stimulation mit Tumornekrosefaktor-α (TNF-α), Interferon-γ (IFN-γ) oder Interleukin-1β (IL-1β) produziert. Eine Überexpression von MCP-1 wird in vielen entzündlichen Erkrankungen wie rheumatoider Arthritis, Multipler Sklerose und Glomerulonephritis gefunden.

Ziel dieser Arbeit war es, molekulare Strategien auf dem Weg zu einer therapeutischen Anwendung zu entwickeln, um die Aktivität z.B. pro-inflammatorischer Chemokine wie MCP-1 und RANTES (*regulated upon activation normal T cell expressed and secreted*) zu modulieren. In der Literatur sind verschiedene erfolgreiche Prinzipien beschrieben, die auf dem Einsatz von kurzen Oligonukleotiden basieren, um die Expression spezifischer Gene zu hemmen. Hierzu gehören die Antisense-Oligonukleotide, *triple helix-forming oligonucleotides* (TFOs) und auch die *small interfering RNA* (siRNA). Im Unterschied zur Wirkung von siRNA und Antisense-Oligonukleotiden auf die mRNA Translation geht es in dieser Arbeit um das Design von therapeutischen Agenzien, die auf der DNA-Ebene durch sequenzspezifische Interaktionen die Transkription verändern können. Dieser Ansatz hat den prinzipiellen Vorteil, dass nur zwei Allele und nicht Tausende von Zielstrukturen (mRNAs) pro Zelle erreicht werden müssen und ist mit der Verfügbarkeit der Genomsequenzen eine viel versprechende Strategie eines neuen molekularbiologischen „Drug Design“. Die dazu eingesetzten TFOs besitzen die Fähigkeit, nach bestimmten Regeln an die doppelsträngige DNA zu binden und stabile Dreifachketten zu bilden. Die Kriterien für die Bindung eines TFOs and die doppelsträngige (ds)DNA sind genau definiert. Eine geeignete Zielsequenz muss in einem der beiden DNA-Stränge aus mindestens 12-15 ununterbrochenen Purinen bestehen. Es existieren zwei verschiedene Bindungsmotive, mit denen das TFO an den Doppelstrang binden kann. Beim Purin-Bindungsmotiv binden die TFOs antiparallel an den Purinstrang der

dsDNA, die Sequenzspezifität wird über die spezifische Bindung von Guanin (G) an Guanin (G):Cytosin (C)- und Adenin (A) (oder auch Thymin) an Adenin (A):Thymin (T)-Basenpaare vermittelt. Beim Pyrimidin-Bindungsmotiv dagegen binden die Oligonukleotide antiparallel zum Purinstrang der dsDNA (Cytosin an Guanin:Cytosin- und Thymin an Adenin:Thymin-Basenpaare) (Chan and Glazer 1997).
TFOs können im Prinzip Änderungen in der Genaktivität (Inhibition der Transkriptions-Initiation oder der Transkriptions-Elongation; oder Aktivierung der Transkription) induzieren (Faria et al. 2000; Intody et al. 2000), oder aber sie werden für strukturelle Änderung in der DNA-Sequenz eingesetzt (Sequenzspezifische DNA-Schädigung und Reparatur oder TFO-vermittelte homologe Rekombination) (Vasquez et al. 2001b). In einem Teil der Publikationen werden sequenzspezifische Effekte von TFOs auf die Genexpression in einem intakten zellulären System beschrieben, viele Untersuchungen zu prinzipiellen Bindungseigenschaften sind allerdings auch in zellfreien Systemen durchgeführt worden. In intakten Zellen wurden erfolgreiche Versuche beschrieben, wenn die TFO Zielsequenzen im Promoterbereich der Gene lagen (Carbone et al. 2004; Cogoi et al. 2000). Hier konkurrierten TFOs mit Transkriptionsfaktoren um die entsprechenden Bindungsstellen. Andererseits werden zur Optimierung der TFO-Technik Reportersysteme beschrieben, in denen die Zielsequenzen in ein Plasmid kloniert und in Zellen transfiziert wurden. Als Kontrollen können Oligonukleotide unterschiedlicher Länge und unterschiedlicher Basenzusammensetzung oder unterschiedlicher Orientierung (parallel statt antiparallel zum purinhaltigen DNA-Strang) verwendet werden. Bei Plasmiden besteht die Möglichkeit, die Targetsequenz zu mutieren und über ein „Nicht-Binden“ der TFOs die Sequenzspezifität zu gewährleisten. Um die Stabilität der TFOs in der Zelle zu erhöhen werden verschiedene chemische Modifikationen der Oligonukleotide angewendet. So können z.B. Phosphorothioat-TFOs, 3’Amino-modifizierte TFOs oder Oligonukleotid-Analoga mit N3’-P5’ Verbindungen gegen endogene Targets eingesetzt werden (Praseuth et al. 1999).

In der vorliegenden Arbeit wurden die beiden Gene der Chemokine MCP-1 und RANTES als TFO-Targets untersucht. In der Promoterregion des humanen MCP-1 Gens befindet sich eine geeignete TFO Zielsequenz in einer Länge von 19 bp. Diese Zielsequenz umfasst die Bindungsstellen für die Transkriptionsfaktoren SP-1 und AP-1, welche sowohl bei der basalen als auch der induzierten Genexpression von MCP-1 eine entscheidende Rolle spielen. Nach den beschriebenen Regeln zur sequenzspezifischen Triplex-Bildung wurde ein 19 nt TFO mit einem purinen Bindungsmotiv (GT) synthetisiert und es konnte im EMSA (*electrophoretic mobility shift assay*) gezeigt werden, dass dieses sequenzspezifisch an die MCP-1 dsDNA (39 bp) bindet. Sequenzspezifität wurde durch ein Kontroll-Oligonukleotid mit gleicher Basenzusammensetzung aber unterschiedlicher Reihenfolge gezeigt, das zu keiner

Triplex-Formation führte. Weiterhin fand keine Triplex-Bildung mit einer RANTES Promotersequenz als Kontroll-Target statt. Wie in einer früheren Arbeit gezeigt (Marchand et al. 2000), konnte in einem Protein-Bindungstest das TFO das Binden von rekombinantem SP-1 und auch von nukleärem Proteinextrakt an den MCP-1 Promoter verhindern; dieses bestätigte zusätzlich die Sequenzspezifität. In der vorliegenden Arbeit konnte die TNF-α induzierte MCP-1 Proteinsekretion in HEK 293 Zellen bei einer Konzentration von 2 µM Phosphorothioat-TFO um 25% im Vergleich zu dem Kontroll-Oligonukleotid inhibiert werden.

Die Suche nach geeigneten Zielsequenzen konnte durch die Entwicklung eines Algorithmus (in Kooperation mit Bill Bruno, Bioinformatiker, New Mexico) optimiert werden. Für ein Genbank Screening wurden folgende Parameter festgelegt: Mindestens 14 Basen Guanin/Adenin mussten in ununterbrochener Reihenfolge vorliegen, und in einer Sequenzlänge von 18 Nukleotiden war nur ein Mismatch (Pyrimidin) erlaubt. Weiterhin musste der Guaningehalt der Zielsequenz mindestens 60 % betragen. Von bisher 2613 mit diesem Algorithmus geprüften Sequenzen konnten 673 als geeignete Zielsequenzen gefunden werden, die als mögliche Zielsequenzen für die *in vitro* Testung zur Verfügung stehen. Ein weiteres Target war das murine RANTES, welches eine wichtige Rolle in der Chemoattraktion von Leukozyten während des Entzündungsprozesses spielt. Im Promoterbereich von -262 bis -235 vom Transkriptionsstart aus befindet sich eine 28 bp TFO-Zielsequenz. +1 entspricht dem Transkriptionsstart wie beschrieben bei Danoff (Danoff et al. 1994). Ein 28 nt TFO mit Purin-Bindungsmotiv (GT) wurde synthetisiert, und Triplex-Bildung mit der RANTES Promoterzielsequenz konnte im EMSA gezeigt werden. Für eine sequenzspezifische Triplex-Formation konnte ein K_d-Wert von 2.5 x 10^{-7} M bestimmt werden. Die Wirkung des TFO mit Phosphorothioat-Modifikation wurde in zwei verschiedenen Zelllinien (T-Lymphozyten und mikrovaskuläre Endothelzellen des Gehirns, b-end3 Zellen) getestet. Hier konnte allerdings kein inhibitorischer Effekt auf die endogene RANTES-Expression festgestellt werden.

Generelle Schwierigkeiten der Oligonukleotid-Technologien wie der Einsatz hoher Konzentrationen, Notwendigkeit chemischer Modifikationen und die Transfektionseffizienz konnten durch die Etablierung von Vektoren zur intrazellulären Generierung von TFOs auf RNA-Basis maßgeblich verbessert werden (Kautz et al. 2005). Dazu wurde der eukaryotische Expressionsvektor pcDNA3.1/Hygro so modifiziert, dass die MCP-1 TFO-Sequenz zusammen mit einem Hygromycin Resistenzgen als Fusionstranskript transkribiert werden konnte. In mit diesem Vektor transfizierten HEK 293 Zellen werden TFO-RNA Moleküle produziert, die als dritter Strang an die MCP-1 Promoter Targetsequenz binden können und damit die Transkription des MCP-1 Gens inhibieren. Für das TFO wurde hier

das Pyrimidin-Bindungsmotiv (Cytosin-Uracil, CU) gewählt, da die Triplex-Bildung mit Oligoribonukleotiden (RNA*DNA:DNA) im Purin-Bindungsmotiv als sehr unwahrscheinlich beschrieben wird (Lacroix et al. 1996). Der Vektor pcDNA3.1/Hygro (ca. 5,6 kb) wurde mit den Restriktionsenzymen *Apa*I und *Sma*I geschnitten, sodass der Bereich zwischen 1002 bp und 2079 bp entfernt wurde. Der *Apa*I Überhang wurde aufgefüllt und der Vektor religiert. Die multiple Klonierungsstelle lag nun im 5' UTR des Hygromycin Resistenzgens unter der Kontrolle des CMV Promoters. Eine Sequenz, die in die multiple Klonierungsstelle kloniert wurde, wurde zusammen mit dem Hygromycin Resistenzgen als Fusionstranskript abgeschrieben. Als Insert wurde ein 49 bp Doppelstrang mit Schnittstellen für die Enzyme *Hind*III, *Xho*I und *Bam*HI synthetisiert. Dieser Doppelstrang enthielt die 19 bp TFO-RNA generierende Sequenz, die als dritter Strang an den MCP-1 Promoter binden sollte. Als Kontrolle wurde ein Vektor mit einer RNA-Sequenz konstruiert, die nicht an die Targetsequenz binden konnte. HEK 293 Zellen wurden stabil mit diesem Vektor und den verschiedenen Kontrollvektoren transfiziert und unter ständigem Selektionsdruck (Hygromycin 250 µg/ml) kultiviert. In Zelllinien, die konstitutiv TFOs generieren, konnte die endogene TNF-α induzierte MCP-1 Protein-Sekretion um 76 ± 10,2% im Vergleich zu Kontrollzelllinien inhibiert werden.

Um eine sequenzspezifische Wirkung der intrazellulär gebildeten TFOs aufzuzeigen, wurde in denselben Zellüberständen sowohl die MCP-1 als auch die Interleukin-8 (IL-8) Proteinkonzentration bestimmt. Hierbei zeigte sich, dass die TNF-α induzierte IL-8 Expression durch das TFO vollkommen unbeeinflusst blieb. Auch in IFN-γ stimulierten Zellen konnte eine Inhibition bis zu 83% erreicht werden, in TNF-α und IFN-γ kostimulierten Zellen bis zu 88%. Die Präsenz der TFOs und der Kontrollen in den verschiedenen Zelllinien konnte über RT-PCR und Northern-Blots bestätigt werden.

Verschiedene Kontrollen wurden *in vitro* durchgeführt, so auch der Nachweis der spezifischen Triplex-Formation mit synthetischen 19 nt Oligoribonukleotiden und dem 39 bp MCP-1 Promoterfragment. Dazu wurden die Oligoribonukleotide (TFO und verschiedene Kontrollen) elektrophoretisch aufgetrennt, auf eine Membran geblottet und anschließend mit der MCP-1 Duplex-DNA inkubiert. Hierbei zeigte sich, dass nur das CU-TFO an die Zielsequenz band. Verschiedene Kontrollen wurden parallel getestet, so z.B. ein Oligoribonukleotid mit gleicher Basensequenz des TFOs, aber mit nur einem Nukleotidaustausch, mit dem Resultat, dass die Kontrollen nicht an die Duplex-DNA banden. Weiterhin wurde ein MCP-1 Promoterfragment mit zwei Nukleotidaustäuschen verwendet, und hier konnte keins der verwendeten Oligoribonukleotide binden. Diese Ergebnisse lassen eindeutig auf eine sequenzspezifische Triplex-Formation schließen.

Schließlich konnte auch gezeigt werden, dass das TFO/Hygromycin-Fusionstranskript an die die MCP-1 Promotersequenz bindet. Dazu wurde ein Biotin/Streptavidin basiertes

magnetisches Abfangen der Triplex-Komplexe etabliert. Die relative Menge der MCP-1-Duplex-DNA, die hierbei an TFO- oder Kontroll-Sequenzen band, wurde über eine semi-quantitative PCR bestimmt. Es zeigte sich, dass das in einem Plasmid eingebettete MCP-1 Promoterfragment dreimal stärker and das TFO-Transkript band als an die Kontrollen. Dieses Ergebnis bestätigt, dass die TFO-Sequenz, eingebettet in ein längeres RNA-Transkript, mit dem MCP-1 Promoterfragment bei einem pH-Wert von 7.0 in einer sequenzspezifischen Art und Weise interagiert.

Neben der TFO-Strategie wurde in dieser Arbeit auch die Möglichkeit von siRNAs untersucht, um die Expression der Chemokine RANTES und MCP-1 zu inhibieren. Für den siRNA Einsatz wurden zwei verschiedene Methoden verwendet, sowohl der Gebrauch synthetisch hergestellter als auch Vektor generierter siRNA. Der Vektor pSUPER besitzt einen Polymerase-III H1-RNA Promoter und kann für die intrazellulare Synthese von siRNA eingesetzt werden (Brummelkamp et al. 2002). Der Einsatz einer intrazellulär generierten siRNA gegen das humane MCP-1 führte zu einer Inhibition der MCP-1 Protein-Sekretion um 35 ± 11% in HEK 293 Zellen. Allerdings zeigte sich auch eine leicht reduzierte Protein Sekretion nach Transfektion mit dem Leervektor ohne codierende siRNA Sequenz um 18 ± 7%; ein geringer inhibitorische Effekt durch die transiente Transfektion des Vektors selbst war also nicht auszuschließen. Weiterhin wurde auch der Effekt von zwei verschiedenen synthetischen siRNA Sequenzen getestet. Eine Sequenz entsprach genau der, die auch in dem Vektor pSUPER verwendet wurde. Hier wurde die MCP-1 Expression um 23% in TNF-α stimulierten und um 30% in unstimulierten Zellen inhibiert. Eine weitere siRNA-Sequenz war eine vom Hersteller validierte Sequenz gegen MCP-1 und erzielte in HEK 293 Zellen eine Inhibition der MCP-1 Protein-Sekretion von 62.3 ± 10.3%. Für weitergehende Versuche wäre es lohnenswert, genau diese erfolgreiche Sequenz in den Vektor pSUPER zu klonieren, um die Effizienz von Vektor generierter und synthetischer siRNA in Bezug auf das Chemokin MCP-1 vergleichen zu können.
Ebenso wurde die siRNA Technik eingesetzt, um murines RANTES in T-Lymphozyten und Endothelzellen (Th1 und b-end3 Zellen) zu inhibieren. Wie beim MCP-1 wurde auch hier eine Vektor-generierte und eine synthetische siRNA untersucht, es zeigte sich allerdings kein inhibitorischer Effekt auf die endogene RANTES Expression in beiden Zelllinien. Zusammenfassend lässt sich sagen, dass für MCP-1 die siRNA-Strategie ein erfolgreicher Ansatz ist, die Expression signifikant zu verringern. Für das Chemokin RANTES scheint es erforderlich, weitere siRNA Sequenzen zu testen, um eine Inhibition erreichen zu können.

Ein weiteres Ziel dieser Arbeit war es, den potentiellen Einsatz von TFO oder siRNA als gentherapeutisches Instrument durch geeignete Transfervektoren zu verbessern. In der

humanen Gentherapie wird eine Vielzahl unterschiedlicher Viren als Gentransfer-Vektoren angewendet, darunter auch die retroviralen Vektoren. Die Verwendung viraler Systeme beruht auf der natürlichen Fähigkeit von Viren, Zellen zu infizieren. Diese Vektoren weisen einige Vorzüge auf, wie etwa die spezifische Bindung an und die Aufnahme in die Zielzellen, den Transport der DNA zum Zellkern und den Schutz der Nukleinsäuren vor Abbau. Die auf Lentiviren basierenden Vektoren weisen zusätzlich einige Vorteile auf, da sie aufgrund eines aktiven Transportes dieser Viren in den Zellkern auch nicht proliferierende Zellen transduzieren können (Naldini et al. 1996). Bei der Herstellung dieser Vektoren werden essentielle Teile des viralen Genoms entfernt und die therapeutisch wirksamen Gensequenzen eingesetzt. Die fehlenden viralen Proteine werden in *trans* von entsprechenden Verpackungsvektoren produziert. Enthält das modifizierte Genom die notwendigen Verpackungssignale, so wird es in den Zellen in virale Hüllen verpackt.
In dieser Arbeit wurden lentivirale Partikel durch eine transiente Transfektion von 239T Zellen mit dem Transfervektor SEW und den notwendigen Verpackungsvektoren hergestellt. Der SEW Vektor enthält als Marker das grüne Fluoreszenzprotein (GFP). Im Anschluss wurden Th1 Zellen mit den infektiösen lentiviralen Vektoren transduziert. Die relative Frequenz an GFP-produzierenden Zellen konnte mittels FACS-Analyse bestimmt werden. Die Transduktionseffizienz lag bei über 82%. Durch diese hohe Transduktionseffizienz ergeben sich auch optimale Bedingungen für den Einsatz von TFO und siRNA. Die erfolgreichen TFO- und siRNA-Sequenzen gegen das humane MCP-1 könnten weiterhin auch lentiviral exprimiert werden, um den Gentransfer zu verbessern. Die Effizienz der beiden Strategien könnte in verschiedenen Zelllinien und letztendlich auch im Tiermodell überprüft werden.

8.3 Journal publications and congress contributions

PUBLICATIONS:

- *"Interference with MCP-1 gene expression by vector generated triple helix-forming RNA oligonucleotides"*
  Kautz K, Schwarz M, Radeke HH
  CMLS, Cell. Mol. Life Sci. 62 (2005): 362-376

ORAL PRESENTATIONS:

- 33. Annual Meeting of the German Society of Immunology,
  Marburg, September 25th-28th, 2002
  "Inhibition of chemokine expression via triple helix-forming oligonucleotides"

- Deutsche Gesellschaft für experimentelle und klinische Pharmakologie und Toxikologie
  Mainz, March 17th-20th, 2003
  „Inhibition der hMCP-1 Expression durch intrazellulär generierte Tripel-Helix bildende Oligonukleotide"

- Deutsche Gesellschaft für experimentelle und klinische Pharmakologie und Toxikologie
  Mainz, March 9th-11th, 2004
  „Inhibition der Chemokin-Genexpression durch Vektor-generierte Tripel-Helix bildende RNA-Oligonukleotide"

POSTER PRESENTATIONS:

- 33. Annual Meeting of the German Society of Immunology,
  Marburg, September 25th-28th, 2002
  "Inhibition of chemokine expression via triple helix-forming oligonucleotides"

- Deutsche Gesellschaft für experimentelle und klinische Pharmakologie und Toxikologie
  Mainz, March 17th-20th, 2003
  „Inhibition der hMCP-1 Expression durch intrazellulär generierte Tripel-Helix bildende Oligonukleotide"

- 34. Annual Meeting of the German Society of Immunology,
  Berlin, September 24th-27th, 2003
  "Specific binding of a vector derived RNA oligonucleotide to a GC-rich double-stranded MCP-1 promoter sequence and inhibition of chemokine gene expression"

- ZAFES, Zentrum für Arzneimittelforschung, -Entwicklung und -Sicherheit
  ZAFES Kick-Off Symposium "Lipid Signaling",
  Frankfurt a. M., October 14th, 2004
  "Sequence specific inhibition of MCP-1 gene transcription by intracellular generated TFOs as a new gene therapeutic approach"

9 Danksagung

Hiermit möchte ich allen danken, die mich bei der Durchführung dieser Arbeit unterstützt und damit zu ihrem Gelingen beigetragen haben:

Herrn Prof. Dr. Heinfried H. Radeke danke ich für die Überlassung des interessanten und anspruchsvollen Themas, für das entgegengebrachte Vertrauen, für viele konstruktive Diskussionen und das stete Interesse an meiner Arbeit. Ich möchte Herrn Prof. Dr. Josef Pfeilschifter für die Unterstützung und das Interesse am Fortgang dieser Arbeit und die angenehme Arbeitsatmosphäre im *pharmazentrum frankfurt* danken. Herrn Prof. Dr. Dieter Steinhilber danke ich vielmals für die externe Betreuung dieser Arbeit und die Begutachtung der Dissertation.
Herrn Dr. Manuel Grez danke ich herzlich für die Bereitstellung des lentiviralen Vektors und für die Möglichkeit, im Georg-Speyer Haus die Arbeiten im S2-Labor durchführen zu können. Dank gilt auch Dr. Stefan Stein und Hana Kunkel für die hilfreiche Unterstützung bei den FACS-Analysen und Transfektionen.
Ein herzliches Dankeschön gilt Dr. Simone Rubant für die schöne Zusammenarbeit, Unterstützung und Freundschaft und aufbauenden Kaffeepausen zwischendurch.
Herzlich danken möchte ich auch Dr. Mario Schwarz für Diskussionsbereitschaft, zahlreiche Anregungen und Unterstützung bei der Durchführung meiner Arbeit.
Martina Herrero San Juan, Sandra Spiegler und Dr. Renate Kinkel möchte ich herzlich danken für die gute Zusammenarbeit im Labor und stete Hilfsbereitschaft auch in stressigen Zeiten.
Dr. Dietmar Falke, Dr. Judith Calderwood und Dr. Kirsten Stoidtner danke ich für viele gute Tipps im Laboralltag und ihre Hilfe, wenn mal wieder nicht alles so lief wie es sollte.
PD Dr. Marietta Kaszkin-Bettag und Dr. Eva Westphal danke ich für konstruktive Kritik in den Doktorandengesprächen.
Allen Doktoranden, Mitarbeitern und Mitarbeiterinnen des *pharmazentrums* danke ich für die gute Zusammenarbeit.
Nicht zuletzt danke ich meinen Eltern, meinem Bruder Matthias, allen Freunden und Bekannten für die vielseitige Unterstützung während meines gesamten Studiums und während der Doktorarbeit. Mein besonderer Dank gilt Alf, der mir in den letzten Jahren immer zur Seite stand und mir Mut und Zuversicht gegeben hat.

10 Lebenslauf

Kautz
Kordula
Schillerstraße 26-28
55116 Mainz
geboren am: 29.11.1972
in Oerlinghausen/Nordrhein-Westfalen

Schulausbildung

1979-1983	Hans Christian Andersen-Grundschule, Bielefeld
1983-1992	Hans Ehrenberg-Gymnasium, Bielefeld
1992	Abitur

Auslandsaufenthalt

Okt. 1992-Feb. 1993	Betreuung eines Jugendlichen mit Lernbehinderungen in London Community Service Volunteers, London

Hochschulausbildung

1993-1999	Studiengang Biologie (Diplom) Johannes Gutenberg-Universität, Mainz
1998-1999	Diplomarbeit im Institut für Allgemeine Botanik zum Thema „Charakterisierung der γ-Tubulin Sequenz in *Nicotiana tabacum*“, Note „sehr gut“
21. Dez. 1999	Abschluss als Diplom-Biologin

Praktische Tätigkeiten

Mai 1998-Juli 1999	Werkstudentin IBM Werk Mainz
Nov. 1999-Feb. 2000	Wissenschaftliche Hilfskraft im Institut für Allgemeine Botanik, Johannes Gutenberg-Universität, Mainz
April 2000-Juni 2000	Mitarbeiterin im Mobilen Sozialen Dienst, Commit-cbf-Ambulante Dienste, Mainz
Juli 2000-April 2001	Praktikum in der Redaktion eines medizinischen Fachverlags, pmi Verlag AG, Frankfurt a. M.

Promotion

Juni 2001-Dezember 2004	Promotion im *pharmazentrum frankfurt*, Institut für Allgemeine Pharmakologie und Toxikologie, Stiftung Immunpharmakologie, Universitätsklinikum Frankfurt a. M., zum Thema “A system for the intracellular generation of triple helix-forming oligonucleotides (TFOs) and the sequence specific inhibition of human MCP-1 gene expression”

Verzeichnis der akademischen Lehrer

Mainz

Botanik	Prof. W. Wernicke, Prof. G.M. Rothe, Prof. J.W. Kadereit
Chemie	Prof. W. Vogt, Prof. K.K. Unger
Mathematik	Prof. W.J. Bühler
Medizinische Mikrobiologie	Prof. R.E. Streeck
Mikrobiologie	Prof. G. Unden, Prof. H. König
Molekulargenetik	Prof. E.R. Schmidt, Prof. W. Sachse
Paläontologie	Prof. J. Boy, Prof. N. Schmidt-Kittler
Pflanzenphysiologie	Prof. A. Wild
Physik	Prof. G. Huber
Tierphysiologie	Prof. J. Markl
Zoologie	Prof. A. Fischer, Prof. A. Dorresteijn, Prof. C. von Campenhausen

Frankfurt a. M.

Biochemie, Pharmazeutische Chemie	Prof. D. Steinhilber
Immunpharmakologie	Prof. H.H. Radeke
Pharmakologie	Prof. J. Pfeilschifter